DOE/ER/04447-124

ELECTROCHEMICAL AND SPECTROSCOPIC STUDIES OF SOME LESS STABLE OXIDATION STATES OF SELECTED LANTHANIDE AND ACTINIDE ELEMENTS

A Dissertation

Presented for the

Doctor of Philosophy

Degree

The University of Tennessee, Knoxville

David Edward Hobart

June 1981

DISCLAIMER

DEDICATION

The author wishes to dedicate this work to his loving wife, Barbara, and lovely daughter, Michelle, for their patience and understanding during the course of this endeavor.

ACKNOWLEDGMENTS

The author wishes to express his gratitude and appreciation to Dr. Joseph R. Peterson, teacher, colleague, and friend, for helpful advice and support throughout the course of this research. The author is indebted to Dr. Kamal Samhoun for valuable collaboration and friendship. His knowledge and technical assistance are greatly appreciated.

Sincere appreciation is extended to Dr. Gleb Mamantov for helpful guidance, suggestions, and encouragement. Dr. Mamantov and Drs. M. H. Lietzke, P. G. Huray, and J. P. Young are acknowledged for helpful discussions and for reading and critiquing this manuscript. Special thanks to Miss Carol Proaps for typing this dissertation.

The author is grateful to the Department of Chemistry, University of Tennessee (Knoxville) for financial support first in the form of a teaching assistantship and then as a research assistantship, sponsored by the U.S. Department of Energy under contract DE-AS05-76ER04447. Appreciation is also extended to the Oak Ridge National Laboratory (ORNL), operated for the U.S. Department of Energy under contract W-7405-eng-26 with the Union Carbide Corporation, and to the Transuranium Research Laboratory (TRL) for the use of their facility.

The support and cooperation of the ORNL Chemistry Division, under the direction of Dr. O. L. Keller, Jr., is recognized and acknowledged. The author is indebted to the entire staff of the TRL for their patience and technical support. In particular, the author

is grateful to Drs. R. L. Hahn, R. G. Haire, G. M. Begun, D. D. Ensor, S. E. Nave, and G. D. O'Kelley for helpful assistance and discussions; Mr. E. L. Earley, Captain T. C. Minton, Mr. K. Sowder, Mr. A. Massey, Mr. J. H. Oliver, Mr. J. Burkhalter, and Mr. J. R. Tarrant for technical assistance; Ms. J. Hamby and Mrs. B. Mercer for thoughtfulness and patience; and to Mr. C. E. Haynes, Mr. W. D. Carden, Mr. T. Collins, Mr. J. Smith, and Mr. B. A. Powers for health physics support.

Appreciation is extended to the author's colleagues, coworkers, and friends, Dr. Lieutenant D. M. Hembree, Mr. M. K. Pastorcich, Mr. V. E. Norvell, Drs. F. David, B. Guillaume, J. Bourges, G. Beall, B. Allard, M. Hara, Ms. I. Schauer, Ms. K. Kelly, Mr. J. Mottern, Mrs. S. A. Morris, and many others for assistance and support.

Special mention is made of persons the author has admired and emulated and who have provided leadership and encouragement, Mr. D. B. Hobart, Mr. A. E. Dempsey, Dr. S. Frome, Dr. G. T. Cochran, and especially, Dr. H. E. Hellwege.

ABSTRACT

The technique of simultaneous observation of electrochemical and spectroscopic properties (spectroelectrochemistry) at optically transparent electrodes (OTE's) has been applied to the generation and characterization of some less stable oxidation states of selected lanthanide and actinide elements (Ce, Pr, Sm, Eu, Tb, Yb, U, Np, Am, and Cm) in complexing and noncomplexing aqueous solutions. Optically transparent electrodes used in this study included reticulated vitreous carbon (RVC) and metal screen OTE's and a new OTE made from porous metal foam (PMF).

Cyclic voltammetry at microelectrodes was used in conjunction with spectroelectrochemistry for the study of oxidation-reduction (redox) couples. In some cases additional analytical techniques were applied for identification of electrochemically generated oxidation state species; these included solution absorption, solid-state reflectance, and laser Raman spectroscopies, X-ray powder diffraction and thermogravimetric-mass spectral analyses, radiochemical measurements, and spectrophotometric and potentiometric redox titrimetry.

The formal reduction potential ($E^{\circ\prime}$) values of the M(III)/M(II) redox couples in 1 M KCl at pH 6 were found by voltammetry to be -0.34 $\pm$ 0.01 V for Eu, -1.18 $\pm$ 0.01 V for Yb, and -1.50 $\pm$ 0.01 V for Sm. Spectropotentiostatic determination of $E^{\circ\prime}$ for the Eu(III)/Eu(II) redox couple yielded a value of -0.391 $\pm$ 0.005 V. Spectropotentiostatic measurement of the Ce(IV)/Ce(III) redox couple in concentrated carbonate solution gave $E^{\circ\prime}$ equal to 0.051 $\pm$ 0.005 V,

which is about 1.7 V less positive than the E°' value in noncomplexing solution. This same difference in potential was observed for the E°' values of the Pr(IV)/Pr(III) and Tb(IV)/Tb(III) redox couples in carbonate solution, and thus Pr(IV) and Tb(IV) were stabilized in this medium. The solution absorption spectra and redox properties of these aqueous species are reported. A solid Tb(IV)-containing compound was also prepared at an RVC electrode in carbonate solution.

The U(VI)/U(V)/U(IV) and U(IV)/U(III) redox couples were studied in 1 M KCl at OTE's. ^{237}Np, ^{243}Am, and ^{248}Cm were studied in containment gloved box facilities. Spectropotentiostatic measurement of the Np(VI)/Np(V) redox couple in 1 M $HClO_4$ gave an E°' value of 1.140 ± 0.005 V. Np(VII) was generated by electrolysis of Np(VI) in 2 M Na_2CO_3 at pH 13, and the solution absorption and laser Raman spectra were recorded, and an E°' value of 0.46 ± 0.01 V for the Np(VII)/Np(VI) couple was found by voltammetry.

Oxidation of Am(III) was studied in concentrated carbonate solution, and a reversible cyclic voltammogram for the Am(IV)/Am(III) couple yielded E°' = 0.92 ± 0.01 V in this medium; this value was used to estimate the standard reduction potential (E°) of the couple as 2.62 ± 0.01 V. The solution absorption spectrum and redox behavior of Am(IV) were compared to those of Am(V) and Am(VI) in this same medium.

Attempts to oxidize Cm(III) in concentrated carbonate solution were not successful which suggests that the predicted E° value for the Cm(IV)/Cm(III) redox couple may be in error.

TABLE OF CONTENTS

LIST OF TABLES

LIST OF FIGURES

FIGURE PAGE

FIGURE PAGE

FIGURE PAGE

CHAPTER I

INTRODUCTION

A. Background

The f-transition series elements, the lanthanides and actinides, constitute nearly 28% of the known chemical elements. Although some of these elements have been known for more than two hundred years,[1] it has only been recently, since the discovery of nuclear fission, that the man-made transuranium elements have been synthesized.

The development of nuclear technology has stimulated considerable interest in the study of the lanthanide and actinide elements. The lanthanides are the major fission products produced in a nuclear reactor and, aside from their important industrial applications, the lanthanide elements exhibit the only truly analogous chemical behavior to that of the transuranium elements. A thorough understanding of lanthanide chemistry can provide valuable information concerning the chemical behavior of the heaviest actinides for which bulk-phase studies are not possible. The actinides include three naturally occurring elements: thorium, protactinium, and uranium. The remaining members of the series, the transuranium elements, are synthesized as a result of neutron-capture processes in a nuclear reactor or as a result of high-energy particle bombardment in an accelerator. A thorough knowledge of the basic physicochemical

properties of the transuranium elements is essential in view of the ever-increasing dependence on nuclear power for energy needs. Additionally, the lanthanides and actinides are unique in the periodic classification of the elements since they are the only elements which exhibit f-electron chemical behavior.

The chemical behavior of any element depends, to a great extent, upon the oxidation states exhibited by that element and upon their relative stabilities. The electrochemical reduction potential, usually expressed in volts, is a thermodynamic measurement of the relative stabilities of oxidation state species. The reduction potential is directly measurable in many cases by using conventional electrochemical analysis techniques such as potentiometry or voltammetry. Furthermore, with voltammetric techniques, it is possible to oxidize and/or reduce species to generate new (different) oxidation states in a convenient, reproducible manner simply by applying the proper electrochemical potential to a system. The control of an oxidation-reduction (redox) process by electrochemical means can be much more precise than is possible by using chemical reagents.[2]

With conventional electrochemical techniques, the identity of the "product" oxidation state is determined by the known value of the reduction potential of the redox couple, or by determining the electron stoichiometry. Both methods are adequate for systems exhibiting electrochemical reversibility under the conditions of the experiment. Oftentimes the systems are not reversible, or the reduction potential is not known for a particular redox couple under

certain conditions; additional characterization techniques are required in these cases.

Absorption spectroscopy has often been used in conjunction with electrochemical methods for unequivocal identification of electrogenerated products. However, the simultaneous application of spectroscopic and electrochemical techniques, called spectroelectrochemistry,[3] provides a much more powerful and versatile analytical tool.

B. Proposed Research

A formal reduction potential can be altered by the degree of complexation of the oxidized and/or reduced species of a redox couple. A complexing ligand which preferentially complexes one of the oxidation states over the other can substantially change the value of the reduction potential. An oxidation state which is unstable in a non-complexing aqueous solution can be stabilized by complexation. The objective of this research was to determine the accessibility of some unusual or unknown oxidation states of the transuranium elements by spectroelectrochemical investigation of complexing aqueous solutions as a means to generate and characterize some less-stable oxidation states of selected lanthanide and actinide elements.

Because of the inherent simplicity and sensitivity of the technique and the advantage of using small sample volumes (usually less than one mL), spectroelectrochemistry is well suited to the electrochemical generation and spectroscopic characterization of less stable oxidation states of the lanthanide and actinide elements.

The technique is particularly well suited to the study of the transplutonium elements since many of these are available only in limited quantities.

Due to the highly radioactive nature and limited availability of the heavier actinides, experiments were performed using the nonradioactive lanthanides and less radioactive lighter actinides as substitutes for the transplutonium elements. The purpose of these experiments was to verify the proper operation of the instrumentation and to determine the correct experimental approach without jeopardizing the fate of the limited amounts of transplutonium materials. Once these experiments were completed, the experiments using the transplutonium elements were performed in a gloved box facility.

C. Spectroelectrochemistry

Here the reader is provided with a brief description and review of the techniques of spectroelectrochemistry with emphasis placed on the applications pertinent to this work. For more detailed and comprehensive treatments, the interested reader is directed to the many excellent journal articles and monographs on the subject.[4,5,6,7,8]

1. Description

The unique combination of spectroscopic and electrochemical techniques has proven to be an effective approach to the study of oxidation-reduction reactions. Oxidation states are changed

electrochemically by the addition or removal of electrons at an electrode surface. Spectroscopic measurements of the solution near the electrode surface are made simultaneously with the electrochemical generation process. Spectroelectrochemical techniques provide a convenient method for obtaining spectra and redox potentials and for investigating subsequent chemical reactions of electrogenerated products.[6]

Many different optical methods have been coupled with electrochemistry but the most frequently used technique is that of absorption spectroscopy in the ultraviolet-visible-near infrared spectral region. Of the three methods of absorption spectroscopy coupled with electrochemistry, transmission spectroscopy, specular reflectance spectroscopy,[9] and internal reflectance spectroscopy,[10,11] the method of transmission spectroscopy is the most simple and convenient method. This method involves the passage of an optical beam directly through an optically transparent electrode (OTE) and the adjacent solution.[3,4,5,12] Two distinctly different configurations of optically transparent electrochemical cells are commonly used in conjunction with transmission spectroscopy. The first configuration is similar to a conventional electrochemical cell in that the electrode is in contact with a solution that is much thicker than the diffusion layer at the electrode surface. In contrast, the second type of cell configuration, the optically transparent thin layer electrode (OTTLE) cell confines a thin layer (<0.2 mm) immediately adjacent to the electrode surface.[4,6] The advantage of this type of cell arrangement is that all the electroactive species within the thin layer can be

rapidly electrolyzed and thus equilibrium for the redox reaction can be quickly achieved (typically 20 to 120 sec).[6]

2. Theory

An electrochemical reaction can be represented by the following

$$Ox + ne^- \rightleftarrows Red, \qquad (1)$$

where an oxidized species, Ox, combines with n number of electrons, e^-, to form a reduced species, Red. The electrochemical potential produced by the reaction is related to the ratio of the activities of the oxidized and reduced species in the Nernst equation

$$E = E^o + \frac{RT}{nF} \ln \frac{a_{ox}}{a_{red}} , \qquad (2)$$

where E is the applied potential; E^o is the standard potential for the specific redox reaction; R, the gas constant; T, the absolute temperature; n, the number of electrons exchanged; F, the Faraday; and a_{ox} and a_{red}, the activities of the oxidized and reduced species, respectively. Under most experimental conditions, the temperature is room temperature (25°C) and the activity coefficients of the oxidized and reduced species are assumed to be unity. Thus a simplified form of the Nernst equation can be written

$$E = E^{o\,\prime} + \frac{0.059}{n} \log \frac{[Ox]}{[Red]} , \qquad (3)$$

where [Ox] and [Red] indicate the molar concentrations of Ox and Red, respectively and $E^{o\,\prime}$ is the formal reduction potential.

With the use of an OTE the concentrations of Ox and Red can be determined spectrophotometrically by Beer's law

$$A = \varepsilon bC, \tag{4}$$

where A is the absorbance of Ox or Red; ε, the molar absorptivity of Ox or Red; b, the path length of the OTE cell; and C, the molar concentration of Ox or Red. Combination of the Nernst equation (3) and Beer's law (4) results in an expression which relates the applied potential to the ratio of concentrations of Ox and Red expressed in terms of spectral parameters

$$E = E^{o'} + \frac{0.059}{n} \log \left(\frac{A_{ox}/\varepsilon_{ox}}{A_{red}/\varepsilon_{red}} \right), \tag{5}$$

where ε_{ox} and ε_{red} are the molar absorptivities of the oxidized and reduced species, respectively. Equation 5 can be used as shown to determine the $E^{o'}$ and n-values of redox couples.

DeAngelis and Heineman[13] presented a more convenient form of equation 5. These authors selected a wavelength where only the oxidized species, for example, absorbed. The absorbance at this wavelength was recorded at potentials corresponding to fully reduced conditions (A_1), partially oxidized conditions (A_2), and fully oxidized conditions (A_3). Under fully oxidized conditions, where the electroactive species is all in its oxidized form, the following holds

$$C_t = \frac{A_3 - A_1}{\varepsilon_{ox} b}, \tag{6}$$

where C_t is the total concentration of electroactive species. The concentration of the oxidized species at a potential corresponding to partially oxidized conditions is

$$[Ox] = \frac{A_2 - A_1}{\varepsilon_{ox} b} . \tag{7}$$

Therefore, the concentration of the reduced species at a potential corresponding to partially oxidized conditions is the difference between the total concentration of electroactive species and the concentration of the oxidized species, i.e.,

$$[Red] = [\frac{(A_3 - A_1)}{\varepsilon_{ox} b} - \frac{(A_2 - A_1)}{\varepsilon_{ox} b}] = \frac{(A_3 - A_2)}{\varepsilon_{ox} b} . \tag{8}$$

The ratio of concentrations of the oxidized species and the reduced species is expressed as

$$\frac{[Ox]}{[Red]} = \frac{(A_2 - A_1)/(\varepsilon_{ox} b)}{(A_3 - A_2)/(\varepsilon_{ox} b)} = \frac{(A_2 - A_1)}{(A_3 - A_2)} . \tag{9}$$

Substitution of Equation 9 into Equation 3 results in

$$E = E^{o'} + \frac{0.059}{n} \log \frac{(A_2 - A_1)}{(A_3 - A_2)} . \tag{10}$$

Experimentally, the absorption of the oxidized species is measured at the selected wavelength at equilibrium at various applied potential values. A plot of the applied potential, E, versus log $(A_2-A_1)/(A_3-A_2)$

for a reversible reaction yields a straight line with slope equal to 0.059/n and intercept equal to the formal reduction potential, $E^{o'}$. This approach eliminates the need to know the molar absorptivity of the absorbing species, the path length of the cell or the total concentration of the electroactive species.

The above description outlines the theory of the spectropotentiostatic technique for the determination of spectra, reduction potentials, and n-values for redox couples. Descriptions of other related spectroelectrochemical techniques can be found elsewhere.[4,12,14,15,16]

3. Literature Review

a. Optically transparent electrodes. In 1964 the use of an OTE for in situ spectral observation of an electrogenerated product was first demonstrated by Kuwana et al.[3]. The OTE was a glass surface which had been coated with a thin transparent film of antimony-doped tin oxide (Nesa glass) which was used for both transmission and internal reflectance spectroscopies. A variety of thin conducting films deposited on transparent substrates for use as OTE's has been reported since then, including metal films such as platinum[17,18] and gold,[18,19] and semi-conductors such as tin oxide,[11,19] indium oxide,[4] carbon film[20] (on quartz or germanium substrates for infrared studies),[21] and pyrolytic carbon.[22] These thin film OTE's are transparent due to the thinness of the metal, metal oxide, or semi-conductor film, but they do exhibit spectral characteristics of the film material.

In 1967 Murray et al.[23] introduced the gold "minigrid" optically transparent electrode in a thin layer configuration (OTTLE). The minigrid consists of a metal (gold,[23] nickel,[6] silver,[6]

platinum,[24] etc.) grid with from 100 to 2000 wires per inch. The transparency of the minigrid electrode (20-80%) is accounted for by the physical holes in the minigrid structure, and therefore the spectral window of these electrodes it not limited by the spectral properties of the construction material.

Mercury transparent electrodes have been prepared by electrodeposition of thin Hg films on a platinum-film OTE[25] and carbon-film OTE,[20] as well as on silver[26] and nickel[27] minigrids. The mercury imparts some of its excellent negative potential range characteristics to the substrate OTE without seriously affecting the transparency of the electrode.

In 1977 Norvell and Mamantov[28] reported the development of an OTE made from a novel electrode material, reticulated vitreous carbon (RVC). The RVC-OTE was quite different from any previous spectroelectrochemical cell in that the cell configuration more nearly resembled the thick (0.8-1.2 mm) conventional OTE, but it exhibited the special characteristics of an OTTLE. This was achieved by the unique structure of the RVC electrode material, composed of glassy carbon struts in a three-dimensional network. The porous nature and large surface-to-volume ratio of the electrode allows the RVC-OTE to behave like a thin layer cell in that electrochemical equilibrium is rapidly achieved, because each electroactive species has a relatively short diffusion path to the electrode surface. In addition, the electrical conductivity and transparency (13-45%) of the RVC-OTE are quite reasonable.

b. Applications. Spectroelectrochemical techniques have been applied to the spectral identification of electrogenerated products such as Mu-pyrazinedecaaminediruthenium (II,III) complexes,[29] ninhydrin,[30]

lithium complexes of 1-hydroxy-9,10-anthraquinone (HOAQ),[31] vitamin B-12,[24] 1,8-dihydroxyanthraquinone and anthraquinone anion radicals,[32] iron (II,III) acetylacetonate,[33] bis-hydroxy methyl ferrocene,[19] o-tolidine,[13,28] permanganate ion[28] and green plant photosystem I.[34] The spectropotentiostatic technique for the measurement of spectra, redox potentials, and n-values has been applied to the study of various metal complexes and biological components.[13,24,32,35,36,37] Additional references can be found in a recent review by Heineman and Kissinger.[38]

c. Related techniques. While many workers have monitored electrochemical generation via spectrophotometry,[39,40,41,42] only one report of simultaneous spectroelectrochemistry of actinide materials had appeared in the literature prior to the work of this author. Young, Mamantov, and Whiting[43] reported the electrochemical generation of uranium(III) at a microelectrode in molten LiF-BeF_2-ZrF_4 located in the optical path of a spectrophotometer.

D. The Lanthanide and Actinide Elements

1. Electronic Structure

The lanthanides are the fourteen elements following lanthanum in the Periodic Table in which the fourteen 4f electrons are consecutively added to the lanthanum configuration. These electrons are added to electron orbitals which are lower in energy than the valence orbitals of lanthanum. Thus the 4f electrons occupy inner shielded orbitals which makes them, for the most part, unavailable for chemical interactions. This accounts for the remarkable similarity in the chemical behavior among the individual members of the lanthanide

series. The electronic configurations of lanthanide atoms and ions are listed in Table I.

In the actinide series the fourteen 5f electrons are consecutively added to the actinium configuration. The electronic configurations of actinide atoms and ions are summarized in Table II. Comparison of these configurations with those of the lanthanides shows an overall similarity with the exception that the lighter actinides (thorium to americium) show an enhanced tendency to retain d electrons. The heavier actinides (curium to lawrencium) show a tendency to retain f electrons rather than d electrons, more paralleling the behavior of the majority of the lanthanides. The result is a greater tendency of the lighter actinides to supply bonding electrons, and thus a greater tendency to exhibit higher oxidation states.[44] The heavier actinides resemble the lanthanides in their oxidation state behavior.[45]

2. Oxidation States

A direct correlation between oxidation state and electronic configuration is the exception rather than the rule in the lanthanide series.[44] The electron configuration of $4f^n6s^2$ is the characteristic one for most of the lanthanide atom ground states (see Table I). Therefore, the divalent state should be accessible for all of the lanthanides with the loss of the two 6s electrons. This is not the situation, however, since the trivalent state is the most common oxidation state for these elements. The loss of the two 6s electrons is usually accompanied by one 4f electron, if a 5d electron is not available.

TABLE I

ELECTRONIC CONFIGURATIONS OF LANTHANIDE ATOMS AND IONS[1,2]

Atomic number	Name	Symbol	Electronic Configuration			
			Atom	M(II)	M(III)	M(IV)
58	Cerium	Ce	$4f^1 5d^1 6s^2$	$4f^2$	$4f^1$	$4f^0$
59	Praseodymium	Pr	$4f^3 6s^2$	$4f^3$	$4f^2$	$4f^1$
60	Neodymium	Nd	$4f^4 6s^2$	$4f^4$	$4f^3$	$4f^2$
61	Promethium	Pm	$4f^5 6s^2$	-	$4f^4$	-
62	Samarium	Sm	$4f^6 6s^2$	$4f^6$	$4f^5$	-
63	Europium	Eu	$4f^7 6s^2$	$4f^7$	$4f^6$	-
64	Gadolinium	Gd	$4f^7 5d^1 6s^2$	$4f^7 5d^1$	$4f^7$	-
65	Terbium	Tb	$4f^9 6s^2$	$4f^9$	$4f^8$	$4f^7$
66	Dysprosium	Dy	$4f^{10} 6s^2$	$4f^{10}$	$4f^9$	$4f^8$
67	Holmium	Ho	$4f^{11} 6s^2$	$4f^{11}$	$4f^{10}$	-
68	Erbium	Er	$4f^{12} 6s^2$	$4f^{12}$	$4f^{11}$	-
69	Thulium	Tm	$4f^{13} 6s^2$	$4f^{13}$	$4f^{12}$	-
70	Ytterbium	Yb	$4f^{14} 6s^2$	$4f^{14}$	$4f^{13}$	-
71	Lutetium	Lu	$4f^{14} 5d^1 6s^2$	-	$4f^{14}$	-

[1]Only the valence-shell electrons, that is, those outside the [Xe] core, are given.

[2]A dash indicates that this oxidation state is not known.

TABLE II

ELECTRONIC CONFIGURATIONS OF ACTINIDE ATOMS AND IONS[1,2]

Atomic number	Name	Symbol	Electronic Configuration					
			Atom	M(II)	M(III)	M(IV)	M(V)	M(VI)
90	Thorium	Th	$5f^0 6d^2 7s^2$			$5f^0$		
91	Protactinium	Pa	$5f^2 6d^1 7s^2$			$5f^1$	$5f^0$	
92	Uranium	U	$5f^3 6d^1 7s^2$		$5f^3$	$5f^2$	$5f^1$	$5f^0$
93	Neptunium	Np	$5f^4 6d^1 7s^2$		$5f^4$	$5f^3$	$5f^2$	$5f^1$
94	Plutonium	Pu	$5f^6 \quad 7s^2$		$5f^5$	$5f^4$	$5f^3$	$5f^2$
95	Americium	Am	$5f^7 \quad 7s^2$	$5f^7$	$5f^6$	$5f^5$	$5f^4$	$5f^3$
96	Curium	Cm	$5f^7 6d^1 7s^2$		$5f^7$	$5f^6$		
97	Berkelium	Bk	$5f^9 \quad 7s^2$		$5f^8$	$5f^7$		
98	Californium	Cf	$5f^{10} \quad 7s^2$	$5f^{10}$	$5f^9$	$5f^8$		
99	Einsteinium	Es	$5f^{11} \quad 7s^2$	$5f^{11}$	$5f^{10}$			
100	Fermium	Fm	$5f^{12} \quad 7s^2$	$5f^{12}$	$5f^{11}$			
101	Mendelevium	Md	$5f^{13} \quad 7s^2$	$5f^{13}$	$5f^{12}$			
102	Nobelium	No	$5f^{14} \quad 7s^2$	$5f^{14}$	$5f^{13}$			
103	Lawrencium	Lr	$5f^{14} 6d^1 7s^2$		$5f^{14}$			

[1]Only the valence-shell electrons, that is, those outside the [Rn] core, are given.

[2]A blank space indicates that this oxidation state is not known or the configuration for this oxidation state is not known.

The M(III) state is the most stable one for the lanthanides in aqueous solution due to a fortuitous combination of ionization and hydration energies rather than a particular electronic configuration.[44] In the solid state the ionization energy is coupled to the lattice or crystal energy, and again the trivalent state is generally the most stable.

To a certain extent, the occurrence of oxidation states other than M(III) for the lanthanides can be correlated with their electronic structures and ionization potentials. As is the case with the d-electron transition metals, there is a certain stability associated with an empty, half-filled, or filled shell. The significance of this stability is evidenced by the existence of M(II) and M(IV) oxidation states of some lanthanides. The oxidation states of the lanthanide elements are summarized in Table III. The states indicated in this table are known to occur in the bulk phase, and although additional oxidation states have been reported, such as inclusions of divalent lanthanides in host lattices, they are not considered in this listing.[1,44,45]

The actinide elements exhibit a greater variety of oxidation states than do the lanthanides. The presently known oxidation states of the actinide elements are presented in Table IV. Only oxidation states which are known in bulk phases are shown. In general, the lighter actinides (Th-Am) show an increased stability for higher oxidation states with increasing atomic number, whereas there is a decrease in the stability of higher oxidation states and an increase in the stability of lower ones in the second half of the series. As is the

TABLE III

OXIDATION STATES OF THE LANTHANIDE ELEMENTS[1,2]

Ce	Pr	Nd	Pm	Sm	Eu	Gd	Tb	Dy	Ho	Er	Tm	Yb	Lu
		(2)		2	2			(2)			(2)	2	
3	3	3	3	3	3	3	3	3	3	3	3	3	3
4	(4)	(4)					(4)	(4)					

[1]Parentheses indicate solid state only or not well characterized.

[2]Underlined numbers indicate most stable oxidation state.

TABLE IV

OXIDATION STATES OF THE ACTINIDE ELEMENTS[1,2]

Th	Pa	U	Np	Pu	Am	Cm	Bk	Cf	Es	Fm	Md	No	Lr
					(2)			2	2	2	2	2	
(3)	3	3	3	3	3	3	3	3	3	3	3	3	3
4	4	4	4	4	4	4	4	4					
	5	5	5	5	5								
		6	6	6	6								
			7	7	(7)								

[1]Parentheses indicate solid state only or not well characterized.

[2]Underlined numbers indicate most stable oxidation state.

case for the lanthanides, the trivalent state is generally the most stable one for the transplutonium elements.

Here again, there is a pronounced preference in the known actinide oxidation states for the f^0, f^7, and f^{14} electronic configurations. However, stability of a given oxidation state is less closely related to electronic configuration than to ionization energy, hydration energy, and lattice energy.[44]

The more extensive spatial projection of the 5f orbitals, over that of the 4f orbitals, into the outer or valence regions of the actinide atoms somewhat reduces the shielding of these electrons, so their binding energy is less, and thus, in general, the actinides exhibit a greater variety of observed oxidation states than do the lanthanides.[44]

a. The Monovalent State. In 1973, Mikheev et al.[46] reported the existence of a stable monovalent, cesium-like ion of mendelevium based on the results of co-crystallization experiments. This was the first report of any monovalent actinide or lanthanide ion in the bulk phase. The existence of Md(I) was attributed to the stabilization provided by its expected $5f^{14}$ electronic configuration. Later experiments by Hulet et al.[47] to reproduce the co-crystallization results were unsuccessful, and these authors concluded that the original claim of the existence of monovalent mendelevium was unsubstantiated. This conclusion was also supported by the results of additional experiments by Samhoun et al.[48] at Oak Ridge, Tennessee (in which this author

participated) and by David et al.[49] at Berkeley, California, using the techniques of radiopolarography[50] and radiocoulometry.[51]

b. The Divalent State. The M(II) state is well-established for the lanthanides Sm, Eu, and Yb in both solutions and in the solid state. Tm(II) and Nd(II) are not well investigated. Eu(II) exhibits a $4f^7$ (half-filled shell) configuration and Yb(II), the $4f^{14}$ (filled shell) configuration. However, the stability of Sm(II), with a $4f^6$ configuration, cannot be explained by electronic configuration alone.[52] The ions of divalent Sm and Yb are unstable in water and are oxidized by air, but Eu(II) is quite stable in aqueous solution.

The actinide elements californium to nobelium are known to exist in the divalent state in aqueous solution. Although the trivalent state is generally the most stable for the heavier actinides in solution, the most stable state of nobelium (homolog of Yb) is No(II).[53] Compounds of the heavier halides of Am(II) have been reported.[54,55] Am(II) and Th(II) may also exist in fused chloride melts.[56] The instability of Am(II) in aqueous solution is surprising, since it is the homolog of Eu and exhibits the $5f^7$ configuration; however, stability of an oxidation state is not based on electronic configuration alone. The behavior of the divalent lanthanides and actinides resembles that of the alkaline earth elements.

c. The Trivalent State. The M(III) state is the characteristic oxidation state for all of the lanthanides and is the most stable in aqueous solution. Gd and Lu form the M(III) ions because of the attainment of the stable $4f^7$ and $4f^{14}$ configurations, respectively.

The trivalent state is well known for all of the actinides with

the exception of protactinium. Only PaI_3 is known, which is a black-colored compound, exhibiting the CeI_3 structure, that might be more properly described as $Pa(IV)(I^-)_3(e^-)$.[57] The M(III) state is generally the most stable one for the actinides with the exception of No. Of the trivalent actinides, U(III) is the most readily oxidized by air or water.[45]

d. The Tetravalent State. Cerium(IV) is the only tetravalent lanthanide species sufficiently stable to exist in aqueous solution as well as in the solid state.[52] In aqueous solution Ce(IV) is a powerful oxidizing agent, and its chemistry resembles that of Zr, Hf, and the tetravalent actinides. The stability of Ce(IV) can be attributed to the attainment of the $4f^0$ (noble gas) configuration.

Pr(IV) is known to exist in only a few solid compounds including the halides and the black nonstoichiometric oxides. The oxide system is complex with stable phases (containing mixed-valence Pr) with formulas between Pr_2O_3 and the true dioxide. Tb(IV) resembles Pr(IV) in that nonstoichiometric compounds are known such as Tb_4O_7 and Tb_7O_{12}. Both Pr(IV) and Tb(IV) oxidize water, so no stable aqueous solutions of these ions are known.[52]

There is some evidence for Nd(IV) and Dy(IV) in the fluorination products of lanthanide/alkali metal mixed salts. Such compounds as Cs_3NdF_7 and Cs_3DyF_7 can be formed to a limited extent.[58,59] Nd(IV) has been reported as being stable when incorporated into barium oxide-based host lattices.[60]

The actinides thorium to californium are known in the tetravalent state. Am(IV) is unstable in most mineral acid solutions. However,

Am(IV) can be stabilized in strongly complexing aqueous solutions.[61,62,63] Cm(IV) has not been prepared by oxidation of any solution of Cm(III), but rather by dissolution of CmF_4 in concentrated aqueous CsF solution.[64] Tetravalent plutonium, like americium, tends to disproportionate rapidly in aqueous solution in the absence of complexing agents. Bk(IV) resembles Ce(IV) in its chemical behavior and stability in aqueous solutions. The tetravalent actinides form the strongest complexes and chelates in the lanthanide-actinide group of elements. Numerous compounds of tetravalent actinides are known, the most common being the dioxides and tetrahalides.[53]

e. The Pentavalent State. This oxidation state is known for the actinides from protactinium to americium. Pentavalent uranium, neptunium, plutonium, and americium are known to exist as the dioxo-cations, MO_2^+, with two short covalent metal to oxygen bonds. Pa(V), on the other hand, does not form such a complex cation and exists in solution as the simple hydrated species. However, at Pa(V) concentrations greater than 10^{-6} M, protactinium forms dimers and polymers which necessarily complicate any experimental work with this species.[65] Pa(V) is the most stable form of protactinium.

The chemistry of the dioxo-cations, MO_2^+ (M = U, Np, Pu, and Am), resembles that of divalent Cd, Ca, or Zn. Uranium(V) is unstable in aqueous solution and disproportionates rapidly unless specific conditions are maintained, including a pH of between 2.0 and 4.0. Attempts to reduce uranium(VI) to uranium(V) usually result in the immediate formation of U(IV) and U(VI), unless adjustments are made to slow the disproportionation rate.[66] Pentavalent uranium is stable in

hydrofluoric acid solutions as the UF_6^- ion. PuO_2^+ and, to a lesser extent, AmO_2^+ are also unstable to disproportionation. Many solid compounds of these pentavalent elements are known which do not contain the dioxo-cation structure, including UF_5, $NpOF_3$, and some tri-oxy compounds like $LiUO_3$.[53]

f. The Hexavalent State. The elements uranium to americium have been shown to exist in this oxidation state. In aqueous solution and in most compounds, the dioxo-cations are present as MO_2^{2+}. UO_2^{2+} is the most stable form of uranium in aqueous solution. The stability of the hexavalent actinides decreases from UO_2^{2+}, with the $5f^o$ configuration, to AmO_2^{2+}, with the $5f^3$ configuration. Many solid compounds are known where the dioxo-cation structure is absent, such as Li_6AmO_6, Pb_3UO_6, UO_3, UF_6, and PuF_6.[53]

g. The Heptavalent State. Russian chemists, in 1967/68, reported the existence of heptavalent neptunium and plutonium. Krot and Gelman[67] reported that ozone oxidation of a NpO_2^{2+} solid suspension in alkali solution resulted in the gradual dissolution of the solid and the formation of a dark green solution of Np(VII). Pu(VII) can be prepared in a similar manner. In alkali solution Np(VII) seems to be reasonably stable and corresponds to the $5f^o$ configuration, whereas Pu(VII) is unstable even in alkali and is reduced by water. These heptavalent species, of the form NpO_5^{3-} and PuO_5^{3-}, can form solid compounds from solution.[53]

Am(VII) is prepared by ozone oxidation of AmO_2^{2+} in alkali at 0 to 7°C. Evidence was presented by the Russian scientists that Am(VII) was indeed the species formed and that it was quite unstable.[68]

3. Oxidation-Reduction Potentials

The relative stabilities of the lanthanide and actinide oxidation state species are reflected in the values of the reduction potentials for their redox couples. Useful correlations of standard reduction potentials for the lanthanide and actinide M(III)/M(II) and M(IV)/M(III) couples were published by Nugent et al.[69] These reduction potentials were derived from (a) direct electrode potential measurements reported in the literature, (b) linear plots of electron-transfer absorption bands and f-d absorption bands versus potential for the various redox couples; and (c) from theoretical calculations based on Jørgensen's[70] refined-electron-spin-pairing-energy theory. These values are displayed graphically in Figures 1 and 2. The most striking feature of these figures is the discontinuity which occurs in the standard reduction potential as the half-filled f-shell is attained for the configuration of the reduced species [Eu(II) and Am(II) in Figure 1 and Gd(III) and Cm(III) in Fig. 2]. This shows evidence of the special stability provided by the f^7 electronic configuration.

These diagrams are particularly useful for correlating the stabilities of species in aqueous solution. For example, Yb(II) is not stable in aqueous solution; it is rapidly oxidized by water. Therefore the point in Figure 1 that corresponds to the Yb(III)/Yb(II) couple is a

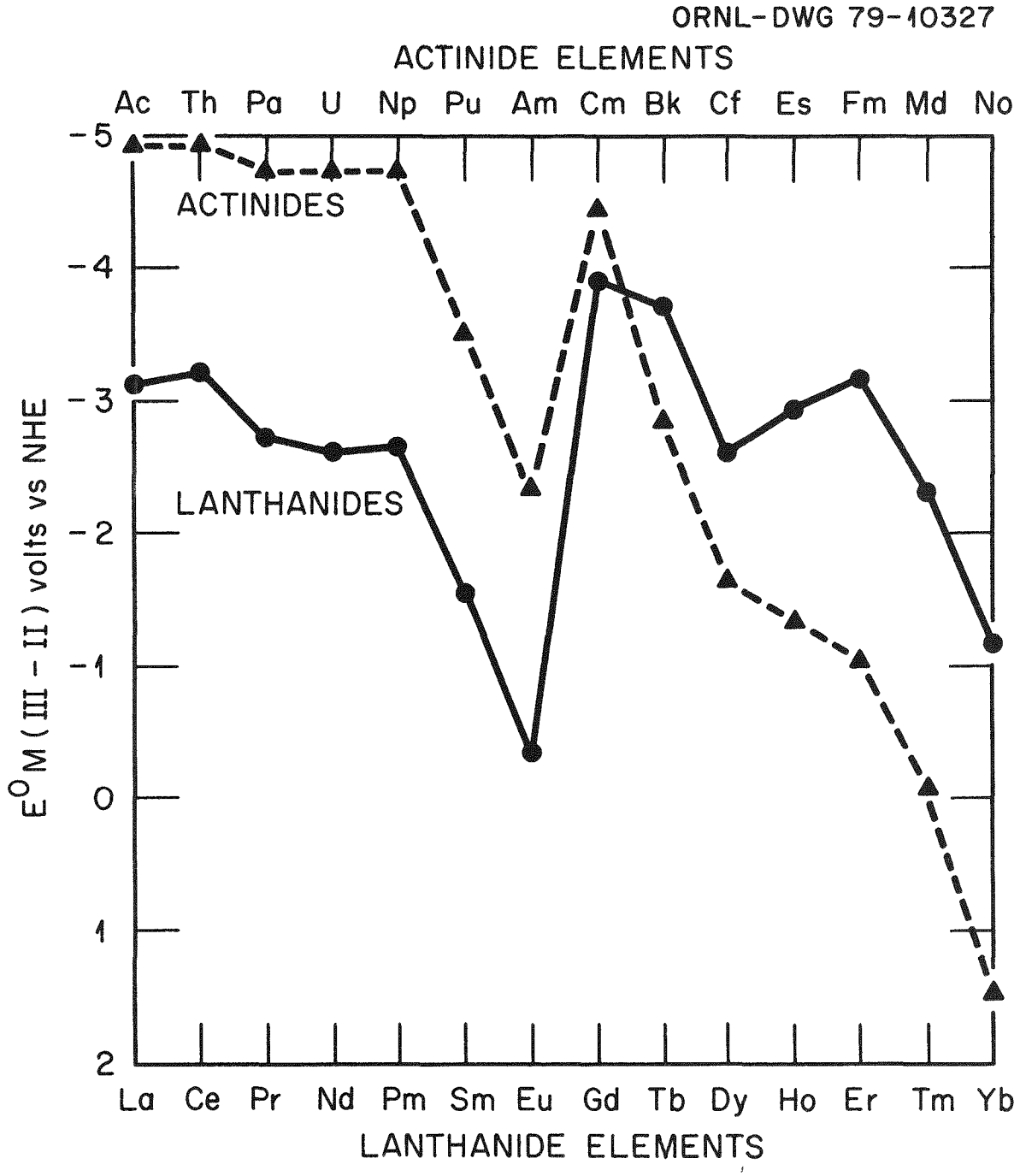

Figure 1. Standard reduction potentials for M(III)/M(II) redox couples of some lanthanide and actinide elements, lanthanum, and actinium.

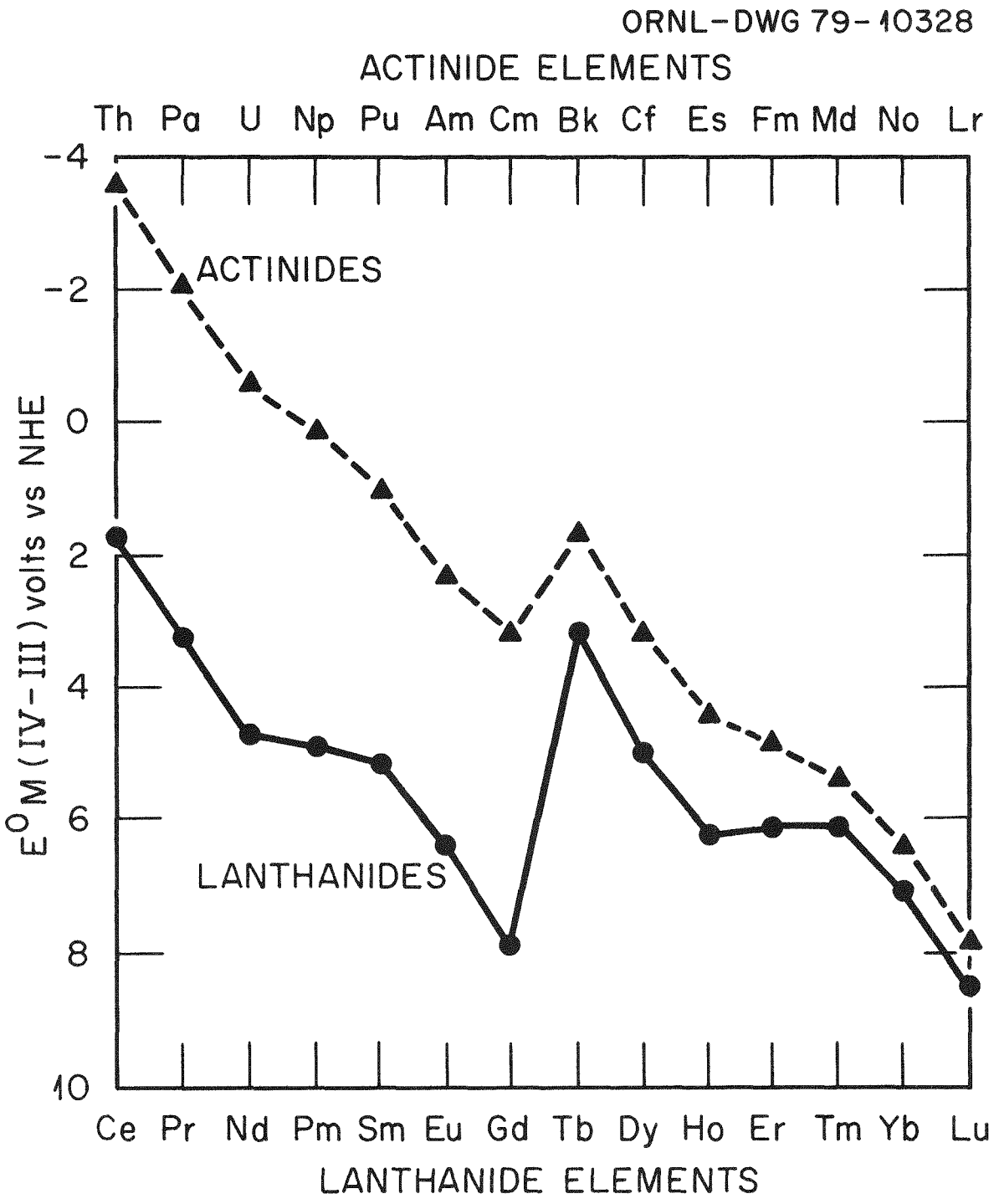

Figure 2. Standard reduction potentials for M(IV)/M(III) redox couples of the lanthanide and actinide elements.

potential at which oxidation by water occurs, as is the case for any point at a more negative potential. The value for the Eu(III)/Eu(II) couple is less negative than that for rapid oxidation by water and so, Eu(II) is quite stable in water. A potential at which water will reduce the oxidized form of the redox couple is the point corresponding to the No(III)/No(II) couple, since No(II) is stable in water and No(III) is not.

Comparison of the chemical properties of the lanthanides and actinides can be made from the correlations in Figures 1 and 2. The points corresponding to the Ce(IV)/Ce(III) and Bk(IV)/Bk(III) couples are at nearly the same potential value, so the chemical behavior of these two redox couples is quite similar. Both Ce(IV) and Bk(IV) are strongly affected by complexation. A high degree of complexation is evidenced by a significant change in the measured redox potential in various complexing solutions. The Ce(IV)/Ce(III) couple exhibits a potential of 1.28 V in 2 M HCl; 1.44 V in 1 M H_2SO_4; 1.61 V in 1 M HNO_3; and 1.7 V in 1 M $HClO_4$.[45,52] The Bk(IV)/Bk(III) couple exhibits a formal reduction potential of 0.022 V in 2 M K_2CO_3; 0.88 V in 7.5 M H_3PO_4; 1.3 V in 1 M HNO_3; and 1.6 V in 1 M $HClO_4$.[69,71] The formal reduction potential of the Am(IV)/Am(III) couple is also changed by complexing solvents, as are the potentials of many of the redox couples that include the tetravalent oxidation state as one member of the couple. This is due to the fact that the tetravalent lanthanide and actinide ions are the most strongly complexed of the f-transition element oxidation states.

The reduction potentials of higher oxidation state couples of some actinides are presented in Table V. These potential values are based on experimental work and theoretical estimates.[45,53,69,72,73]

4. Solution Absorption Spectra

The f orbital electrons of the lanthanide and, to a lesser extent, the actinide ions are shielded from the surrounding chemical environment, and thus absorption spectral bands due to f-f electronic transitions are extremely sharp bands and are, for the most part, unaffected by complexing ligands. The absorption spectra of the trivalent lanthanides and of many oxidation states of the actinides typically exhibit this line-like character with most absorption bands appearing in the visible and near-UV spectral regions. These f-f transitions are of low probability due to the "forbidden" nature of the transition as described by quantum mechanical selection rules. The actinide f-f absorption bands are generally an order of magnitude greater in intensity than those of the lanthanides.[44]

The absorption spectra of the di- and tetravalent lanthanide and certain actinide ions exhibit broad-band transitions arising from f-d or ligand-metal charge-transfer mechanisms. These "allowed" transitions result in high molar absorptivities, several orders of magnitude greater than those of the f-f transitions. These bands are strongly affected by the surrounding chemical environment. This is especially true for the charge-transfer bands, since the electron originates from the ligand itself.

TABLE V

REDUCTION POTENTIALS OF HIGHER OXIDATION STATE COUPLES OF SOME ACTINIDE ELEMENTS[a]

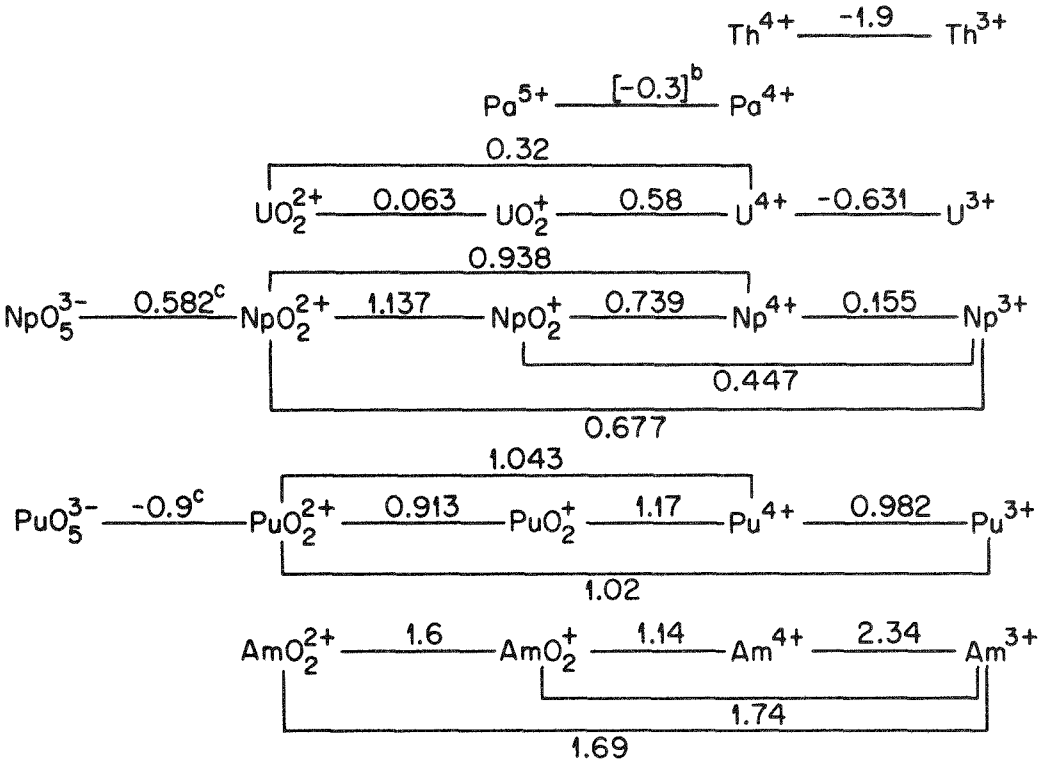

[a]Values reported in volts vs NHE in 1 M $HClO_4$ at 25°C, unless otherwise specified.

[b]Brackets indicate estimated value.

[c]Values reported in 1 M hydroxide solution.

CHAPTER II

EXPERIMENTAL DETAILS

A. Introduction

1. Spectrophotometers

Solution absorption spectra and solid state reflectance spectra of nonradioactive samples were recorded using a Cary Model 14-M spectrophotometer. Solution absorption spectra of inactive as well as radioactive materials were recorded with a Cary Model 14-H spectrophotometer (see Figure 3). Solution absorption spectra of some inactive samples were recorded using a Tektronix silicon-vidicon based rapid-scan spectrophotometer.[74] Solid state absorption spectra of radioactive, microgram-sized samples sealed in quartz capillaries were recorded with a microscope spectrophotometer/Tektronix 4051 data acquisition facility.[75]

2. Voltammeter

Electrochemical measurements were performed with an EG&G PARC Model 173D/179D/175 potentiostat/coulometer/universal programmer complemented by an Esterline Angus Model XY530 recorder (see Figure 3).

3. Gloved Boxes

A basic requirement in the handling of radioactive materials is that all operations be performed in a suitable enclosure that provides necessary containment.

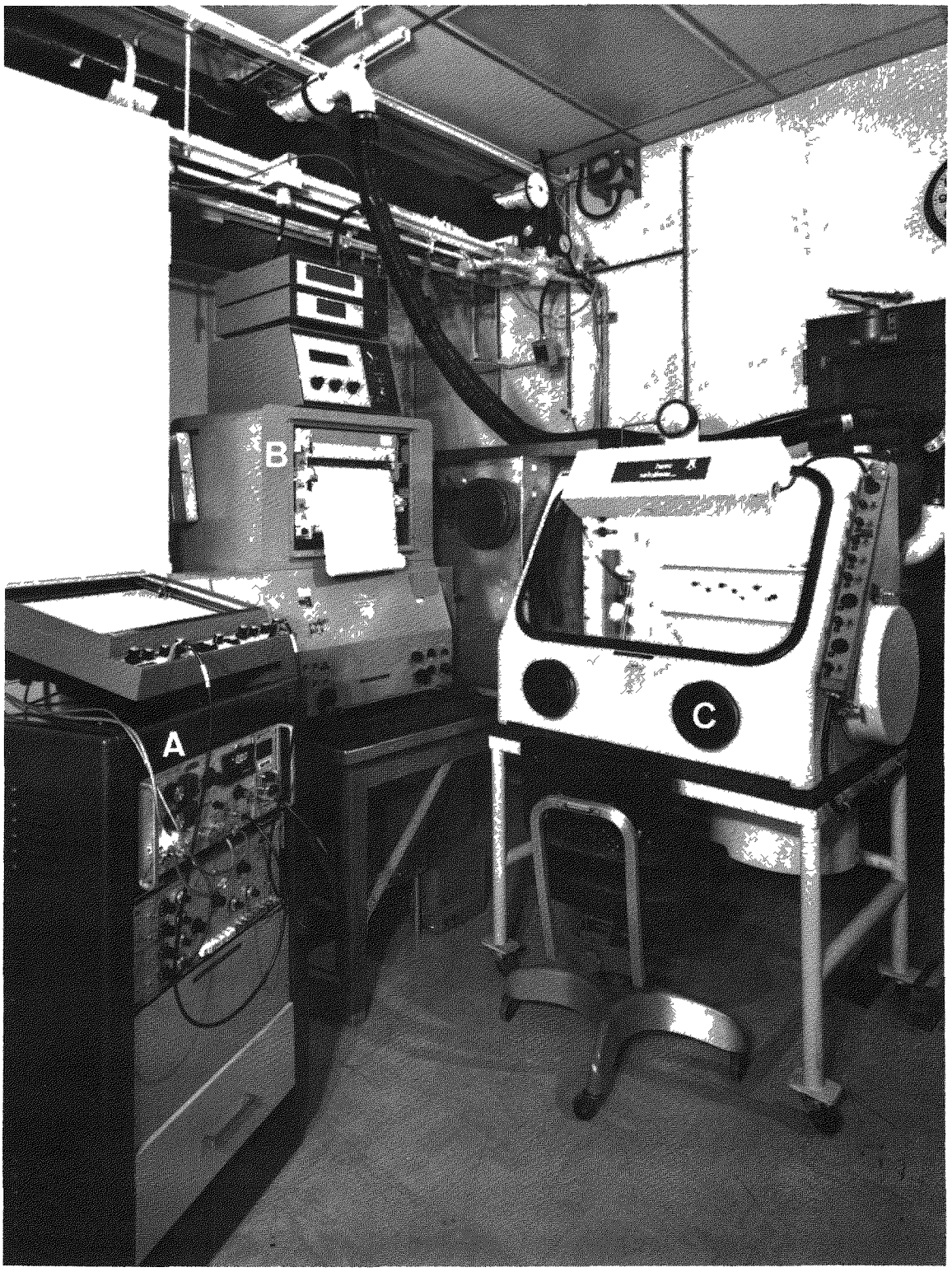

Figure 3. Equipment for spectroelectrochemical studies of radioactive actinide elements. Voltammeter (A), spectrophotometer (B), and modified gloved-box (C).

a. Preparative gloved box. Chemical manipulations of larger quantities (>10 mg) of radioactive actinides were performed in a conventional three-foot, standard-flow, air-ventilated gloved box. This box was equipped with a centrifuge, hot plate, and bulk-head connections for the input of various gases and electrical power.

b. Modified gloved box. A conventional three-foot gloved box was modified with an appendage, fitted with quartz windows, which slides into the sample compartment of the Cary Model 14-H spectrophotometer (see Figures 3 and 4). Bulk-head connections were made to the voltammeter for performing simultaneous electrochemical and spectroscopic measurements of radioactive actinides.

c. Inert atmosphere gloved box. An inert (helium) atmosphere gloved box was used for preparation of anhydrous fluorides. An RF-heated Monel tube furnace, which could be pressurized with fluorine, was installed in the rear of the box for this purpose.

4. Accessory Equipment

a. pH meter. A Corning Model 130 pH meter was used in conjunction with a Fisher Scientific Company Model E-5A combination glass electrode with a silver/silver chloride internal reference electrode.

b. Alpha detection equipment. Alpha spectra were taken with a silicon surface-barrier detector and a Tracor/Northern Model TN-1710, 4096-channel analyzer. Gross alpha counting was performed with a gas-flow proportional counter.

c. X-ray spectrometer. A General Electric Model XRD-6 X-ray generator with a fine-focus copper X-ray tube was used with a nickel filter to perform X-ray powder diffraction analysis. Powder patterns

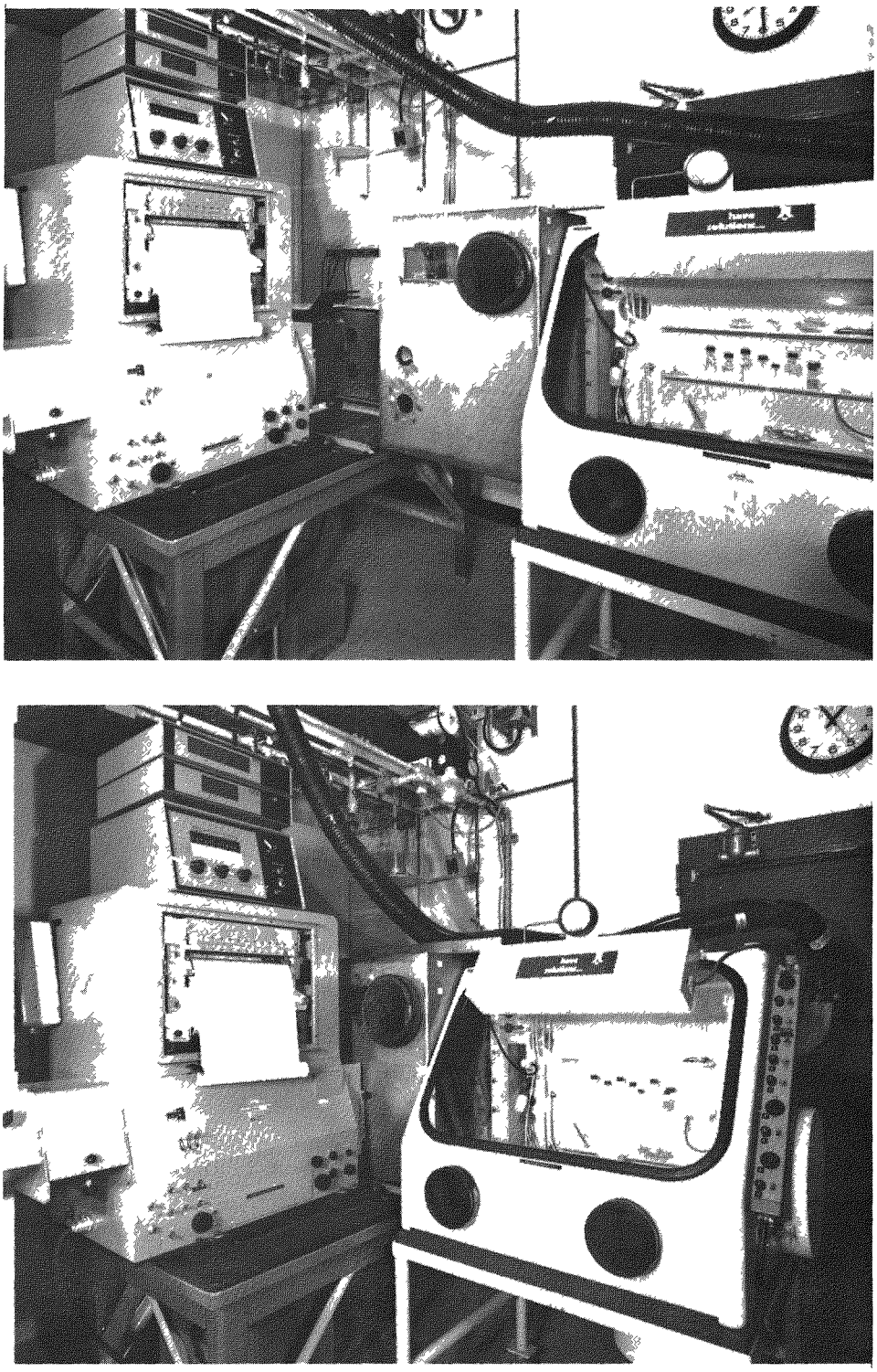

Figure 4. Spectrophotometer/modified gloved box assembly. Gloved box removed from spectrophotometer (upper photo) and installed in spectrophotometer (lower photo).

were recorded with a Norelco/Phillips Debye-Scherrer-type powder camera (57 mm dia.) using Kodirex 35 mm X-ray film.

d. Raman spectrophotometer. Raman spectra were recorded with a Ramanor Model HG 2S spectrophotometer (Instruments SA). This instrument employs a double monochromator with curved holographic gratings, photoelectric detection, and pulse counting electronics.

B. Electrodes and Cells

1. Conventional Working Electrodes

Microelectrodes used in this research include: (a) a hanging mercury drop electrode (HMDE)(PARC Model 9323), (b) an 18-gauge platinum wire, (c) an 18-gauge nickel wire, (d) a 22-gauge gold wire, and (e) a microelectrode made of reticulated vitreous carbon (RVC) (Fluorocarbon, Anaheim, CA). All of the metal wire electrodes (Engelhard Mining and Minerals, Newark, NJ) were made by sealing the wire into the end of a glass tube with epoxy, with the exception of platinum, which was sealed by fusing the end of the glass tube. The RVC microelectrode was constructed by sealing a small section of 10 pores per inch (ppi) RVC in the end of a glass tube with epoxy. Electrical contact was made by threading a copper wire through the RVC matrix and packing UCAR C-34 carbon cement (Union Carbide Corporation, New York, NY) around the contact, followed by curing at 110°C for 24 hr.

Larger conventional electrodes for bulk electrolyses of solutions were made from (a) sections of 10 ppi RVC, with electrical contact provided as described above, and (b) sections of 40-mesh platinum screen (Engelhard Mining and Minerals), which were soldered to copper

wires for electrical contact. These electrodes were partially submerged such that only the electrode material was in contact with the solution.

2. Optically Transparent Electrodes

a. Reticulated vitreous carbon optically transparent electrodes (RVC-OTE's). RVC-OTE's were constructed based on directions by Norvell and Mamantov[28] but with some modifications. Slices of various porosity grades (10-100 ppi) of RVC were sectioned with a diamond saw to various thicknesses from 0.62 mm for 100 ppi to 5 mm for 10 ppi. Electrical contact was made as described above. The RVC slices, with contacts in place, were then sandwiched between two quartz microscope slides. The edges were epoxied on three sides, with the RVC positioned a few mm from the open bottom of the cell. A small diameter plastic suction tube was epoxied into the top of the cell. Epoxy (W. J. Ruscoe Company, Akron, OH) was extended to coat the entire external portion of the RVC, which extended beyond the cell, as well as the electrical contact, to ensure mechanical stability. A completed RVC-OTE is shown in Figure 5.

b. Platinum screen OTE's. Sheets of 40-mesh platinum screen were trimmed into sections approximately 2.5 x 7.5 cm. Electrical contact was made by soldering a copper wire to the edge of the platinum screens. The electrodes were then sandwiched between two quartz plates as described above.

c. Gold screen OTE's. Trimmed sections of silver screen (40 mesh) were soldered to copper wire leads and were then electroplated with gold (Sel-Rex "Original Bright Gold" patented process, Sel-Rex Corp., Nutley, N.J.). These gold screens were then sandwiched between quartz plates as described above.

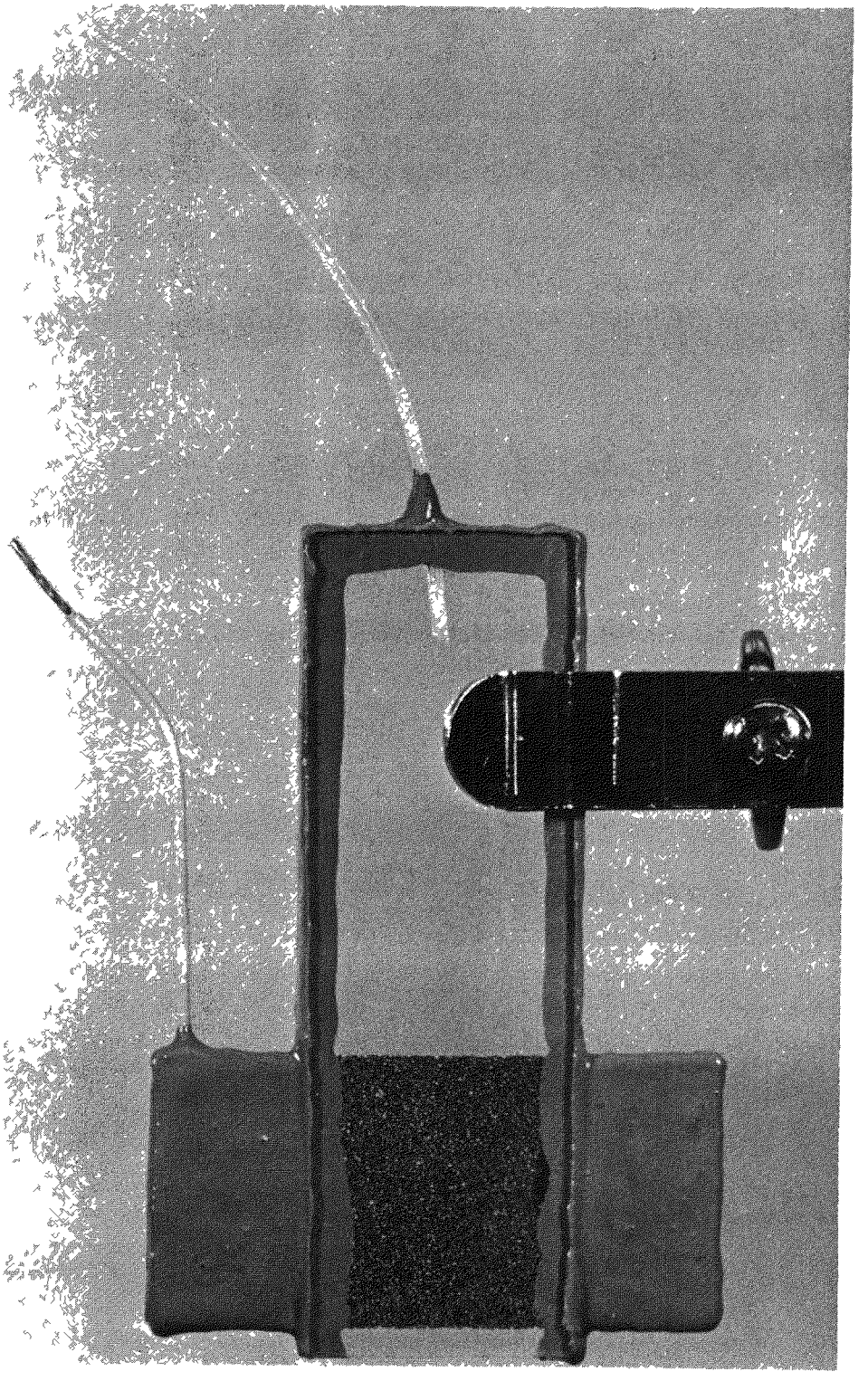

Figure 5. A reticulated vitreous carbon optically transparent electrode (RVC-OTE).

d. Porous metal foam OTE's (PMF-OTE's).[76] Porous metal foam (Astro Met Associates, Cincinnati, OH) was obtained as the copper and nickel material (series 280-5) in bulk sheets which were sectioned into electrodes between 3 and 5 mm thick. The PMF was electroplated with Pt, by the Oak Ridge Gaseous Diffusion Plant, using a proprietary process, or with Au, by ORNL using the Sel-Rex process, or was amalgamated.[27] Electrode coverage was checked by voltammetry.

e. Amalgam OTE's. Nickel PMF, silver screen, and gold screen OTE's were plated with mercury using a procedure described by Heineman et al.[27] after they were sealed between quartz plates. This plating procedure was followed by dipping the electrodes in clean, dry mercury. The excess mercury was dislodged by vigorous shaking of the OTE's.

3. Reference Electrodes

Saturated calomel reference electrodes (SCE's) (Altex-Beckman Instruments, Irvine, CA and Corning Scientific Instruments, Medfield, MA) of the semi-micro type with fiber junctions were used for all potential measurements.

4. Counter Electrodes

An 18-gauge platinum wire (2 cm in length), sealed in a glass tube, or a 40-mesh platinum screen (about 1 x 3 cm) was used as the counter electrode.

5. Teflon Cell Holder

A specially designed Teflon cell holder was constructed which positions a quartz cell (0.5-cm pathlength and 0.75 mL volume to

2.0-cm pathlength and 1 mL volume) in the sample beam of the spectrophotometer. The cell holder is fitted with a sliding lid in which three electrodes are mounted: a working electrode (RVC, PMF, or metal screen OTE), an SCE reference electrode, and a platinum wire counter electrode (see Figure 6). When the lid is lowered (see Figure 7), the three electrodes are immersed in the electroactive solution for spectroelectrochemical measurements.

C. Reagents

The common inorganic acids, bases, and salts used in this work were of standard ACS-certified reagent grade and were obtained from one or more of the following: Mallinckrodt Inc., Paris, KY; J. T. Baker Chemical Company, Fairlawn, NJ; Fisher Scientific Company, Pittsburgh, PA; or Allied Chemicals. Morristown, NJ.

Uranium salts and oxides (99.0% purity), cesium fluoride (99.9%), cesium carbonate (99.9%), potassium hydroxide (ultra-pure), potassium carbonate (ultra-pure), and deuterochloride and deuterated water were obtained from Thiokol-Ventron, Alfa Products, Danvers, MA.

Lanthanide salts (99.9%) were obtained from Thiokol-Ventron, Alfa Products and from Research Chemicals-NUCOR, Phoenix, AZ. Europium, samarium, and praseodymium chlorides were obtained in high purity (Cerac-pure) from Cerac, Inc., Milwaukee, WI.

Multimilligram quantities of the transuranium elements used in this work were obtained as the chloride salts from the High Flux Isotope Reactor/Transuranium Processing Plant (HFIR/TRU) complex of ORNL under the Department of Energy's program of transuranium element production and research.

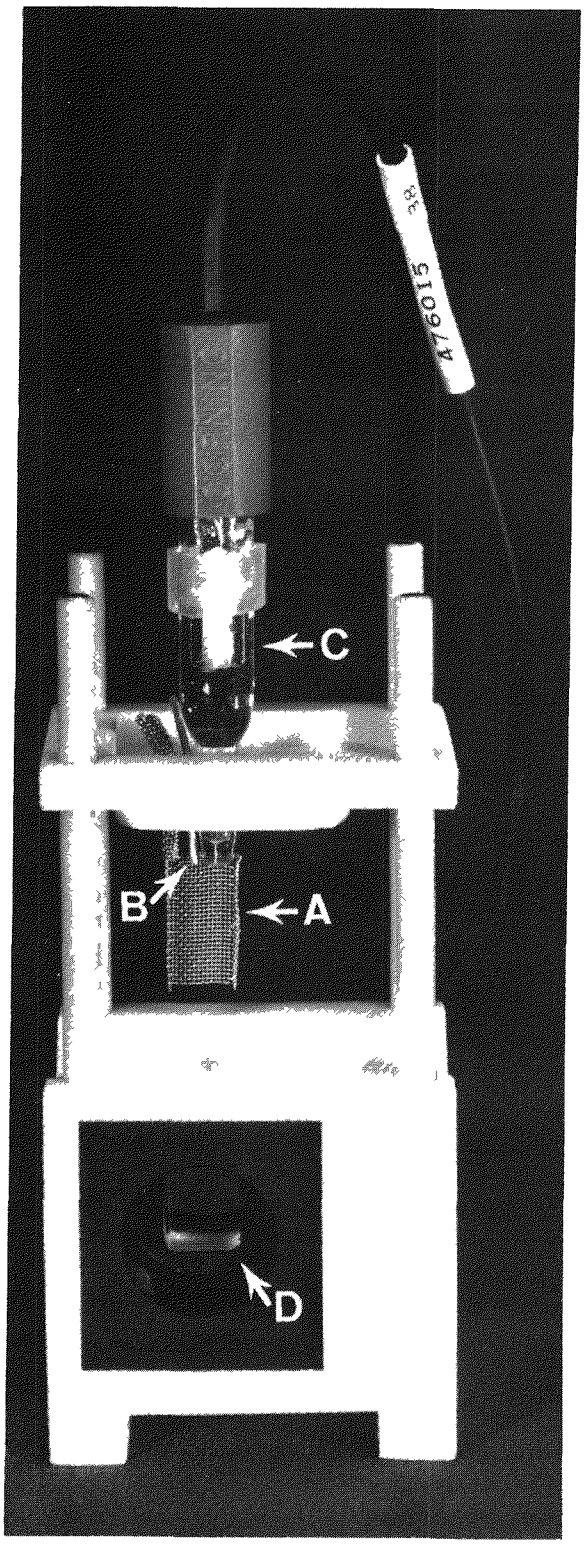

Figure 6. Teflon cell holder with lid in "up" position. Platinum screen working electrode (A), platinum counter electrode (B), SCE reference electrode (C), and optical path through quartz cell (D).

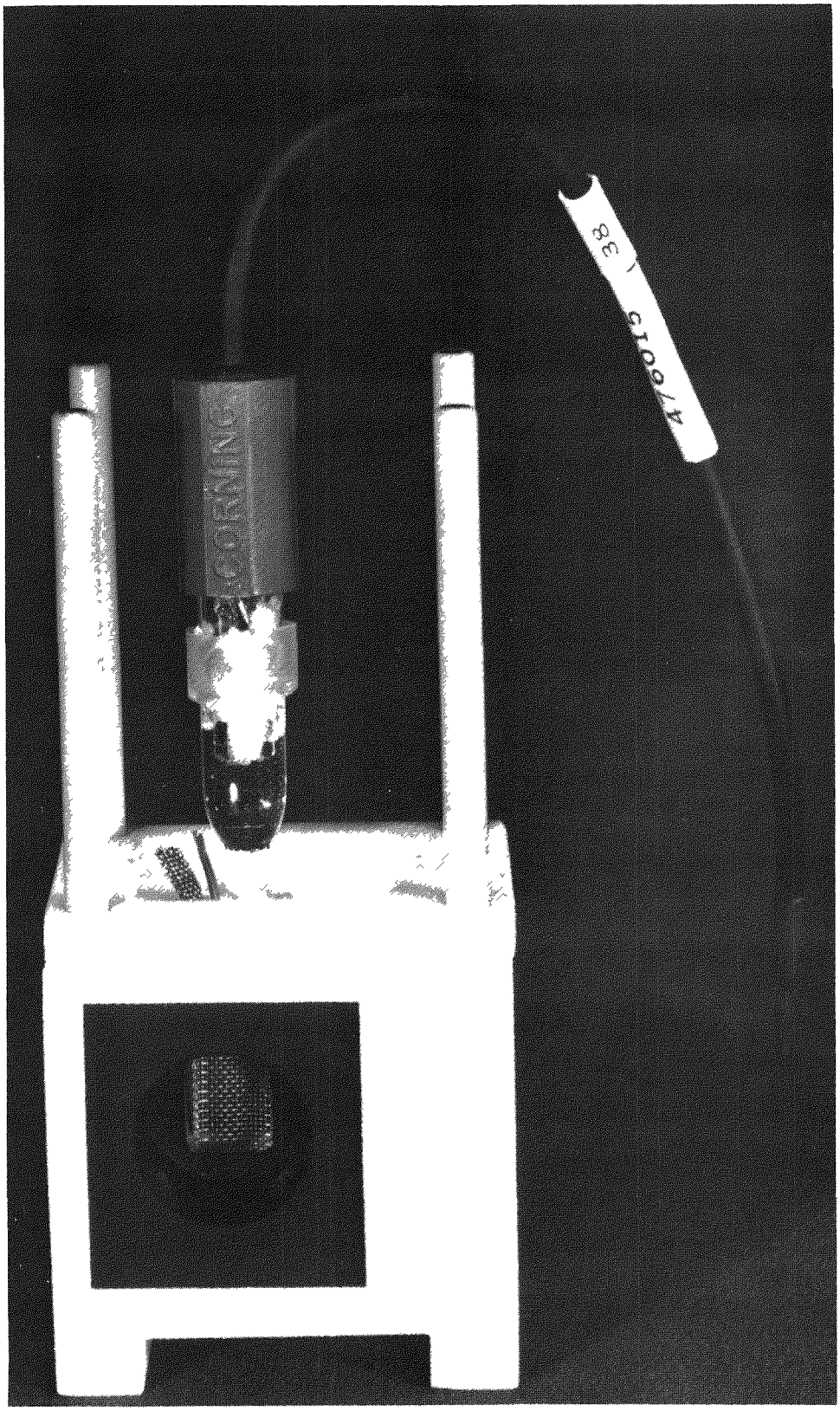

Figure 7. Teflon cell holder with lid in "down" position.

Stock solutions were prepared with distilled-deionized water unless otherwise indicated.

Nitrogen gas (99.9%) was obtained from Linde/Union Carbide Corporation, New York, NY. Ozone (10% by volume) was prepared by passing oxygen (99.5%) (Holston Oxygen Company, Knoxville, TN) through a high-voltage arc-discharge apparatus.

D. Procedures

1. General Procedures

Initial electrochemical investigations of redox couples involved the use of cyclic voltammetry for the determination of (a) the proper potential required to generate products, (b) the reversibility of the reaction, and (c) the existence of possible interfering side reactions. In most cases the same electrode material was used for spectroelectrochemistry as was used for voltammetry.

Initial spectral investigations of redox couples were performed by (a) recording the solution absorption spectrum of the electroactive species in its initial oxidation state, (b) oxidizing or reducing this species with chemical reagents to obtain the desired product oxidation state, and (c) recording the absorption spectrum of this product species. The spectra were used to determine the identity of the product and the proper monitoring wavelength(s), corresponding to absorption maxima, for constant wavelength spectroelectrochemistry.

After the initial experiments, or in lieu of these, absorbance vs time spectroelectrochemical experiments were performed. A potential step was applied to the redox system, in equilibrium, in order to

generate the product oxidation state. The generation of product was monitored by measuring the absorbance of the product (or reactant) at a constant wavelength as a function of time or by recording the entire spectrum as a function of time.

Spectropotentiostatic determinations of thermodynamic parameters (formal reduction potential and n-value) were then applied to amenable redox systems in the following manner. The absorbance of the product (or reactant) oxidation state was measured at various values of applied potential in equilibrium. These data were then used to construct a potential vs log ([Ox]/[Red]) (Nernstian) plot.

2. Lanthanide Elements

a. M(III)/M(II) redox couples. Solutions of from 10^{-1} to 10^{-3} M Sm(III), Eu(III), and Yb(III) were prepared separately by dissolving weighed quantities of the appropriate chloride salts in a 1 M KCl. The pH of the resultant solutions was measured with a glass electrode and was adjusted to pH 6 by the addition of KOH. Since the lanthanide chloride salts were hydrated with an unknown number (from 6 to 9) of water molecules, an exact weighing to have a known concentration was not possible; therefore, the concentrations of the lanthanide solutions were approximate. In experiments where accurately known concentrations of lanthanides were required, the solutions were submitted to ORNL Analytical Chemistry Division for quantitative analysis.

Cyclic voltammograms of the Sm(III), Eu(III), and Yb(III) chloride solutions in 1 M KCl at pH 6 were recorded with an HMDE. Cyclic

voltammograms of the Eu(III) solution were recorded using an RVC-OTE (100 ppi, 0.62 mm pathlength). The solutions were purged with nitrogen gas for 15 min prior to voltammetric analysis in order to remove dissolved oxygen.

The Eu(III)/Eu(II) redox couple was investigated using RVC and Pt screen OTE's via spectroelectrochemistry. About 5 mL of 5.0×10^{-3} M Eu(III) in 1 M KCl at pH 6 was placed in a teflon boat. An optical mask was placed on the OTE to prevent edge effects.[36] The OTE was then dipped in the bulk solution and, with the use of a hypodermic syringe, a portion of the bulk solution was drawn up into the OTE cell. This assembly was placed in the sample beam of the spectrophotometer. With the addition of an SCE and a Pt wire electrode placed in the bulk solution, below the OTE, spectroelectrochemistry was performed. Spectropotentiostatic experiments were performed to determine the formal reduction potential of the Eu(III)/Eu(II) redox couple and the n-value in the RVC-OTE. Equilibrium attainment was determined by monitoring the absorbance vs time curve of the system after each potential step.

Spectra were recorded as a function of time using the Cary Model 14-H and the silicon-vidicon rapid-scan spectrometers during the generation of Yb(II) by electrolysis of Yb(III) using a silver amalgam screen OTE. The reduction of Sm(III) was also studied with this OTE.

b. M(IV)/M(III) redox couples. Solutions of from 10^{-1} to 10^{-2} M in Ce(III), Pr(III), and Tb(III) were prepared separately by dissolving the chloride salts in (a) 5.5 M K_2CO_3, (b) 2 M $(NH_4)_2CO_3$,

(c) 2 M Na_2CO_3, and (d) 5 M Cs_2CO_3. In order to eliminate chloride ion, some solutions of the above-mentioned lanthanides were prepared by precipitating the lanthanide hydroxide with KOH followed by centrifugation and washing and dissolution of the wet hydroxide in the various carbonate solutions. The hydroxide ion concentration of all of the carbonate solutions, with the exception of the ammonium carbonate solution, was adjusted to about 1 M by the addition of KOH.

Initial spectra were recorded in 1-cm quartz cuvets with the appropriate carbonate solution placed in the reference cell. For bulk electrolysis approximately 20 mL of the lanthanide carbonate solution was placed in a small beaker, and a large conventional RVC or Pt screen working, the reference, and the counter electrodes were immersed. Stirring of the solution was provided by the bubbling of nitrogen or by electrochemically generated oxygen. The solutions were electrolyzed for periods of time ranging from 10 min to 3 hr before absorption spectra were recorded. For highly absorbing solutions, quartz spacers were used to reduce the optical pathlength to 3 mm or to 1 mm.

The spectropotentiostatic method was applied to the determinations of the formal reduction potential and n-value of the Ce(IV)/Ce(III) redox couple in 5.5 M K_2CO_3 using an RVC-OTE (100 ppi, 1 mm pathlength).

A solid oxidation product, formed at the RVC electrode during electrolysis of the Tb(III) carbonate solution (5.5 M K_2CO_3, 1 M OH^- ion), was collected, rinsed with alcohol, dried, and investigated by X-ray powder diffraction and solid state reflectance and laser Raman

spectroscopies. The sample was also submitted to ORNL Analytical Chemistry Division for thermogravimetric/mass spectral and X-ray fluorescence analyses.

Chemical oxidation of the Pr(III) and Tb(III) carbonate solutions was accomplished by bubbling ozone through the solutions for a few hours to ensure sufficient oxidation of the lanthanide species.

3. Actinide Elements

a. Uranium. Solutions of from 10^{-1} to 10^{-2} M U(IV) and U(VI) were made separately by dissolving UCl_4 and UO_2Cl_2 in 1 M KCl. The pH of these solutions was adjusted to desired values by the addition of HCl or KOH. Solutions of from 0.1 to 0.5 M U(VI) were prepared in 1 M KCl in 99.8% D_2O by first dissolving a weighed quantity of UO_3 in DCl followed by evaporation to near dryness and subsequent dissolution of the salt in the KCl/D_2O solution. The pH (pD) was adjusted by addition of DCl.

Cyclic voltammograms of the uranium solutions at various pH values were recorded at an HMDE and a Pt wire microelectrode.

Initial absorption spectra of the U(IV) and U(VI) solutions were recorded prior to chemical reduction of the uranium species by zinc amalgam. The U(VI)/KCl/D_2O solution was treated with Eu(II) to reduce the U(VI) species. Spectra of the reduced species were then recorded.

Absorbance vs time spectroelectrochemical experiments were performed using the U(VI) solutions at various pH values. Absorbance vs time curves were recorded during the electrochemical reduction of U(IV) to U(III) in 1 M KCl (pH 0) in a silver screen amalgam OTE. The

complete spectra of these species were also recorded as a function of time during the electrolysis.

An RVC-OTE was used while absorbance vs time curves and complete spectra as a function of time were recorded during the electrochemical reduction of U(VI) at various pH values in 1 M KCl.

b. Neptunium. Multimilligram quantities of neptunium-237 were obtained as the oxide, NpO_2, which was dissolved in nitric aid and heated to dryness. The resultant salt was fumed to dryness in perchloric acid, thus oxidizing the Np to the hexavalent state. The $NpO_2(ClO_4)_2$ solid was dissolved in 1 M perchloric acid, resulting in a stock solution which was about 2 M Np(VI). Aliquots of this solution were diluted separately with 1 M $HClO_4$, 2 M Na_2CO_3, and 5.5 M K_2CO_3 to prepare solutions between 10^{-2} and 10^{-3} M Np(VI).

A stock solution of oxidation-state pure Np(V) was prepared[77] by mixing equal quantities of Np(IV) and Np(VI) in perchloric acid. The Np(IV) was prepared by peroxide reduction of a mixture of Np(V) and Np(IV), obtained by direct dissolution of the mixed oxide in nitric acid. Excess peroxide was eliminated by heating.

Initial spectra of the Np solutions were recorded prior to electrochemical studies. Cyclic voltammograms of the Np solutions were recorded with the Pt and RVC microelectrodes using a 1-mL aliquot of solution in a small beaker or in a quartz cell in the teflon cell holder.

The absorption spectra of Np(VI) and Np(V) were recorded in an RVC-OTE as a function of time during the electrolytic reduction of Np(VI) in 1 M $HClO_4$. Absorbance vs time curves were also

recorded, as well as data for the spectropotentiostatic determinations of $E^{o'}$ and n for the Np(VI)/Np(V) redox couple in 1 M $HClO_4$.

Np(VI) in 2 M Na_2CO_3 was first reduced to Np(V) and the spectrum was recorded. The Np(VI) stock solution was then adjusted to pH 13 by the addition of hydroxide ion, and the solution was investigated by cyclic voltammetry and by recording complete spectra as a function of time during electrolysis at a large-surface platinum screen electrode. An $E^{o'}$ value for the Np(VII)/Np(VI) redox couple was derived from the voltammogram. The Raman spectra of both Np(VI) and electrogenerated Np(VII) in 2 M Na_2CO_3 were recorded by removing the samples from the gloved box in sealed capillaries by a technique described elsewhere.[78]

c. Americium. Multimilligram quantities of americium-243 were purified at TRU/ORNL by chromatographic separations described elsewhere.[79] The americium was received as an air-dried chloride salt, $AmCl_3.nH_2O$, which resulted from evaporation of the eluant from the final ion-exchange column. This chloride salt was dissolved directly in various carbonate solutions [2 M $(NH_4)_2CO_3$, 2 M Na_2CO_3, 5.5 M K_2CO_3, and 5 M Cs_2CO_3]. In order to eliminate chloride ion, some solutions were prepared by dissolving the $AmCl_3.nH_2O$ in water and by precipitating $Am(OH)_3$ by the addition of hydroxide ion. After centrifugation and washing with dilute base and then with water, the $Am(OH)_3$ was dissolved in the various carbonate solutions. The hydroxide concentrations of the carbonate solutions containing Am(III) were measured with a pH glass electrode which was calibrated with solutions of known NaOH concentration.

Chemical oxidation of the Am(III) carbonate solutions was accomplished by using peroxydisulfate-silver(I) oxide.[53] Spectra of the initial solutions and the oxidized solutions were recorded. Cyclic voltammograms of the Am(III) carbonate solutions were recorded at various pH values.

Aliquots of from 0.75 to 1.5 mL of the Am(III) carbonate solutions, which were from 1.2×10^{-2} to 4.0×10^{-3} M Am(III), were placed in quartz cells in the teflon cell holder. Initial spectra were recorded and then aliquots of the solutions were removed for alpha counting. The electrodes (RVC or Pt OTE's) were immersed in the solutions, and an initial potential applied to the cell. The potential was made more positive until a change in the spectrum was noted or until visual observation confirmed an oxidation reaction. Depending on the pH of the solution and the type of OTE used, some spectra were recorded only after a potential was no longer imposed or after the electrodes were completely removed from the solution.

The precipitate formed by the electrochemical oxidation of Am(III) in potassium carbonate solution was collected, washed, and centrifuged. The solid was then dissolved in 1 M perchloric acid, and the solution spectrum was recorded. The solid was also analyzed by X-ray powder diffraction.

Additional characterization of the oxidized Am species in carbonate solutions included spectrophotometric and potentiometric titrations with $K_4Fe(CN)_6$ in 2 M Na_2CO_3.

Solid anhydrous AmF_4 and Cs_3AmF_7 were prepared and dissolved in concentrated HF solution saturated with CsF. Spectra were recorded both prior to and following bulk solution electrolysis.

d. Curium. Multimilligram quantities of curium-248 were purified at TRU/ORNL as described elsewhere.[79] Received as the solid $CmCl_3.nH_2O$ salt, it was dissolved in water, and the curium was precipitated by the addition of KOH. The resulting precipitate was washed with dilute KOH and was centrifuged and dissolved separately in 5.5 M K_2CO_3 and in 2 M Cs_2CO_3.

Initial spectra of Cm(III) in the carbonate media were recorded prior to electrochemical oxidation with large-surface RVC and Pt electrodes. The spectra of the resultant solutions were also recorded.

4. Data Treatment

Data obtained from the spectropotentiostatic experiments for the determinations of $E^{o'}$ and n for redox couples were analyzed by a linear least squares program using a Tektronix 4051 microcomputer. The program is described in the Tektronix "PLOT 50" 4050A10 Software Package, Volume 4, Program 9. This program, using the least squares method, fits a user-defined function (the Nernst equation), where optimal parameter values are found by minimizing the sum of the squares of the differences between the observed and calculated values.

The Nernstian plot and attendant parameters were displayed on the Tektronix 4051 CRT display and printed by a Tektronix 4631 Hard Copy Unit. Drawings were then made from the hard copy output.

Error limits reported in this work are based on one standard deviation and do not include estimates of systematic errors. The errors associated with the determination of formal reduction potentials by voltammetric measurements depend upon (a) the accuracy and stability of the reference electrode, (b) the ambient temperature variation in the laboratory, (c) the proper calibration of the potentiostat/recorder, and (d) the reproducibility of the voltammetric response of the redox system.

The error limits reported for the spectropotentiostatic determinations of the formal reduction potentials reflect a conservative estimate of the accuracy of the determination and not necesarily the full extent of the precision indicated by the least squares program.

CHAPTER III

RESULTS AND DISCUSSION

A. Lanthanide Elements

1. M(III)/M(II) Redox Couples

The only divalent lanthanide ions sufficiently stable to exist in aqueous solution are those of samarium, europium, and ytterbium, and therefore, these M(III)/M(II) redox couples are amenable to spectroelectrochemical investigation in aqueous solution. The pH range in which these redox couples can be studied is limited. Above pH 7 the hydrolysis of the M(III) ions proceeds and precipitation of the ions occurs. At lower pH values interference from hydrogen gas evolution, at potentials required to generate the M(II) ions, is substantial. Thus pH 6 was selected as the optimum value for investigation of these redox couples.[80]

a. Voltammetry. Initial electrochemical investigations of the M(III)/M(II) redox couples were performed by recording cyclic voltammograms of the systems at an HMDE. Cyclic voltammetry is an effective technique for initial electrochemical study of new systems. A great deal of information about fairly complicated systems can be derived in a single experiment.[81] The HMDE was selected because of the cathodic potentials required to generate lanthanide M(II) oxidation states. The HMDE provides a cathodic range of from about 0 to -1.8 V in 1 M KCl at pH 6. [All potential measurements in this

document are reported versus the NHE unless otherwise indicated: SCE = 0.2415 V vs NHE.] At potentials more negative than -1.8 V, the evolution of hydrogen gas and/or the reduction of potassium ions occurs at the electrode surface.

Cyclic voltammograms of the Eu(III)/Eu(II), Yb(III)/Yb(II), and Sm(III)/Sm(II) redox couples in 1 M KCl at pH 6 are displayed in Figure 8. The lack of complete electrochemical reversibility of the Eu(III)/Eu(II) redox couple was evidenced by the large difference between the anodic and cathodic peak potentials. In addition, the recording of consecutive cyclic potential sweeps also indicated the lack of complete reversibility in that the peak potential values changed with each scan. The peak separation grew larger with each potential scan. The Eu redox couple is not completely irreversible, however, because the anodic peak current is approximately equal to the cathodic peak current. This behavior of the Eu redox system has been noted by others.[82]

The formal reduction potential, $E^{o'}$, obtained from the cyclic voltammogram was -0.34 $\pm$ 0.01 V. This approximate value was determined by calculating the mid-point between the anodic and cathodic peak potentials.[13,83] The cyclic voltammogram of the Eu redox couple in an RVC-OTE in 1 M KCl at pH 6 is shown in Figure 9. The sweep rate used was quite slow (5 mV/s) and was necessary because of the relatively high internal resistance of the RVC electrode. Essentially the same behavior of the Eu couple was observed at the RVC electrode as was observed at the HMDE. The difference between the two was, however, a shift in the $E^{o'}$ value; at the RVC electrode, it was -0.43 $\pm$ 0.01 V. The lack of total reversibility of the Eu(III)/Eu(II)

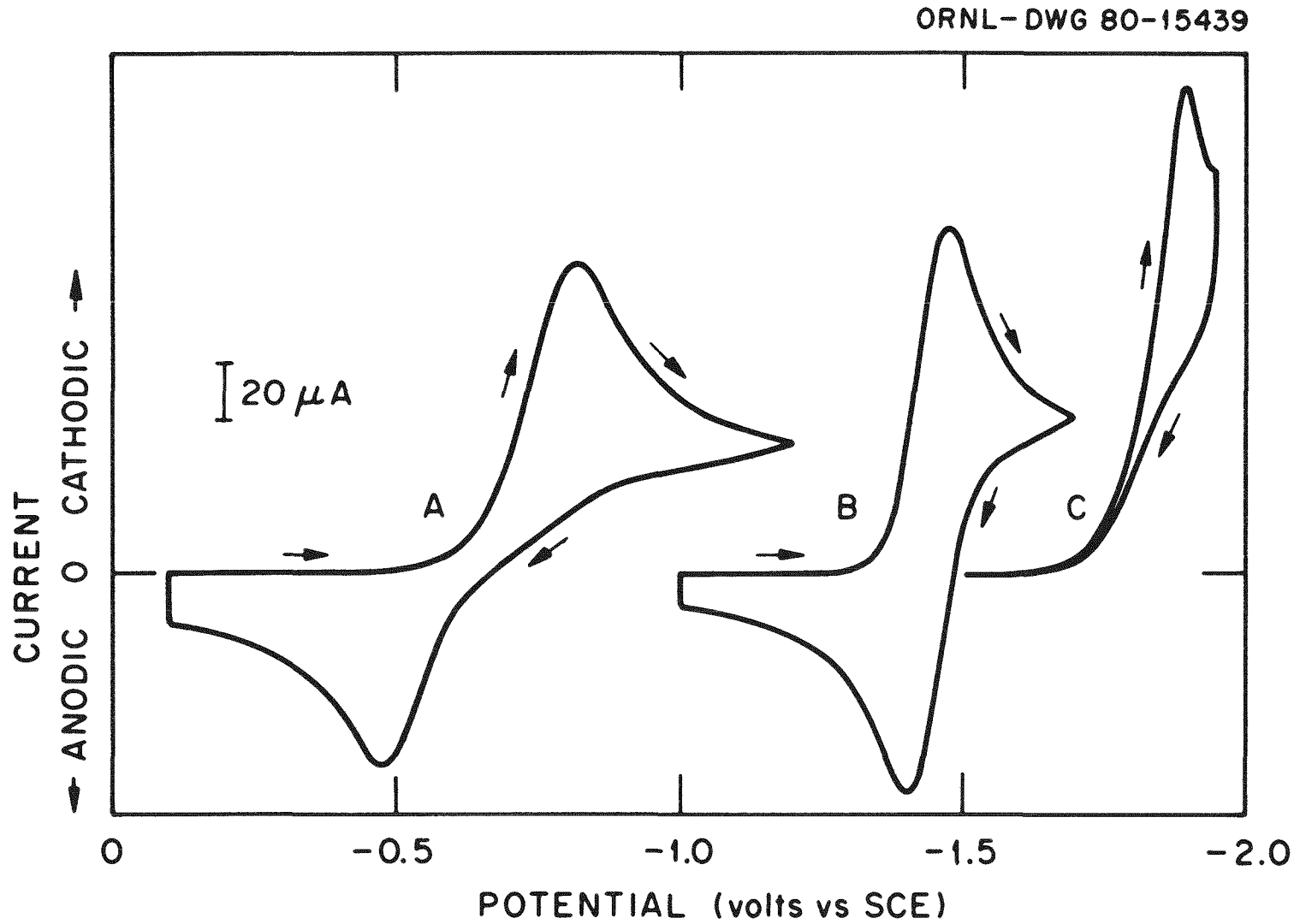

Figure 8. Cyclic voltammograms of M(III) species of Eu (A) Yb (B), and Sm (C) in 1 M KCl. pH 6, HMDE, sweep rate: 200 mV/s, [M(III)] = 1.0×10^{-2} M.

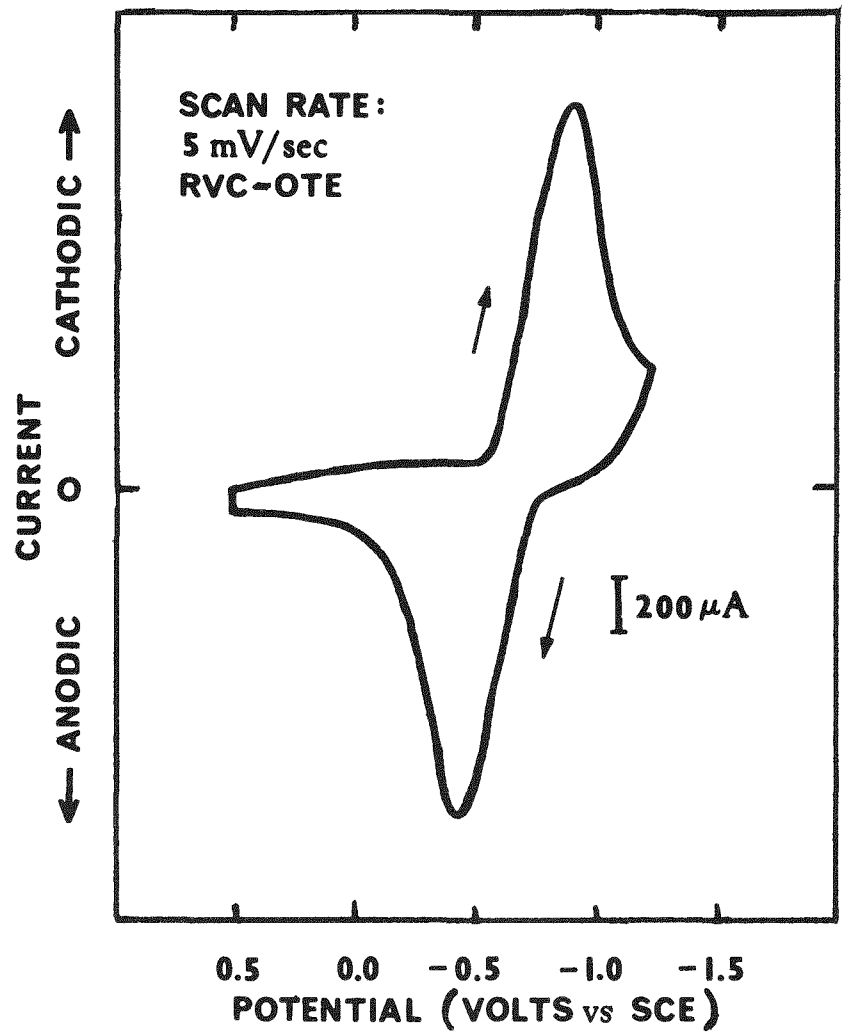

Figure 9. Cyclic voltammogram of Eu(III) in 1 M KCl in an RVC-OTE. pH 6, RVC-OTE: 100 ppi, 0.62 mm path length, [Eu(III)] = 1.0×10^{-4} M.

redox couple did not preclude the spectroelectrochemical investigation of this couple.

The cyclic voltammogram of the Yb(III)/Yb(II) redox couple in 1 M KCl at pH 6 (see Figure 8, page 52) displayed electrochemical reversibility in that the peak potential separation for the anodic and cathodic peaks was 65 mV, much less than that for the Eu case. In addition, the anodic peak current for the Yb system was equal to the cathodic peak current. Consecutive potential scans showed a reduction in peak current but complete reproducibility in the peak potential values. The $E^{o'}$ value determined for this couple in the stated medium, derived from the cyclic voltammogram, was -1.18 $\pm$ 0.01 V.

Complete cyclic voltammograms of the Yb system at the RVC electrode were not possible due to the limited cathodic range of RVC. The RVC electrode exhibited a potential range of from +1.4 to -1.0 V in 1 M KCl at pH 6. Cyclic voltammograms of the Yb system at a nickel amalgam wire microelectrode were possible, but the voltammograms exhibited a shape indicative of a less-than-reversible redox couple. This was shown by the fact that the anodic and cathodic peak potentials were greatly separated. The shape of the voltammogram was similar to that of the Eu system at the HMDE.

The cyclic voltammogram of the Sm(III)/Sm(II) redox couple in 1 M KCl at pH 6 is shown in Figure 8, page 52. The cathodic peak is clearly visible, indicating the reduction of Sm(III), but the anodic peak is

absent, which indicates an irreversible redox couple at the electrode. The reasons for this irreversibility are as follows. The reduction of the Sm(III) species occurs at a potential at which hydrogen gas is evolved at the HMDE. The H_2 gas probably carries the reduced species away from the electrode surface; thus, Sm(II) may no longer be present at the electrode to be oxidized during the anodic sweep. Also the Sm(II) species reacts rather quickly with the solvent to form H_2 and Sm(III), and therefore, no Sm(II) is present at the electrode to be oxidized and give rise to an anodic peak. The $E^{o'}$ value for the Sm(III)/Sm(II) redox couple in the stated medium was estimated from the cyclic voltammogram to be -1.50 ± 0.01 V. This value was calculated by using the boundary condition equations for a totally irreversible wave, as described by Bard and Faulkner.[81]

The $E^{o'}$ values determined in these three cases are in good agreement with the values of the standard reduction potentials reported by Nugent et al.[69] of -0.35 V for Eu(III)/Eu(II), -1.15 V for Yb(III)/Yb(II), and -1.55 V for Sm(III)/Sm(II).

b. Spectrophotometry. The solution absorption spectra of the tri- and divalent ions of europium, ytterbium, and samarium are displayed in Figures 10, 11, and 12, respectively. These spectra are adapted from those of Carnall[84] and are of the species in 1 M $HClO_4$. The spectra of the lanthanide species in 1 M KCl are essentially identical to those in Figures 10, 11, and 12.

The divalent species were prepared chemically by zinc amalgam reduction of the trivalent species in deoxygenated solvent, with the

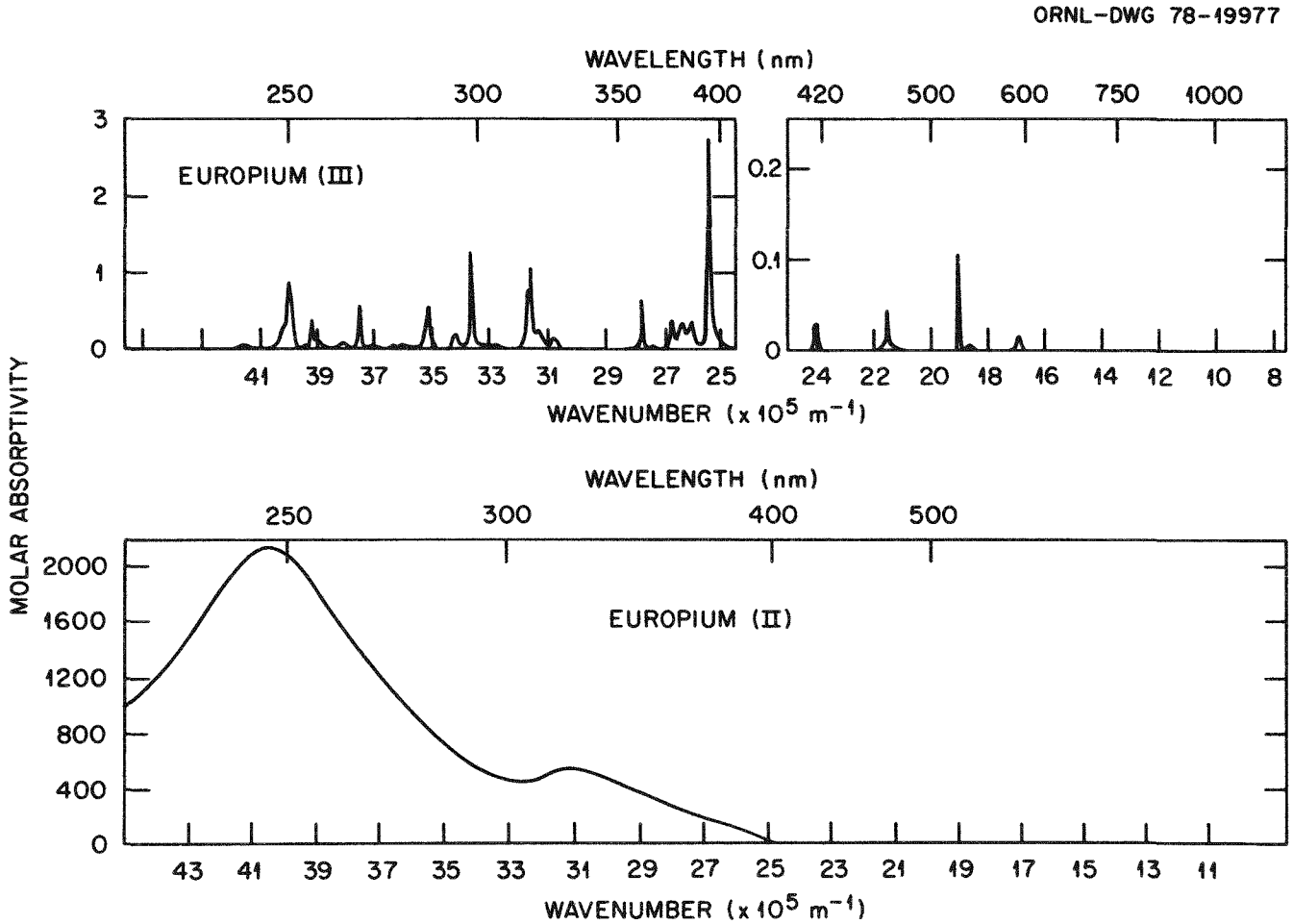

Figure 10. Solution absorption spectra of Eu(III) and Eu(II) in 1 M $HClO_4$.

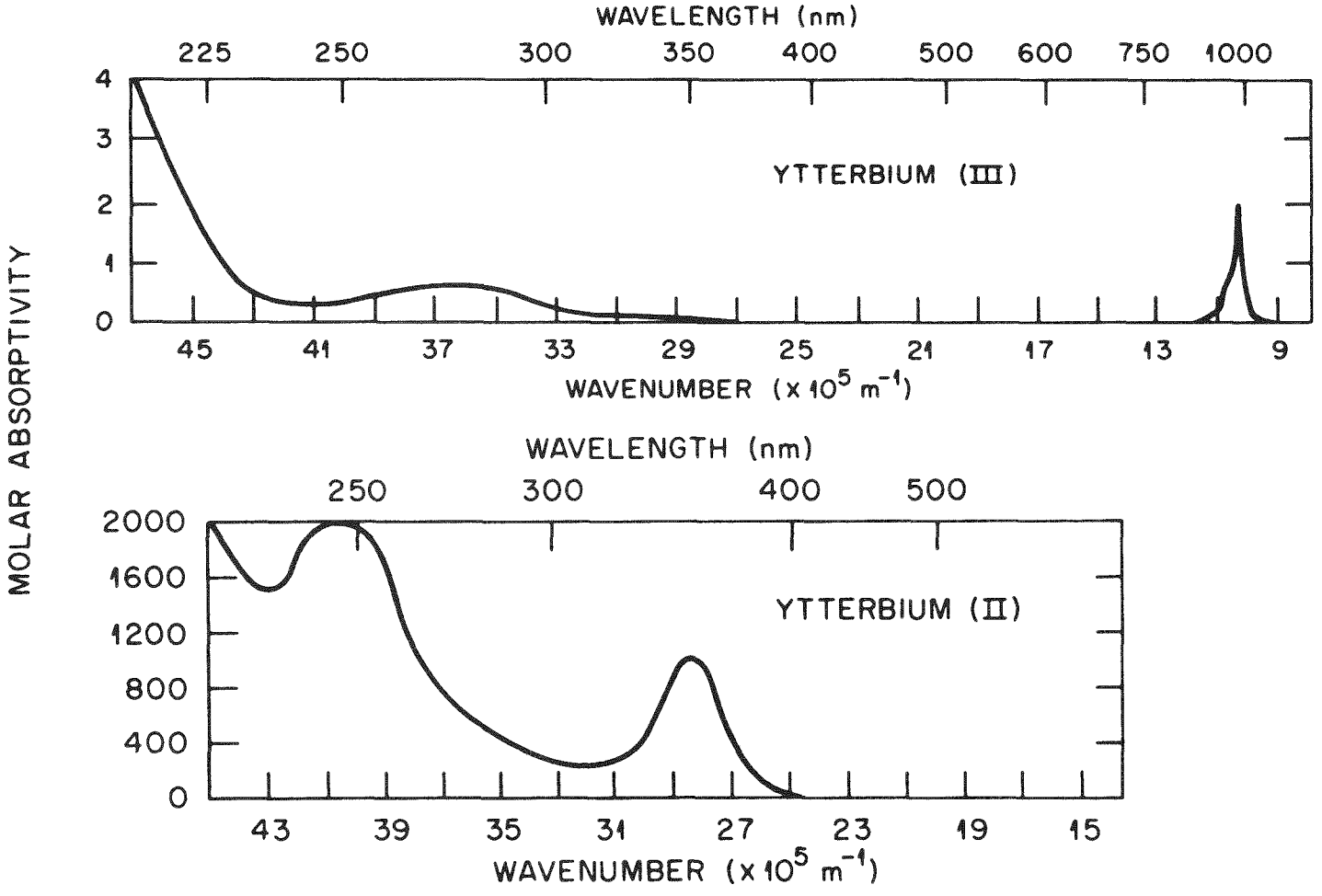

Figure 11. Solution absorption spectra of Yb(III) and Yb(II) in 1 M $HClO_4$.

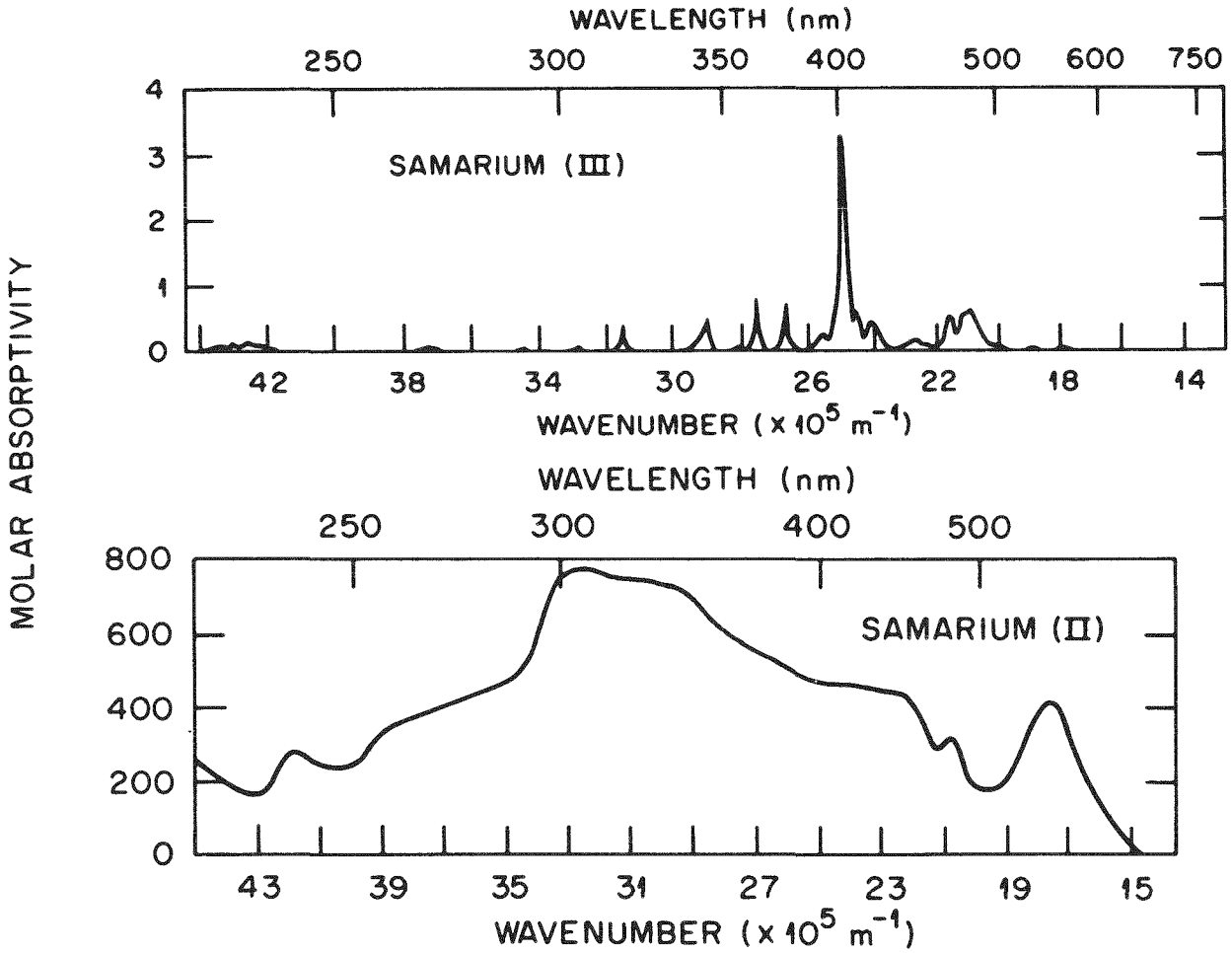

Figure 12. Solution absorption spectra of Sm(III) and Sm(II) in 1 M $HClO_4$.

exception of Sm(II), which was generated by dissolution of samarium metal in dilute HCl. It was not possible to record a complete spectrum of the blood-red solution of Sm(II) due to the interference from hydrogen gas evolution.

c. Spectroelectrochemistry. The Eu(III)/Eu(II) redox couple in 1 M KCl at pH 6 was studied using Pt screen and RVC optically transparent electrodes. Although the Pt screen OTE allowed for electrochemical generation and spectral identification of Eu(II), it did not provide a sufficient cathodic potential range for complete spectropotentiostatic study of this couple. The RVC-OTE was therefore used to perform this study.

The absorbance vs time curve for a selected potential-step electrolysis for the reduction of Eu(III) in an RVC-OTE is shown in Figure 13. The wavelength monitored was 320 nm, corresponding to an absorption maximum in the Eu(II) spectrum. The absorbance vs time curve is quite similar in shape to a current vs time curve for the reaction. Both absorbance and current are direct measurements of the quantity of electroactive species reacted. Equilibrium is attained, throughout the total path length of the OTE illuminated by the sample beam, when there is no change in the absorbance with time (at 30 min for the curve in Figure 13). Such absorbance vs time curves were recorded for all potential-step electrolyses to ensure the attainment of equilibrium prior to recording the complete spectrum.

Absorption spectra of Eu(III) and Eu(II) at various values of applied potential, in equilibrium, are shown in Figure 14. Due to the large difference between the molar absorptivities of the Eu(III) and

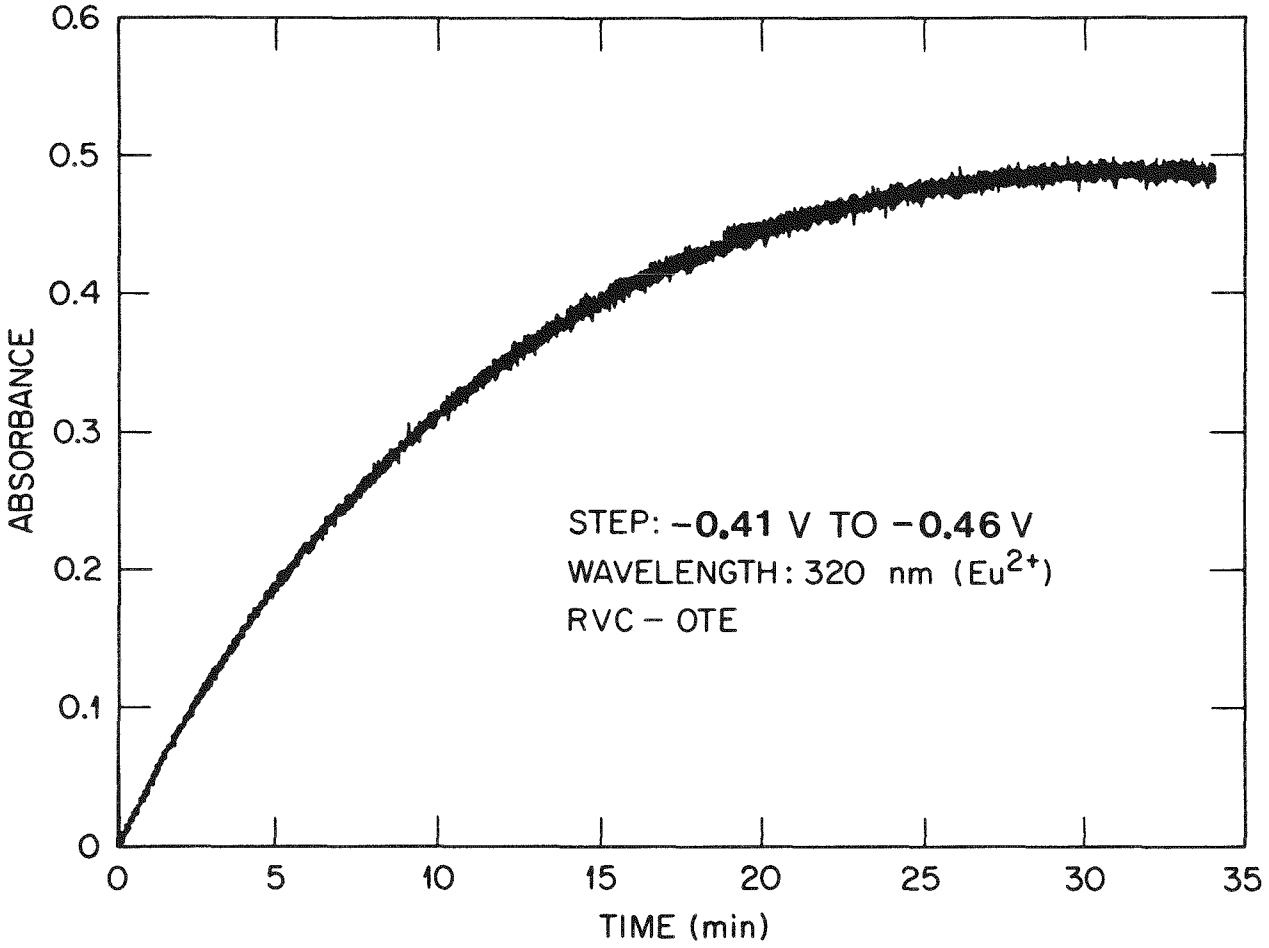

Figure 13. Absorbance vs time curve for the potential-step electrolysis of Eu(III) in an RVC-OTE. RVC: 100 ppi, 1 mm path length, [Eu(III)] = 1.0×10^{-2} M, potential step: -0.41 V to -0.46 V.

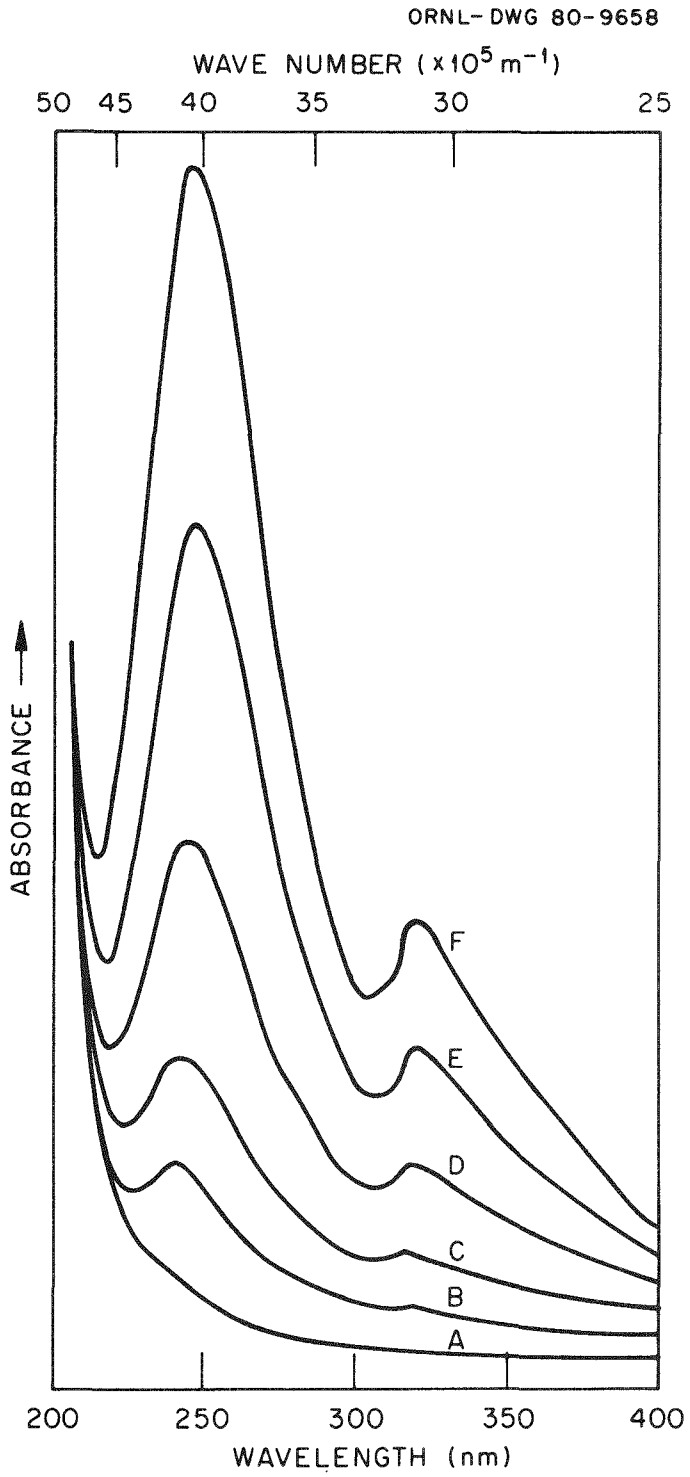

Figure 14. Solution absorption spectra of Eu(III) and Eu(II) at various values of applied potential in an RVC-OTE. 0.242 V (A), -0.309 V (B), -0.334 V (C), -0.359 V (D), -0.384 V (E), and -0.409 V (F). RVC-OTE: 100 ppi, 0.62 mm pathlength, [Eu(III)] = 5.0 x 10^{-3} M in 1 M KCl at pH 6.

Eu(II) species (see Figure 12, page 56), it was necessary to select an initial concentration of Eu(III) which was too low to observe any absorption peaks due to Eu(III) (spectrum A, Figure 14). As more negative potentials were applied to the RVC electrode, absorbance peaks due to Eu(II) grew in (spectra B through F). The potential range selected for the experiment was based on the value of $E^{o'}$ obtained from the cyclic voltammogram of the Eu(III)/Eu(II) redox couple. The potentials were chosen to provide both fully reduced and fully oxidized conditions so that sufficient data were collected to generate an accurate Nernstian plot.[13]

A tabulation of the data for the spectropotentiostatic determination of thermodynamic parameters ($E^{o'}$ and n) for the Eu(III)/Eu(II) redox couple in 1 M KCl is given in Table VI. The data were derived from the absorbance of Eu(II), at 320 nm, in equilibrium, at the various values of applied potential. The notation used in Table VI is defined in Chapter I, page 7. The Nernstian plot, obtained by plotting the applied potential versus the log of absorbance ratio, is shown in Figure 15. The data points fall on a straight line, as required by the Nernst equation. The slope of the line yields an n-value of 1.007 (corresponding to a one-electron reduction), and the y-intercept yields an $E^{o'}$ value of -0.391 $\pm$ 0.005 V. This value is in reasonable agreement with the values reported by Morss and Haug[85] (-0.35 $\pm$ 0.03 V) and Biedermann and Silber[86] (-0.379 $\pm$ 0.001 V).

The spectroelectrochemical behavior of the Yb(III)/Yb(II) redox couple was studied in 1 M KCl at pH 6 using a silver amalgam screen

TABLE VI

DATA FOR SPECTROPOTENTIOSTATIC DETERMINATION OF THERMODYNAMIC PARAMETERS FOR THE Eu(III)/Eu(II) REDOX COUPLE

Potential (volts vs SCE)	Absorbance A_2	A_2-A_1	A_3-A_2	A_2-A_1/A_3-A_2	$\log(A_2-A_1/A_3-A_2)$
0	$(0.098)=A_1$	-	-	-	-
-0.550	0.150	0.052	1.217	0.043	-1.369
-0.575	0.215	0.117	1.152	0.102	-0.993
-0.600	0.388	0.290	0.979	0.296	-0.528
-0.625	0.650	0.552	0.717	0.770	-0.114
-0.650	0.950	0.852	0.417	2.043	0.310
-0.675	1.165	1.067	0.202	5.282	0.723
-0.700	1.278	1.180	0.089	13.26	1.123
-1.000	$(1.367)=A_3$	-	-	-	-

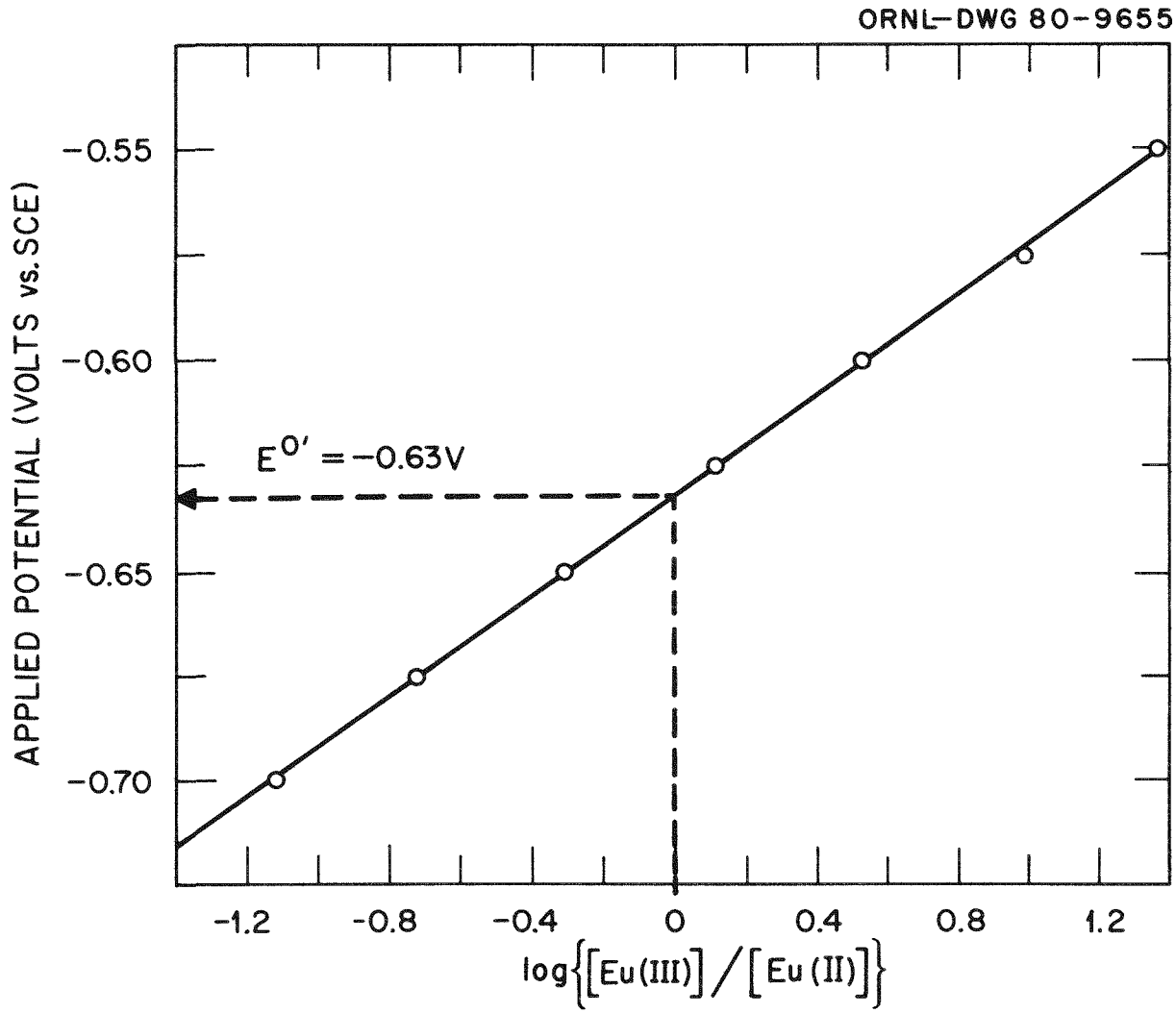

Figure 15. Nernstian plot for the Eu(III)/Eu(II) redox couple in 1 M KCl. pH 6.

OTE. It was necessary to use this electrode because the reduction potential of the Yb couple exceeds the cathodic potential range of both the Pt screen and RVC OTE's. A Tektronix silicon-vidicon based rapid-scan spectrophotometer was used to monitor the silver amalgam OTE during the potential-step electrolysis of Yb(III). The absorbance vs time curve for this reaction, monitored at 353 nm, is reproduced in Figure 16. Note that equilibrium occurs in less than three minutes. This time to equilibrium was much shorter than that for the Eu couple (see Figure 13, page 59). The reasons for this were: (a) the concentration of Yb(III) was a factor of ten less than that of Eu(III), (b) the path length of the Ag amalgam screen OTE was 0.62 mm vs the 1 mm path length of the RVC-OTE, (c) the silver amalgam screen has a lower electrical resistance than that of RVC, and (d) the potential step applied to the Yb system (-0.76 to -1.56 V) was much greater than the small steps (0.05 V) used to study the Eu system. The rather large potential-step was an effort to generate quickly the Yb(II) before interference from gross hydrogen gas evolution was encountered. The cathodic potential range of the silver amalgam screen OTE did not allow for the complete spectropotentiostatic study of this redox couple. Due to the requirement that equilibrium be attained at more negative potentials than that for the evolution of hydrogen gas at the Ag amalgam OTE (corresponding to a potential where Yb(III) is completely reduced), no measurement of the formal reduction potential via spectroelectrochemistry was performed.

The absorption spectra of Yb(III) and Yb(II) as a function of time during the potential-step electrolysis of Yb(III) are shown in

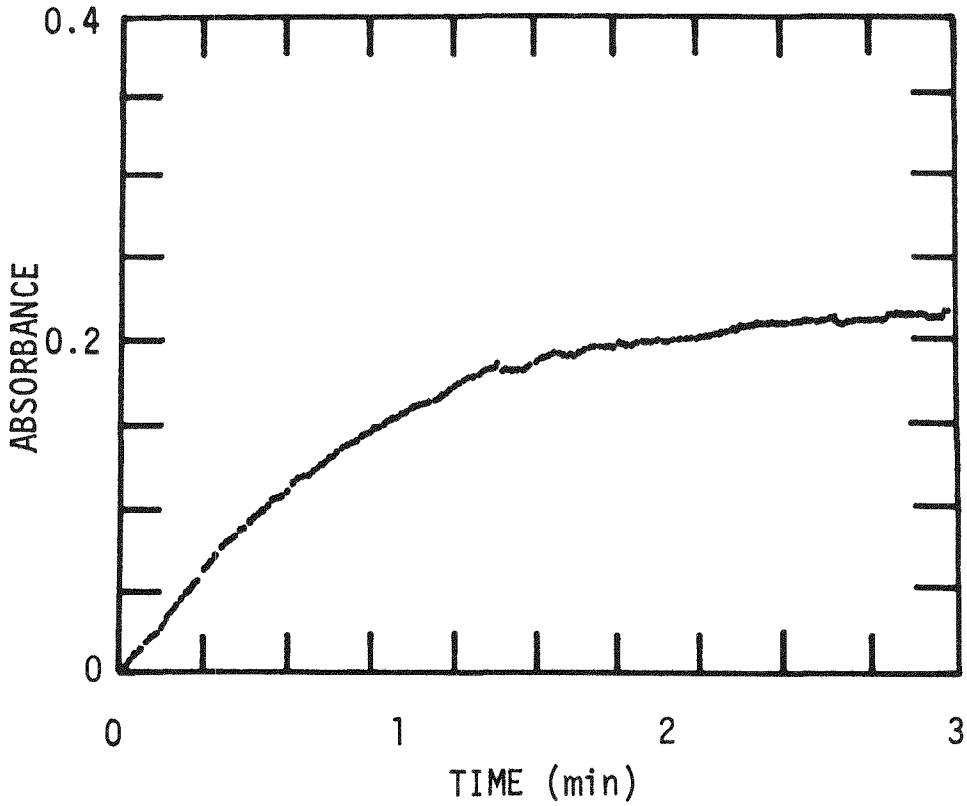

Figure 16. Absorbance vs time curve for the potential-step electrolysis of Yb(III) using a silver amalgam screen OTE. Ag(Hg)-OTE: 0.62 mm path length, wavelength constant: 353 nm, potential step: -0.76 V to -1.56 V.

Figure 17. The characteristic Yb(II) absorption peak, at about 353 nm, was observed to increase with the time of electrolysis. The other major peak in the Yb(II) absorption spectrum, at 240 nm, is not clearly defined, in Figure 17, due to the insufficient light output of the UV source lamp used with the rapid-scan spectrophotometer. Figures 16 and 17 are hand-drawn copies of the photographs taken of the CRT output of the rapid-scan spectrophotometer.

Additional experiments with more concentrated solutions of Yb(III) in the stated medium were conducted using the Cary Model 14-H spectrophotometer. The initial colorless solution of Yb(III) was reduced in a silver amalgam screen OTE, and a lemon-yellow color was observed in the cell. The spectrum of this solution verified the presence of Yb(II).

Spectroelectrochemical investigations of the Sm(III)/Sm(II) redox couple in 1 M KCl at pH 6 were not successful using any of the OTE's. The reduction potential for the redox couple was beyond the cathodic limitations of the electrodes. No indication of the electrochemical generation of divalent samarium was noted visually, and hydrogen evolution at the electrode prevented spectral analysis.

2. M(IV)/M(III) Redox Couples

a. Cerium. The only tetravalent lanthanide ion sufficiently stable to exist in aqueous solution is cerium(IV). The Ce(IV)/Ce(III) redox couple is therefore amenable to spectroelectrochemical study in this medium. The formal reduction potential of the Ce(IV)/Ce(III) redox couple varies considerably in different mineral acid solutions

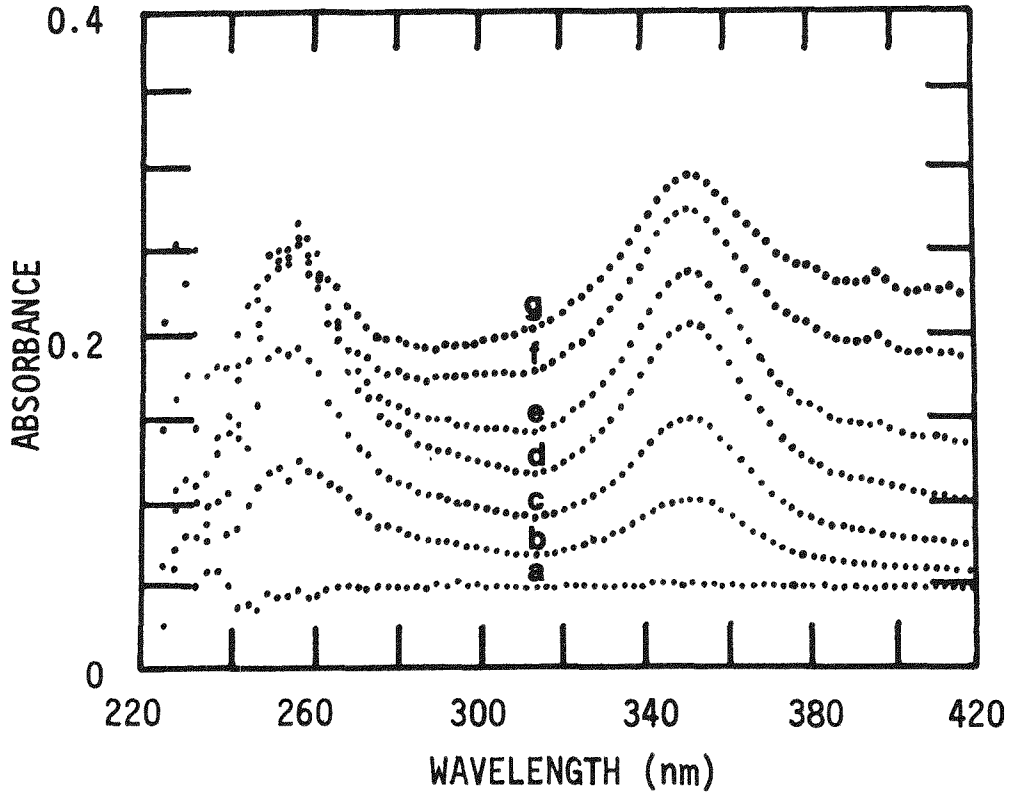

Figure 17. Solution absorption spectra of Yb(III) and Yb(II) as a function of time during the potential-step electrolysis of Yb(III) in 1 M KCl. 1 sec (a), 15 sec (b), 30 sec (c), 60 sec (d), 90 sec (e), 120 sec (f), and 150 sec (g); Ag(Hg)-OTE: 0.62 mm path length, potential-step: -0.76 to -1.56 V.

and is dependent upon the degree of complexation of the cerium ions by the anions of the various acids. A complexing agent providing a more stable Ce(IV) complex than that of Ce(III) enables the oxidation reaction to occur at a more favorable (less negative) potential.

Various complexing aqueous solutions were investigated using the Ce(IV)/Ce(III) couple in an effort to find a medium in which Ce(IV) could be generated most easily, such that other less stable M(IV) oxidation states of the lanthanide and actinide elements might also be generated in this same medium. The solubility of trivalent cerium was investigated in concentrated aqueous solutions of cesium fluoride, phosphoric acid, alkali metal oxalates, and alkali metal carbonates. Although the M(IV) states of the actinide elements were reported to be soluble and quite stable in concentrated fluoride media,[61,64] the trivalent states are quite insoluble, as was clearly demonstrated in experiments with Ce(III) salts. Solutions of concentrated phosphoric acid dissolved Ce(III) to a large extent, as did the alkali metal carbonates. The alkali metal oxalates themselves had limited solubility in water, and it was not possible to obtain a solution of oxalate ion much greater than 1 or 2 M.

Spectroelectrochemical experiments with Ce(III) chloride dissolved in about 15 M phosphoric acid were performed to determine the formal reduction potential of the Ce(IV)/Ce(III) redox couple. The Ce(III) solution was placed in a RVC-OTE and a gold screen OTE and increasingly more positive potentials were applied, until a change in the absorption spectrum indicated the appearance of Ce(IV). The absorption spectra of Ce(III) and Ce(IV) are shown in Figure 18. The

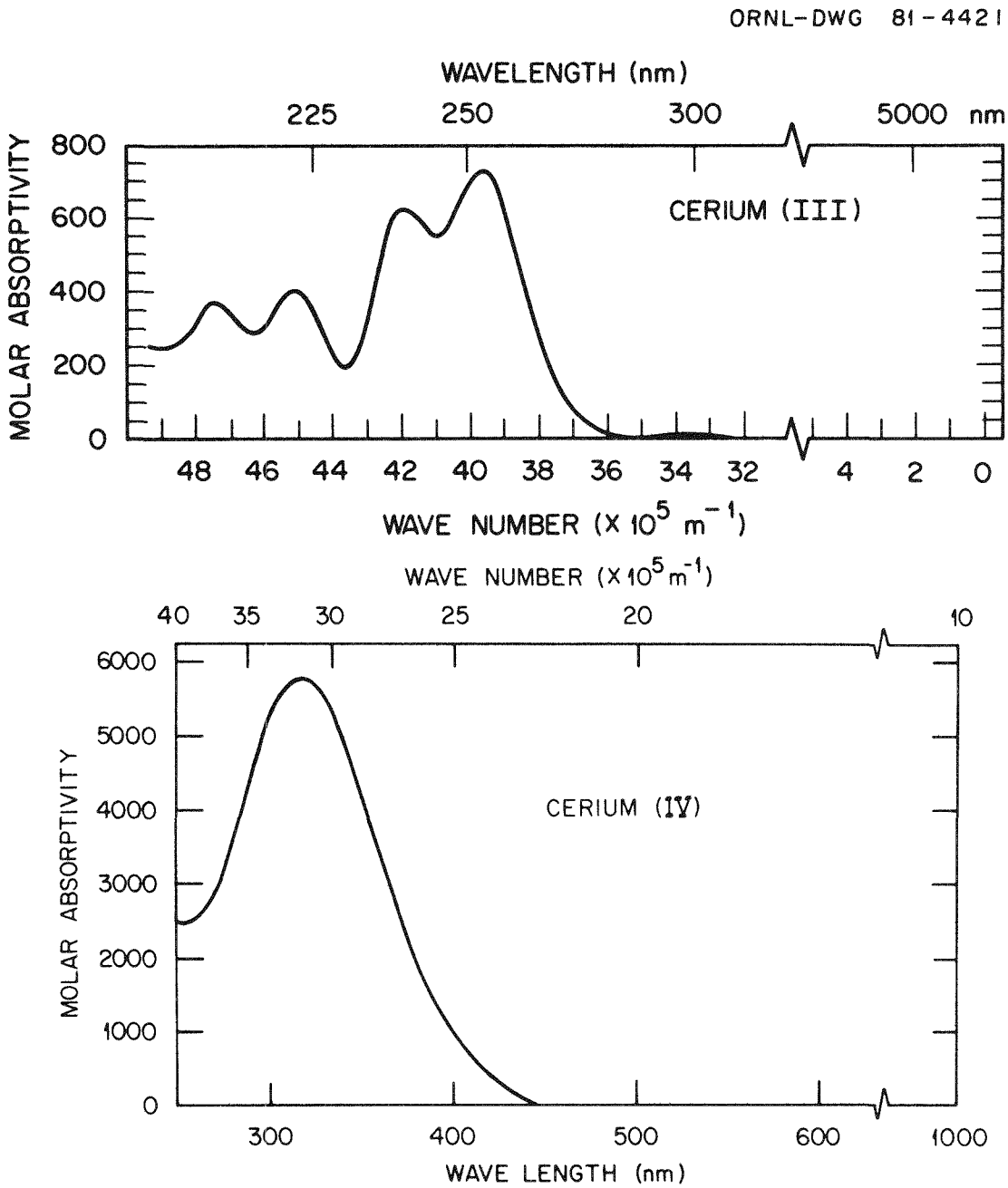

Figure 18. Solution absorption spectra of Ce(III) in 1 M $HClO_4$ and Ce(IV) in 1 M H_2SO_4.

Ce(III) spectrum was adapted from the work of Carnall[84] and was obtained in 1 M $HClO_4$. The Ce(IV) spectrum was recorded with the Cary Model 14-H spectrophotometer from an aqueous solution of ceric ammonium sulfate in 1 M H_2SO_4.

It was determined that concentrated phosphoric acid provided a potential shift of only about 1 V from the reduction potential of the Ce(IV)/Ce(III) redox couple in perchloric acid (1.7 V). This is an insufficient shift in potential to allow for the generation of any other lanthanide M(IV) states. Aside from this result, both the RVC and gold screen OTE's were damaged at high anodic potentials in H_3PO_4. Phosphoric acid studies were discontinued.

Rather surprising results were obtained from the first solubility experiments with Ce(III) chloride in 5.5 M K_2CO_3. The colorless salt was dissolved in the carbonate solution by vigorous shaking of the container, followed by mild heating. The Ce(III) salt appeared to change, while still in the solid form, from a clear sand-like material to a more opaque solid, followed by complete dissolution. This new solid material was probably cerium hydroxide, or hydrated oxide, which then dissolved. The pH of pure 5.5 M K_2CO_3 was measured at a glass electrode to be about 12.5. The most interesting result of these dissolution experiments was that, upon standing for a few minutes, freshly prepared, colorless solutions of Ce(III) in the carbonate solution became tinted yellow at the solution surface. The spectrum confirmed the presence of Ce(IV), which must have been the result of

oxidation by atmospheric oxygen. This suggested a substantial shift in the value of the formal reduction potential in concentrated carbonate solution.

The use of voltammetry in concentrated carbonate media was severely limited by the poor voltammograms obtained with both the Pt and RVC electrodes. It was not possible to observe reproducible current-voltage curves attributed to the cerium couple. This was in part due to the limited anodic potential range of these electrodes. The oxygen evolution wave occurred at a low anodic potential (+1.0 V for Pt and +0.7 for RVC) because of the high hydroxide ion concentration in the solutions. Only an estimate of the value of $E^{o'}$ (-0.13 V) was derived from the voltammogram.

The spectropotentiostatic method was applied to the cerium redox system in 5.5 M potassium carbonate to determine the formal reduction potential of the couple. An RVC-OTE (100 ppi, 1 mm path length) was used for this experiment. The absorption spectra of Ce(IV) and Ce(III) at various values of applied potential in 5.5 M K_2CO_3 are shown in Figure 19. Spectrum A was recorded at a potential where cerium was completely in the reduced form. As more positive potentials were applied (B through D) absorption due to the oxidized form was observed to increase. At the potential at which spectrum E was recorded, cerium was completely in the oxidized form. The potential range selected for this experiment was based on the $E^{o'}$ value obtained from the cyclic voltammograms.

The data from the spectropotentiostatic experiment are collected in Table VII. The absorbance values, recorded at 304 nm, are values

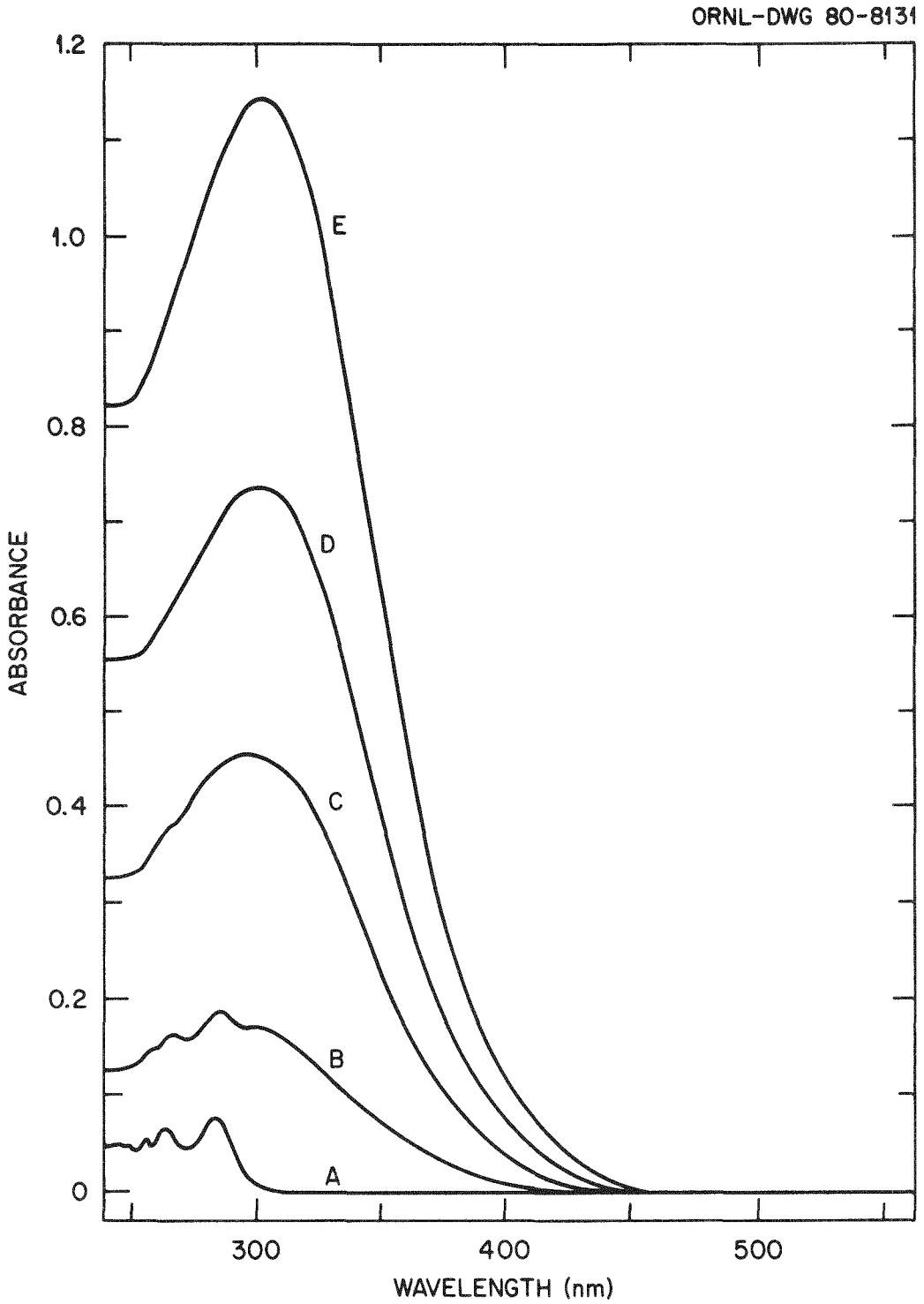

Figure 19. Solution absorption spectra of Ce(IV) and Ce(III) at various values of applied potential in 5.5 M K_2CO_3. -0.26 V (A), 0.002 V (B), 0.04 V (C), 0.06 V (D), 0.44 V (E). RVC-OTE: 100 ppi, 1 mm path length, [Ce(III)] = 1.0×10^{-3} M.

TABLE VII

DATA FOR SPECTROPOTENTIOSTATIC DETERMINATION OF THERMODYNAMIC PARAMETERS FOR THE Ce(IV)/Ce(III) REDOX COUPLE

Potential (volts vs SCE)	Absorbance A_2	A_2-A_1	A_3-A_2	A_2-A_1/A_3-A_2	$\log(A_2-A_1/A_3-A_2)$
		Data Set A			
-1.00	$(0.0528)=A_1$	-	-	-	-
-0.28	0.0750	0.0222	0.9824	0.0226	-1.6459
-0.24	0.1690	0.1162	0.8884	0.1308	-0.8834
-0.20	0.4500	0.3972	0.6074	0.6539	-0.1845
-0.18	0.6718	0.6190	0.3856	1.6053	0.2056
0.20	$(1.0574)=A_3$	-	-	-	-
		Data Set B			
-1.00	$(0.0061)=A_1$	-	-	-	-
-0.24	0.1780	0.1720	0.9220	0.1866	-0.7292
-0.20	0.4702	0.4640	0.6301	0.7365	-0.1328
-0.16	0.8450	0.8390	0.2550	3.2900	0.5172
-0.12	1.0450	1.0390	0.0610	17.032	1.2313
0.20	$(1.1000)=A_3$	-	-	-	-

from two separate experiments. The Nernstian plot derived from these data in Table VII is shown in Figure 20. The slope yielded an n-value of 0.95, corresponding to a one-electron exchange.

It was found[87] that the formal reduction potential of the Ce(IV)/Ce(III) redox couple was 0.051 ± 0.005 V in 5.5 M potassium carbonate solution. This is a significant shift from the value of 1.7 V reported in noncomplexing, perchloric acid solution.[69] Assuming a similar potential difference for other M(IV)/M(III) redox couples of the lanthanide elements, only praseodymium and terbium would have $E^{o'}$ values in the range to provide stability for the M(IV) species in concentrated carbonate solution (see Figure 2, page 25).

b. Praseodymium. Trivalent praseodymium, as the chloride or hydroxide compound, was dissolved in 5.5 M potassium carbonate. The spectrum of the resulting light green solution is shown in Figure 21. This spectrum is typical of the trivalent lanthanides, consisting of sharp f-f transitions of low molar absorptivity. The Pr(III) carbonate solution was placed in an electrolysis cell. Increasingly more positive potentials were applied to a Pt-screen anode until a change was noted visually, or spectrally, as a result of transferring the solution to a quartz cuvet and recording the absorption spectrum. At first the results of the electrolysis experiments were not reproducible. It was then determined that the solution pH was critical. It was first discovered by working with the terbium system (see below) that pH 14 (1 M hydroxide ion) was necessary for bulk stability of the M(IV) species. Thus after proper adjustment of the OH^- ion concentration and at a potential of 1.4 V (at a platinum

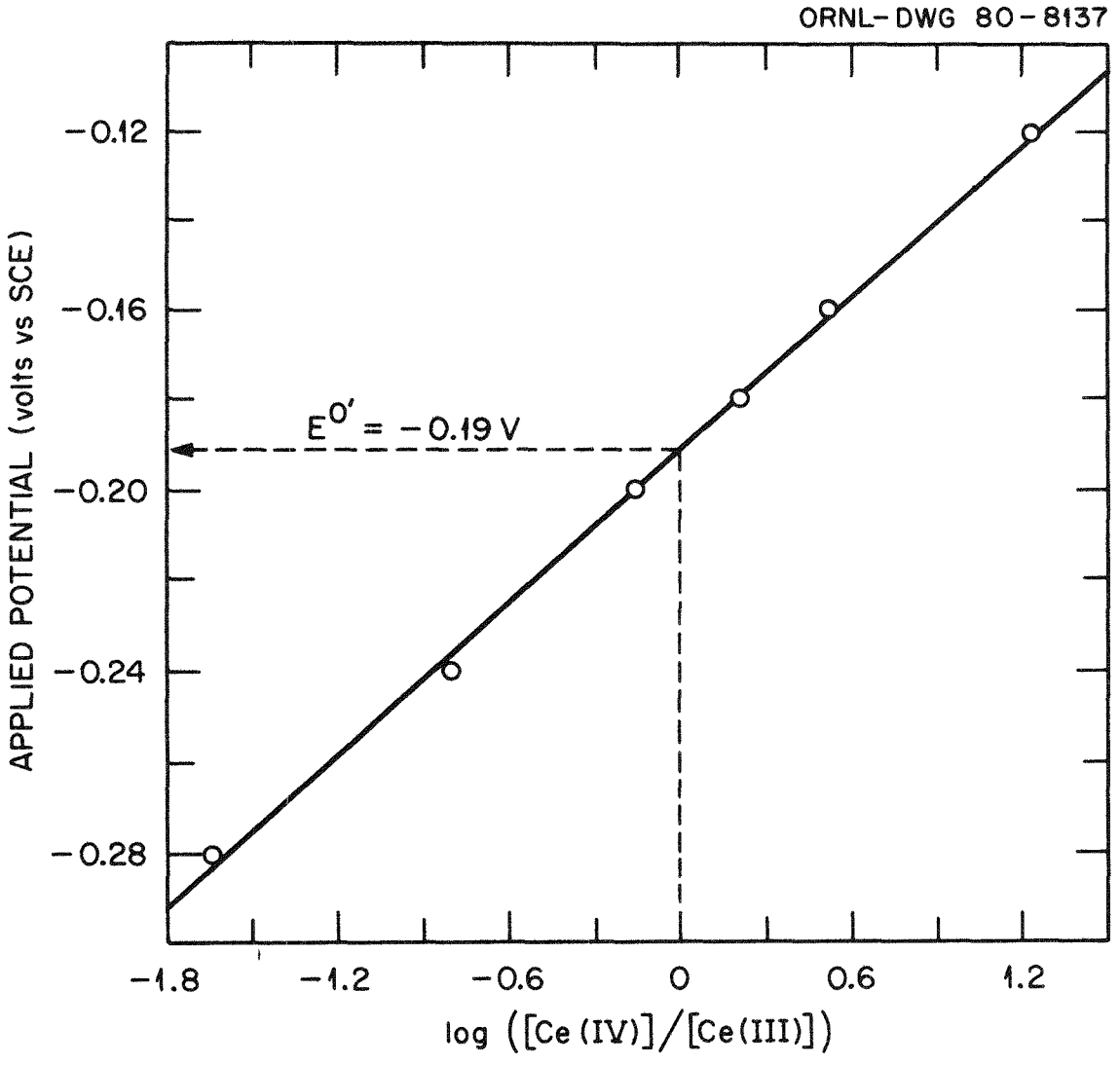

Figure 20. Nernstian plot for the Ce(IV)/Ce(III) redox couple in 5.5 M K_2CO_3.

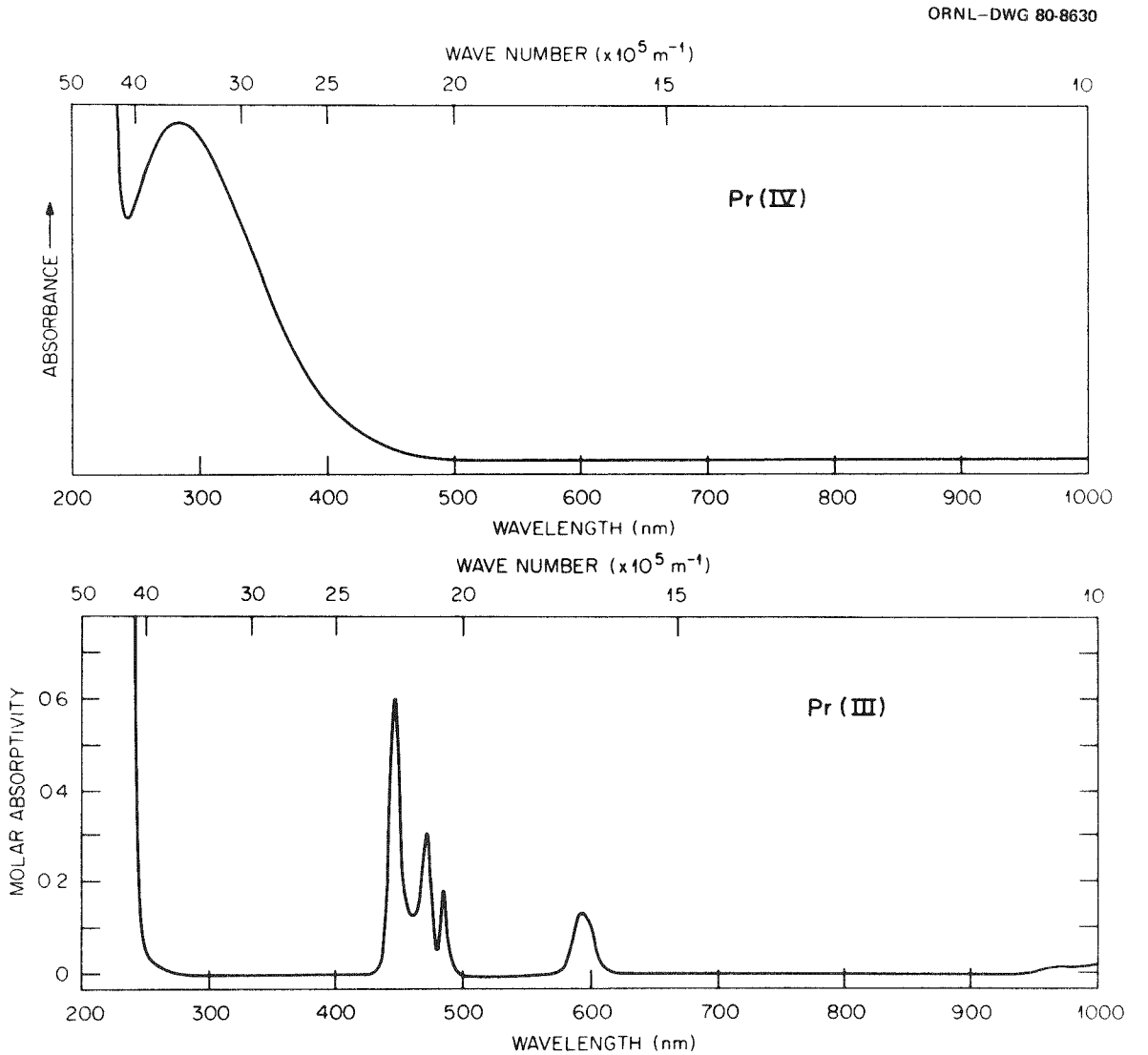

Figure 21. Solution absorption spectra of Pr(III) and Pr(IV) in 5.5 M K_2CO_3.

screen anode), Pr(III) was oxidized to Pr(IV). The resulting yellow solution of Pr(IV) exhibited the spectrum shown in Figure 21. The Pr(IV) spectrum is characterized by a broad-band absorption (f-d or charge-transfer) with a maximum at 283 nm. The molar absorptivity of this maximum was estimated to be greater than 1000. This was determined by correlating, in various partially oxidized solutions, a measured decrease in absorbance of a Pr(III) absorption peak of known molar absorptivity with the measured increase in absorbance of the 283 nm peak of Pr(IV).

Spectroelectrochemical experiments were performed using the rapid-scan spectrophotometer to further investigate the Pr(IV)/Pr(III) redox couple in carbonate solution using the RVC and Pt screen OTE's. The results of potential-step electrolysis and simultaneous recording of complete spectra, as a function of time, verified the previous results. It was also determined that carbonate solutions of Pr(IV) were susceptible to photolytic reduction by the source lamp of the rapid-scan spectrophotometer.

c. Terbium. Trivalent terbium, as the chloride or hydroxide compound was dissolved in 5.5 M K_2CO_3. The colorless solution which resulted exhibited the spectrum shown in Figure 22. This solution was placed in an electrolysis cell and increasingly more positive potentials were applied to a platinum screen anode until a change was noted. At a potential of 1.3 V a golden-brown color appeared at the surface of the Pt screen. This color dissipated into the bulk of the solution. It was found that this color would remain throughout the bulk of the solution if the OH^- ion concentration were adjusted to about 1 M. The

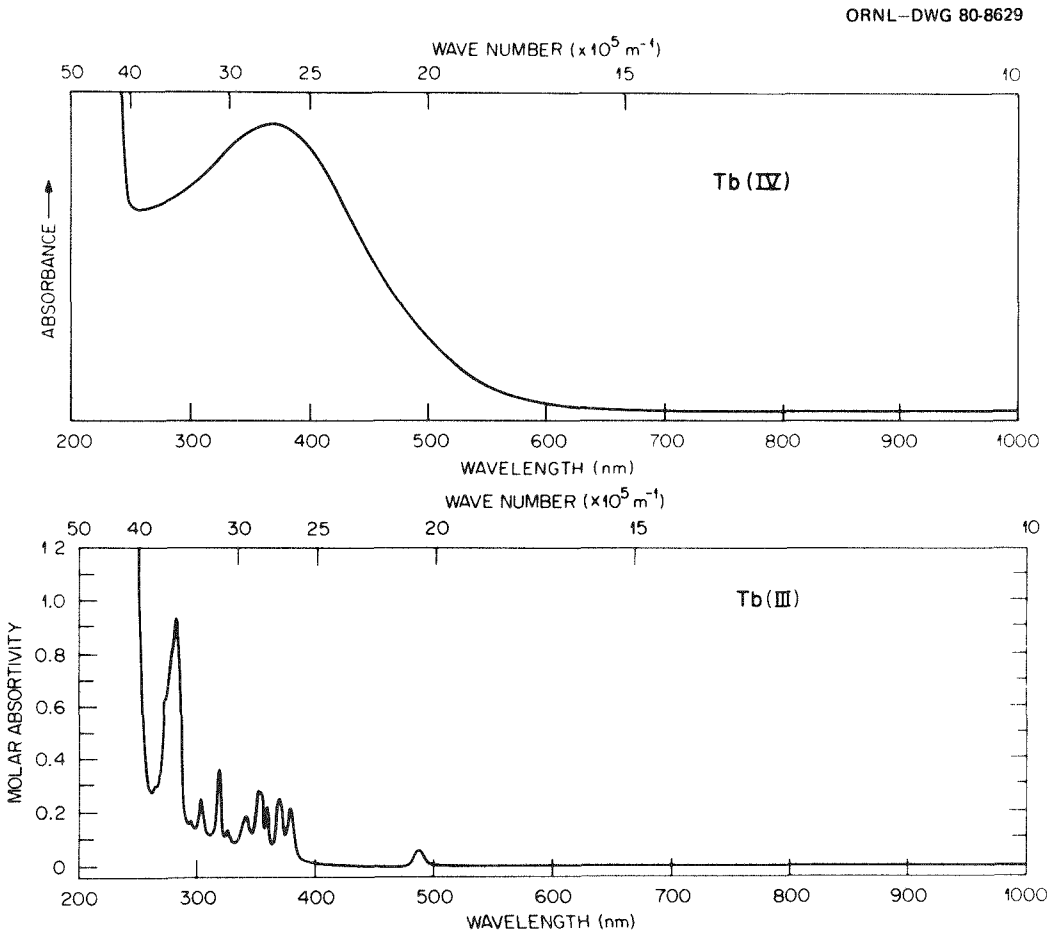

Figure 22. Solution absorption spectra of Tb(III) and Tb(IV) in 5.5 M K_2CO_3.

resulting red-brown Tb(IV) solution exhibited the spectrum shown in Figure 22. It is characterized by a broad-band transition with a maximum at 365 nm and with a molar absorptivity greater than 1000. The molar absorptivity was estimated by the same method as that described for Pr(IV). The colors of solutions of Pr(III), Pr(IV), Tb(III), and Tb(IV) in 5.5 M K_2CO_3 are displayed in Figure 23.

Spectroelectrochemical experiments at the RVC-OTE were not reproducible for reasons other than pH. RVC was not inert at potentials higher than about 1 V in concentrated carbonate media. RVC was apparently oxidized to produce a yellow coloration of the solution. This color gave a featureless spectrum starting at about 400 nm and extended as a shoulder into the UV spectral region. Pt electrodes were therefore used for all subsequent electrochemistry in concentrated carbonate media when anodic potentials exceeding 1 V were required.

Both Pr(IV) and Tb(IV) were electrochemically generated in 5 M Cs_2CO_3 and 2 M Na_2CO_3 at pH 14. The spectra recorded in these solutions were identical to those in potassium carbonate solution. Pr(IV) and Tb(IV) were also both chemically generated in potassium carbonate by ozone oxidation. The solutions were adjusted to the proper pH prior to bubbling of the ozone through the solutions for three hours. The resultant spectra were the same as those recorded after electrochemical oxidation. A literature value reported for the ozone redox couple in basic media is about 1.24 V.[88] This is the approximate potential which was applied to the anode to obtain these M(IV) states.

Chemical oxidation of trivalent praseodymium[89] and terbium[90] in aqueous solutions of potassium phosphotungstate has been previously

AFFIX COLOR

PHOTO HERE

Figure 23. Solutions of Pr(III) (A), Pr(IV) (B), Tb(III) (C), and Tb(IV) (D) in 5.5 M K_2CO_3.

reported. Propst[91] reported the preparation of a solid Tb(IV) compound by electrolytic deposition. However, the electrochemical generation of soluble Pr(IV) and Tb(IV) species in aqueous media has not, to the knowledge of this author, been previously reported.

A solid compound was prepared by the electrochemical oxidation of a Tb(III) carbonate solution at an RVC electrode. The red-brown, powder-like solid exhibited the solid-state reflectance spectrum shown in Figure 24. For comparison, the reflectance spectra of solid Tb(III) carbonate and Tb_7O_{12} are also displayed in Figure 24. The arrow in this figure indicates the maximum absorbance of the Tb(IV)-carbonate solution spectrum. The data suggest that this red-brown solid consists of Tb in an oxidation state greater than M(III).

X-ray diffraction patterns of the red-brown solid were made but the results were not particularly conclusive due to the noncrystalline nature of the solid. The X-ray data do suggest, however, that the solid is probably a mixed-valence state compound consisting of both Tb(III) and Tb(IV).

Thermogravimetric-mass spectra analysis (TGA-MS) indicated at least two carbonate ions were associated with a terbium atom.[92] Two "water" peaks at different temperatures in the TGA-MS data indicated waters of hydration in an outer sphere configuration and an inner sphere moiety, probably hydroxide ions. Similar data were found for closely related compounds by Sastry et al.[93]

The solid compound seems to be a mixed-valence compound of Tb(III) and Tb(IV) with carbonate and hydroxide ions as part of the structure.

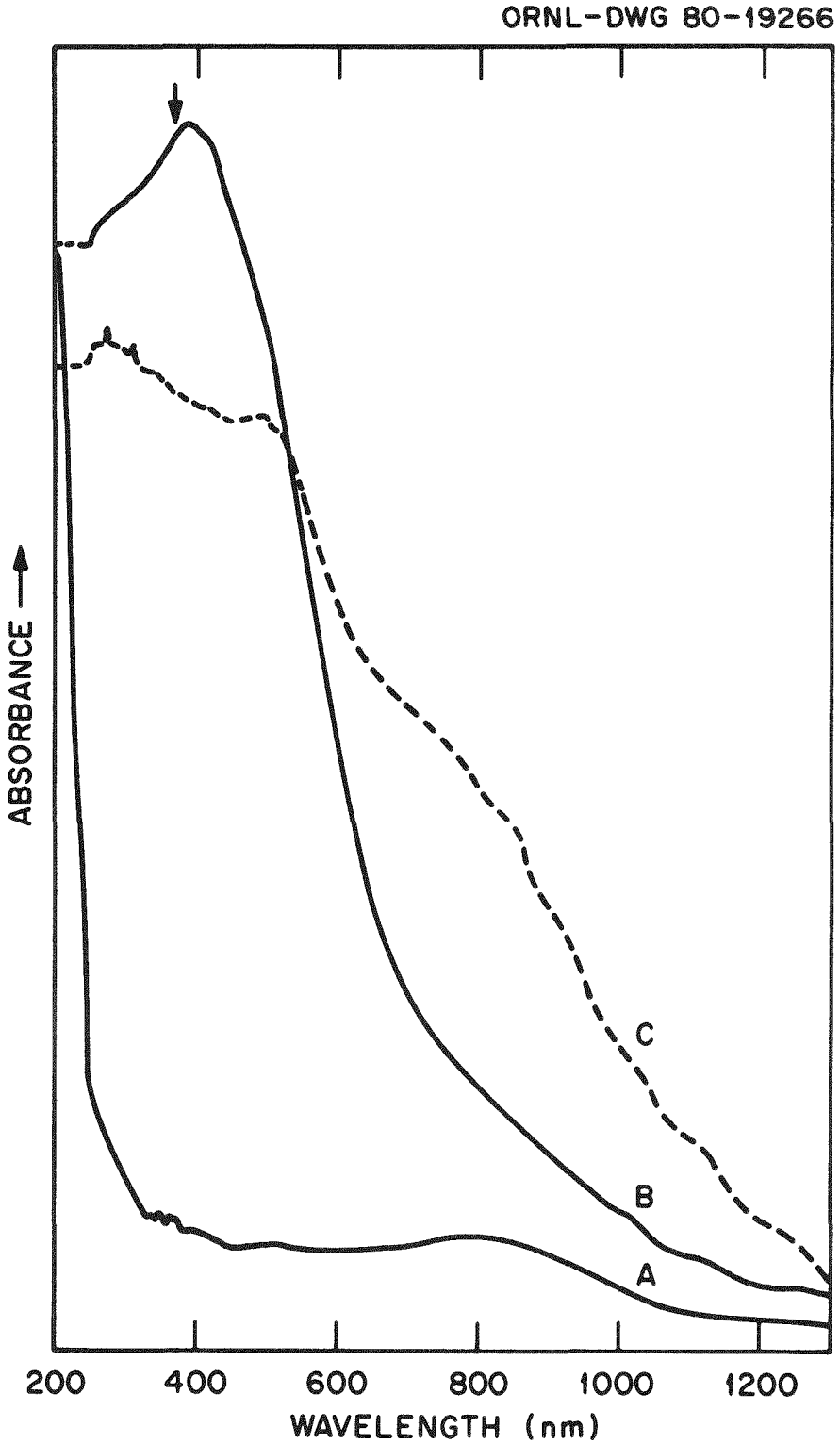

Figure 24. Solid-state reflectance spectra of $Tb_2(CO_3)_3$ (A), unknown solid (B), and Tb_7O_{12} (C). Arrow indicates absorption maximum of Tb(IV) in carbonate solution.

The significance of the preparation of such a compound by electrochemical oxidation is that perhaps compounds of the actinides may be prepared in a similar manner.

B. Actinide Elements

1. Uranium

The chemistry of uranium in aqueous solution is well known. The relatively low-level radioactivity of naturally occurring uranium-238 and the variety of oxidation states exhibited by this element (see Table IV, page 17) make it an excellent substitute for the heavier, more radioactive actinides in preliminary electrochemical and spectroscopic studies.

a. U(VI)/U(V)/U(IV) redox couples. The known oxidation states of uranium are well characterized, with the exception of U(V). The U(V) species UO_2^+ is unstable in aqueous solution and tends to disproportionate. It is also easily oxidized to the very stable U(VI) species, UO_2^{2+}.[66] It was expected that spectroelectrochemical techniques could be used to generate electrochemically and identify spectrally the U(V) oxidation state before it could disproportionate.

The redox couples involving U(VI), U(V), and U(IV) were studied by the reduction of the yellow UO_2^{2+} ion in 1 M KCl at various pH values. KCl was selected for the extended potential range of electrodes in this solvent.

Voltammograms of the UO_2^{2+} solution were recorded at an HMDE and platinum microelectrode, at various pH values, in 1 M KCl. These

voltammograms are shown in Figure 25. Voltammogram A was recorded at an HMDE at pH 0 and displays an irreversible reaction curve. A peak was observed for the reduction of U(VI) to U(V),[94] but no peak was noted during the anodic scan. This same solution was studied at a platinum wire electrode (voltammogram B) to determine if an oxidation wave occurred at potentials more positive than those attainable at an HMDE. The reduction wave was less pronounced, because of the hydrogen wave at platinum at pH 0, but still no oxidation wave was noted. At pH 0 the UO_2^+ species is unstable;[66] immediately after it forms by the reduction of UO_2^{2+}, it disproportionates before it can be oxidized at the electrode surface. It should be mentioned that voltammograms A and B in Figure 25 are the third scans of multiple scans. That is, due to the "catalytic current wave" of the U(VI) reduction (disproportionation and regeneration of the reactant), it was necessary to take several scans before reproducibility was attained. The first scans had very large current values, unrelated to the concentration of uranium. Voltammogram C in Figure 25 is of the UO_2^{2+} solution at pH 3 at a platinum electrode. An oxidation wave was noted in this case, indicating a certain stability of the UO_2^+ species at pH 3. This is in agreement with literature data which indicate that U(V) is somewhat stable at pH values between 2 and 4 in aqueous media.[94]

Solution absorption spectra of U(VI), U(V), U(IV), and U(III) are shown in Figure 26. These spectra are adapted from literature sources[95,96] and are indistinguishable from those spectra recorded in

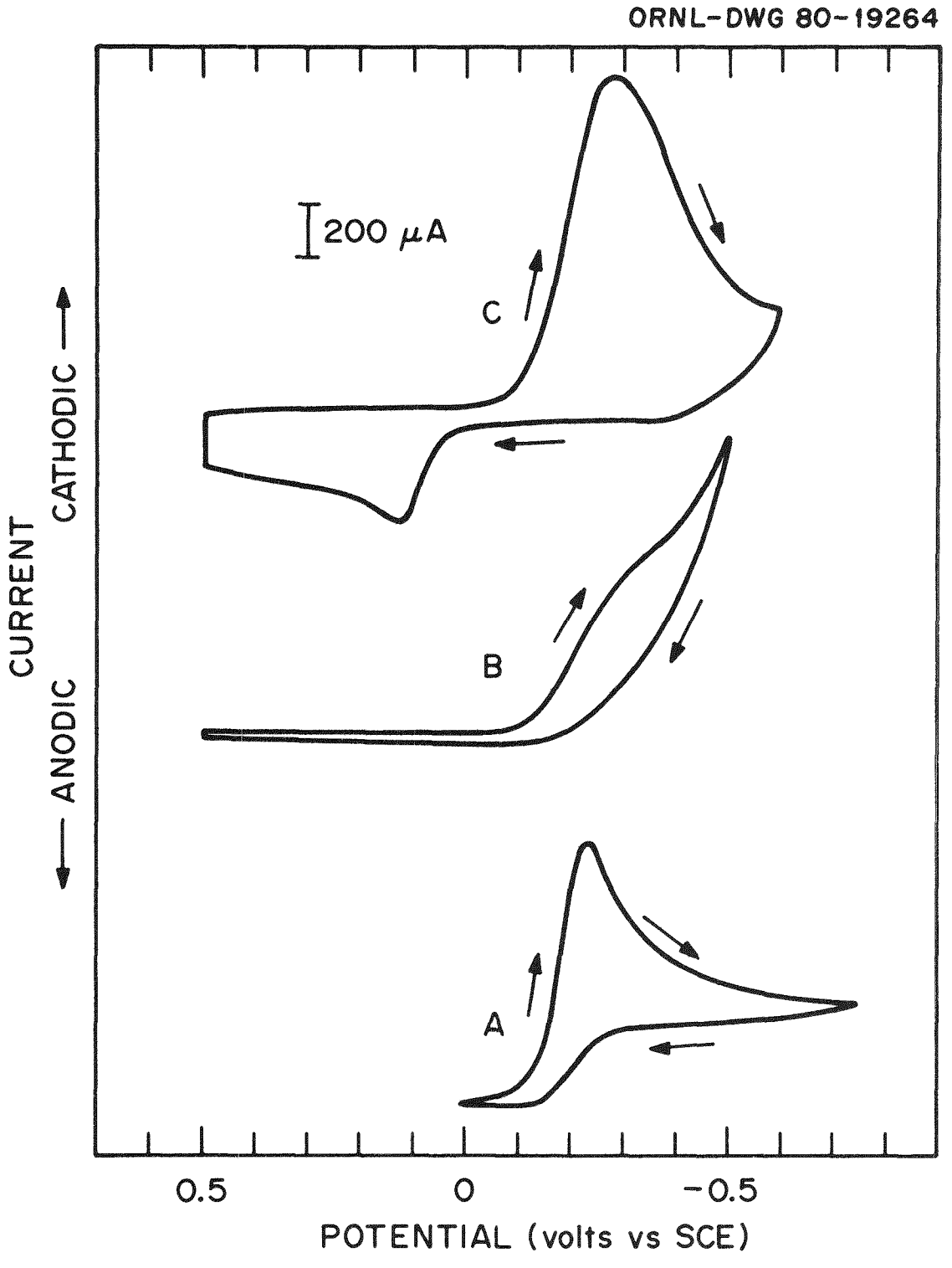

Figure 25. Cyclic voltammograms of U(VI) in 1 M KCl. pH 0 at HMDE (A), pH 0 at Pt (B), and pH 3 at Pt (C). Scan rate: 200 mV/s, [U(VI)] = 1.0×10^{-2} M.

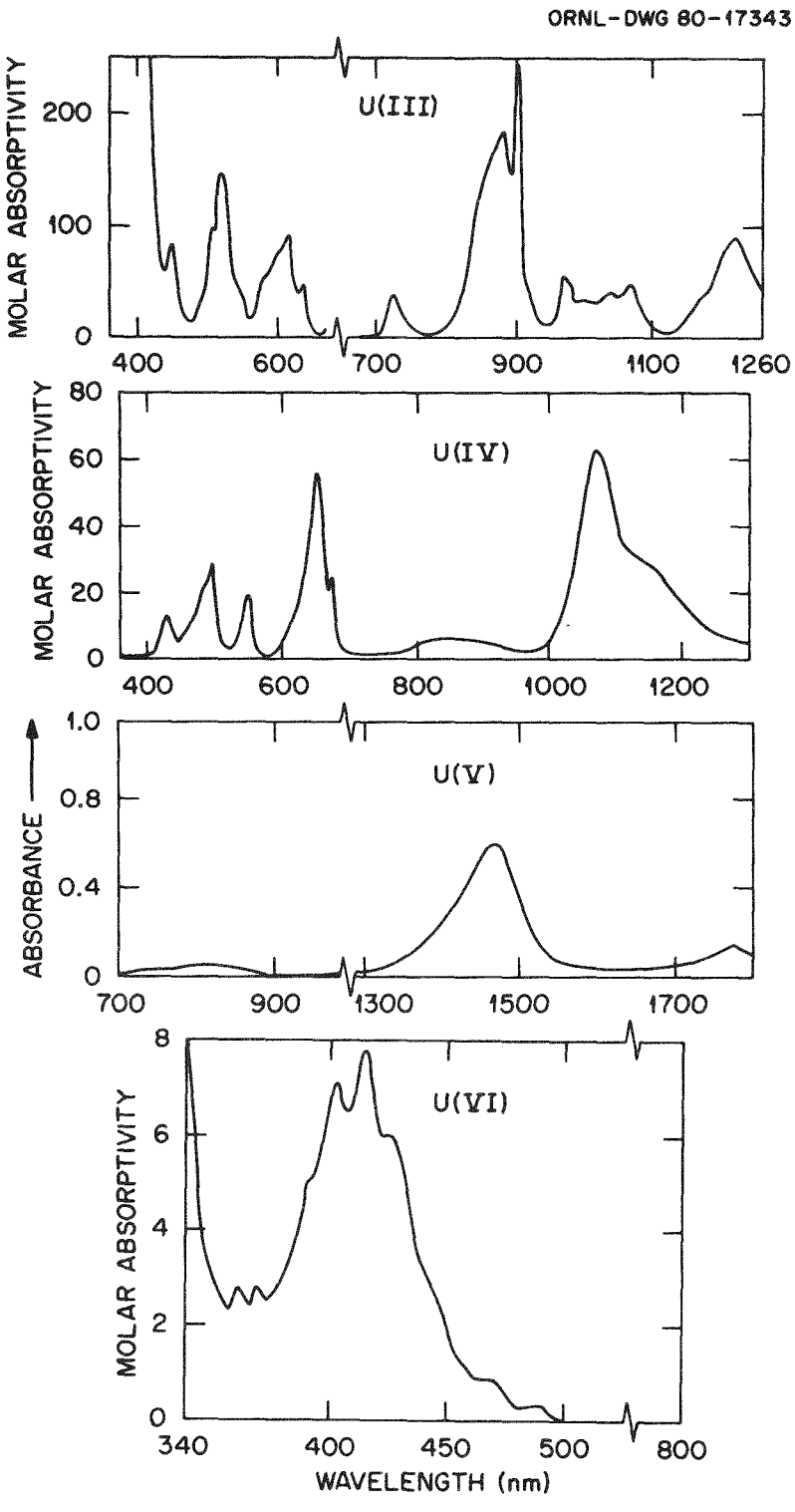

Figure 26. Solution absorption spectra of U(VI, V, IV, and III). In 1 M $HClO_4$ except U(III) in $DClO_4$ at pH (pD) 3.09.

this work. The spectra of the U(VI), U(V), and U(IV) ions were obtained from solutions in which the uranium species was generated by chemical reactions rather than by electrochemical reactions. The U(VI) (yellow) solution spectrum was recorded, and then the pH of the solution adjusted to 0. Zinc amalgam was placed in the solution, a green color appeared, and the resultant U(IV) spectrum was obtained. In order to record the spectrum of colorless U(V), it was necessary to adjust the U(VI) solution to pH 3 and add Eu(II) [which was prepared by zinc amalgam reduction of Eu(III)]. The reductant Eu(II) solution was also adjusted to pH 3 prior to mixing with the U(VI).

Attempts were made to record the Raman spectrum of U(V) as the UO_2^+ ion in 1 M KCl. A spectrum of the U(VI) species was obtained, but no signal attributed to U(V) was observed. It was determined that the beam of the argon-ion laser was heating the solution and increasing the speed of the disproportionation reaction. A dark green solid was noted in the bottom of the Raman sample tube. This was U(IV) oxide which results from the disproportionation at pH 3.

Spectroelectrochemical investigation of the U(VI)/U(V)/U(IV) redox couples was performed at pH 0 and pH 3. The U(VI)-KCl solution was adjusted to pH 0 and placed in the RVC-OTE (100 ppi, 1 mm) in the beam of the Cary Model 14-H spectrophotometer. A potential-step was applied which was much greater than the cathodic peak potential in the U(VI) solution voltammogram. This was from 0.24 V to -0.80 V. Complete absorption spectra were recorded as a function of time during the potential-step electrolysis and are displayed in Figure 27. Spectrum A is due to the starting material UO_2^{2+}. As the electrolysis proceeded (spectra B and C), the yellow color disappeared and a green

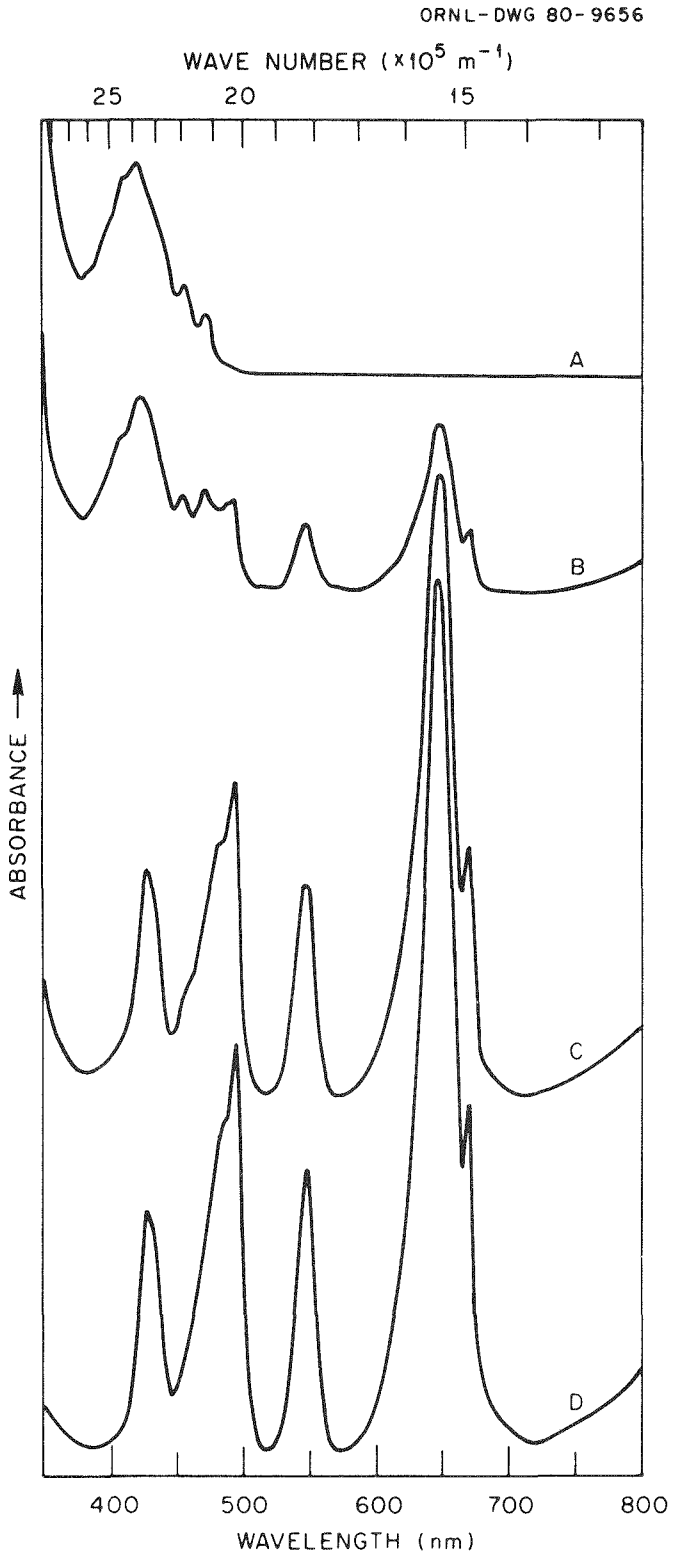

Figure 27. Solution absorption spectra of U(VI) and U(IV) as a function of time during potential-step electrolysis of U(VI). Initial spectrum (A), 10 min (B), 30 min (C), and 50 min (D). RVC-OTE: 100 ppi, 1 mm path length, potential step: 0.24 V to -0.8 V, spectra off-set for clarity.

color was observed, with the concomitant appearance of spectral peaks attributed to U(IV). Spectrum D is the result of complete reduction to the product U(IV). The absorbance of the U(VI) and U(IV) peaks accounted for 100% of the uranium present as calculated by Beer's law and thus no measurable U(V) was formed.

The RVC-OTE was filled with a solution of U(VI) in 1 M KCl/DCl at pH (pD) 3. A potential of -0.26 V was applied to the cell and the spectrum of U(V) shown in Figure 28, was recorded before interference caused by the formation of solid U(IV) oxide occurred. It was necessary to use a relatively high concentration (greater than 0.1 M) of U(VI) in the starting solution due to the short path length of the OTE and the low molar absorptivity of UO_2^+.

b. U(IV)/U(III) redox couple. This couple was studied in 1 M KCl, at various pH values, by reduction of U(IV) stock solutions. U(III) is unstable in aqueous solution and is easily oxidized by water and air.[45]

Cyclic voltammograms of the U(IV)/U(III) redox couple, recorded at an HMDE, are shown in Figure 29. Voltammogram A displays a reversible wave from which an $E^{o'}$ value of -0.65 $\pm$ 0.01 V was derived (pH 0). This value is in good agreement with the value reported by Nugent et al.[69] of -0.631 V. At pH 1 (voltammogram B) the cathodic peak potential is more negative than that of A and is a less reversible wave. At pH 2 (voltammogram C) the redox couple is even less reversible, as indicated by the radical change in peak potential values and the lower current values. The cathodic peak current does not equal the anodic peak current in C, also indicating a less than reversible electrode reaction.

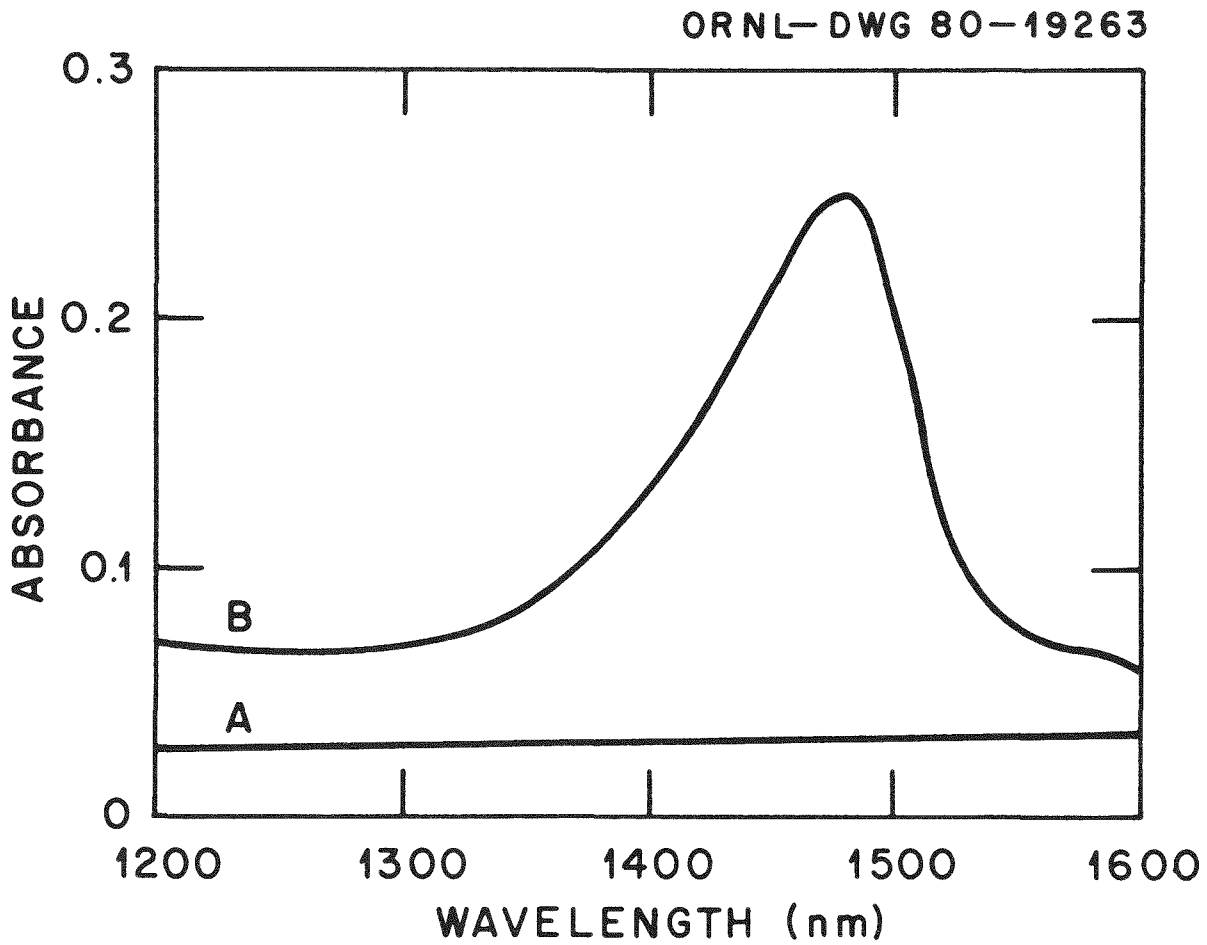

Figure 28. Solution absorption spectra of U(VI) and U(V) in an RVC-OTE. U(VI) initial solution (A) and electrogenerated U(V) (B). RVC-OTE: 100 ppi, 1 mm path length, 1 M KCl/D_2O at pH (pD) 3, adjusted with DCl, [U(VI)] = 5.0×10^{-1} M.

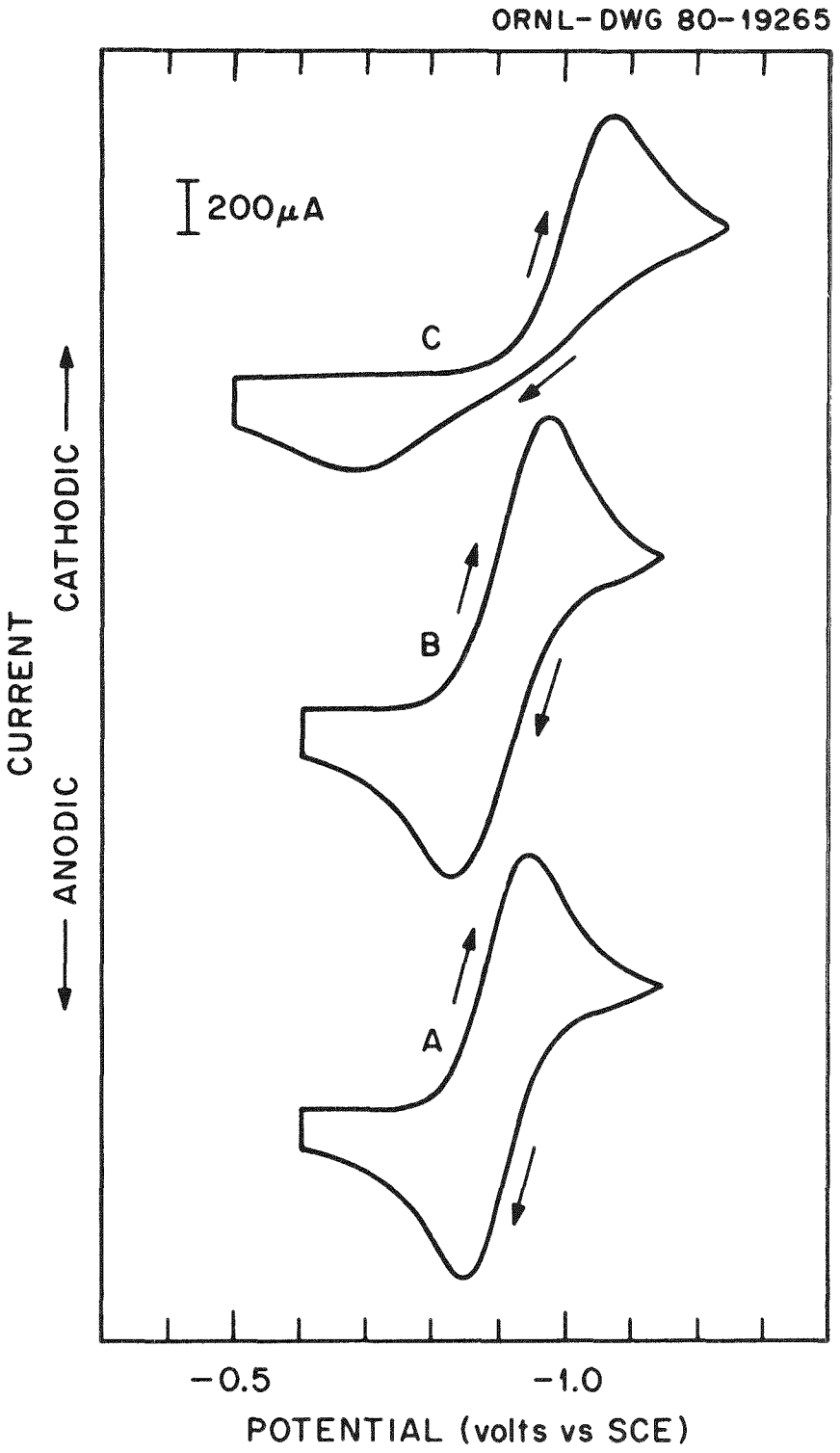

Figure 29. Cyclic voltammograms of U(IV) in 1 M KCl at an HMDE. pH 0 (A), pH 1 (B), and pH 2 (C). [U(IV)] = 1.0×10^{-1} M, sweep rate: 200 mV/s.

Solution absorption spectra of U(IV) and U(III) were obtained by recording the spectrum of the U(IV) stock solution in a 1-cm quartz cuvet followed by reduction with zinc analgam in a deoxygenated solution to obtain U(III). The initial green color of U(IV) gave way to a much darker green or nearly black solution, which yielded the characteristic U(III) spectrum.

Spectroelectrochemistry of the U(IV)/U(III) redox couple in 1 M KCl at pH 0 was performed in a silver amalgam screen OTE and a porous nickel metal amalgam foam OTE. These electrodes were used because of the requirement to attain a substantially cathodic potential in molar acid solution. These electrodes combine the characteristics of mercury with the optically transparent quality of the substrate metal materials. Absorption spectra of U(IV) and U(III) as a function of time during potential-step electrolysis in the silver amalgam screen OTE are shown in Figure 30. Spectrum A is that of U(IV) only. As the electrolysis proceeded, absorption peaks due to U(III) were observed to appear (spectrum B). Spectrum C is exclusively that of U(III) indicating complete reduction in the OTE. The potential-step was from no potential applied to -1 V vs SCE. It was not possible to determine the $E^{o'}$ value of this couple by spectropotentiostatic methods due to the interference from hydrogen gas evolution at the potential corresponding to complete reduction at equilibrium conditions.

2. Neptunium

Neptunium-237 has sufficient radioactivity associated with quantities greater than a few milligrams to require that all manipulations be performed in containment gloved box facilities. The

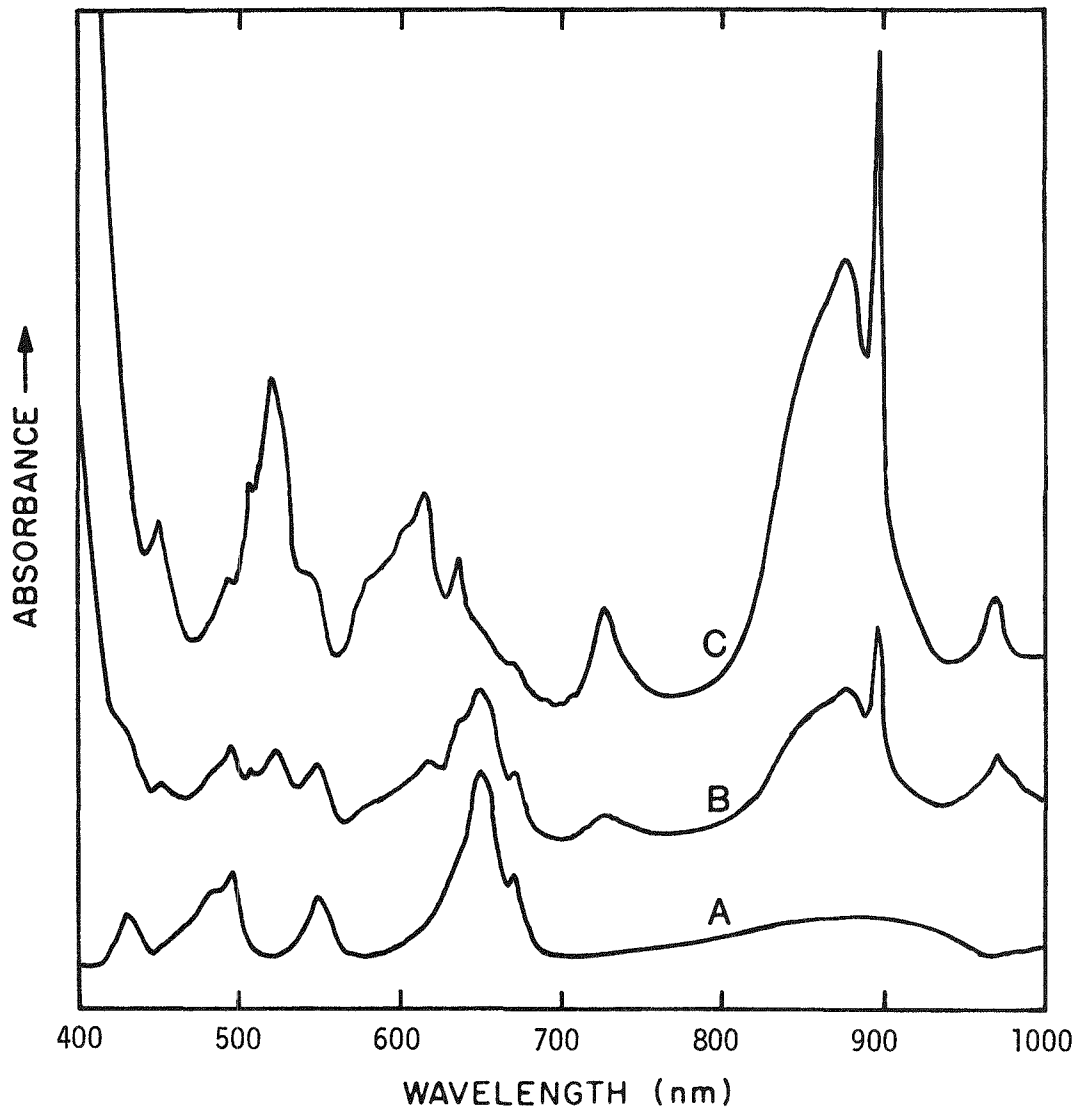

Figure 30. Solution absorption spectra of U(IV) and U(III) as a function of time during the potential-step electrolysis of U(IV). 0 min (A), 10 min (B), 20 min (C). Silver amalgam screen OTE: 0.62 mm path length, potential-step: 0.24 V to -0.76 V [U(IV)] = 1.0×10^{-2} M in 1 M KCl at pH 0.

variety of oxidation states accessible within a narrow potential range in aqueous solution and the characteristic absorption spectrum associated with each oxidation state make neptunium an excellent candidate for spectroelectrochemical studies. In addition, the heptavalent oxidation state is accessible in complexing aqueous solutions.

a. Np(VI)/Np(V) redox couple. The stable Np(V) species, NpO_2^+, can be oxidized to reasonably stable Np(VI), NpO_2^{2+}, in aqueous solution. This redox couple was investigated in 1 M $HClO_4$, a noncomplexing medium.

Voltammograms of the Np(VI)/Np(V) couple in 1 M $HClO_4$ were recorded at platinum wire and RVC microelectrodes. A representative voltammogram is shown in Figure 31. The $E^{o'}$ value obtained from this voltammogram was 1.11 ± 0.01 V, in good agreement with the literature value of 1.137 V.[69]

Solution absorption spectra of emerald green Np(V) and red-purple Np(VI) in 1 M $HClO_4$ are shown in Figure 32. These spectra were adapted from literature spectra;[97,98] spectra obtained in this work were identical. The spectra of Np(VI) and Np(V) were obtained from the corresponding stock solutions in 0.5-cm quartz cuvets containing 1 ml of solution.

Spectropotentiostatic determinations of $E^{o'}$ and n for the Np(VI)/Np(V) redox couple in 1 M $HClO_4$ were performed using an RVC-OTE. Current vs time curves were recorded simultaneously with absorbance vs time curves during the potential-step electrolysis of Np(VI). After attainment of equilibrium, complete spectra were recorded at various

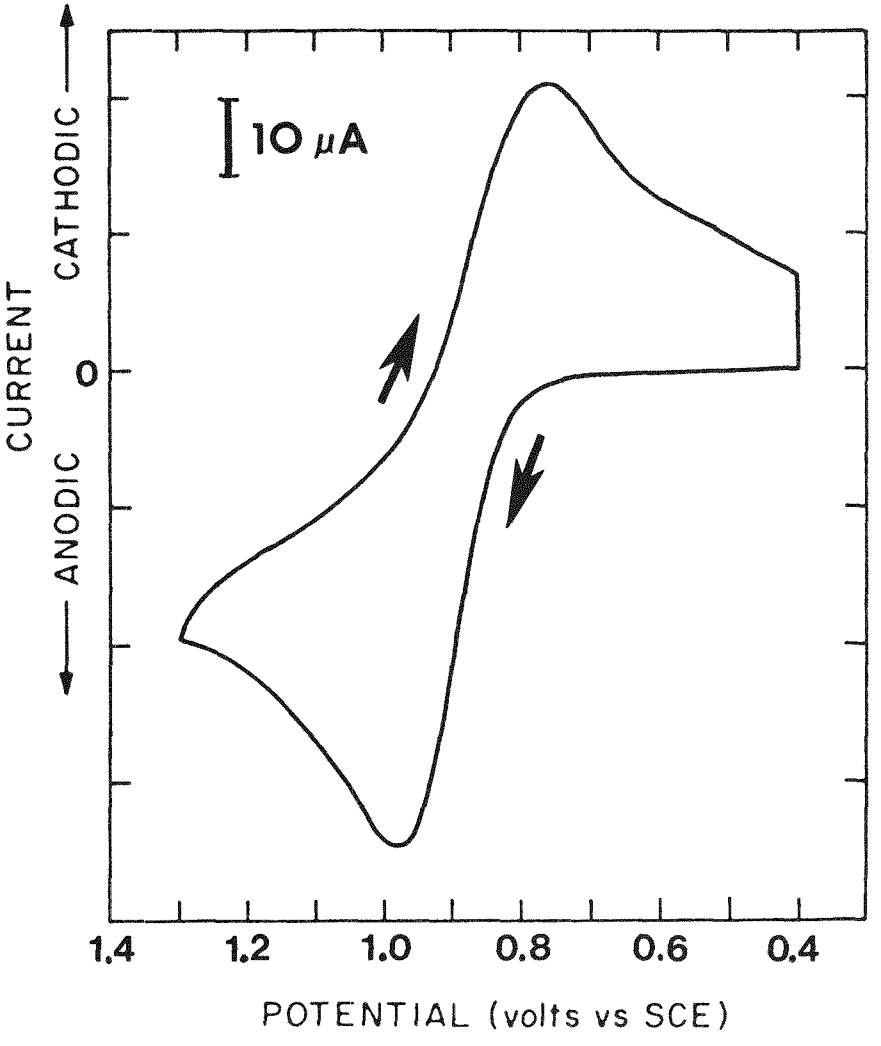

Figure 31. Cyclic voltammogram of Np(V) in 1 M $HClO_4$. Pt electrode, sweep rate: 100 mV/s, [Np(V)] = 3.3 x 10^{-2} M.

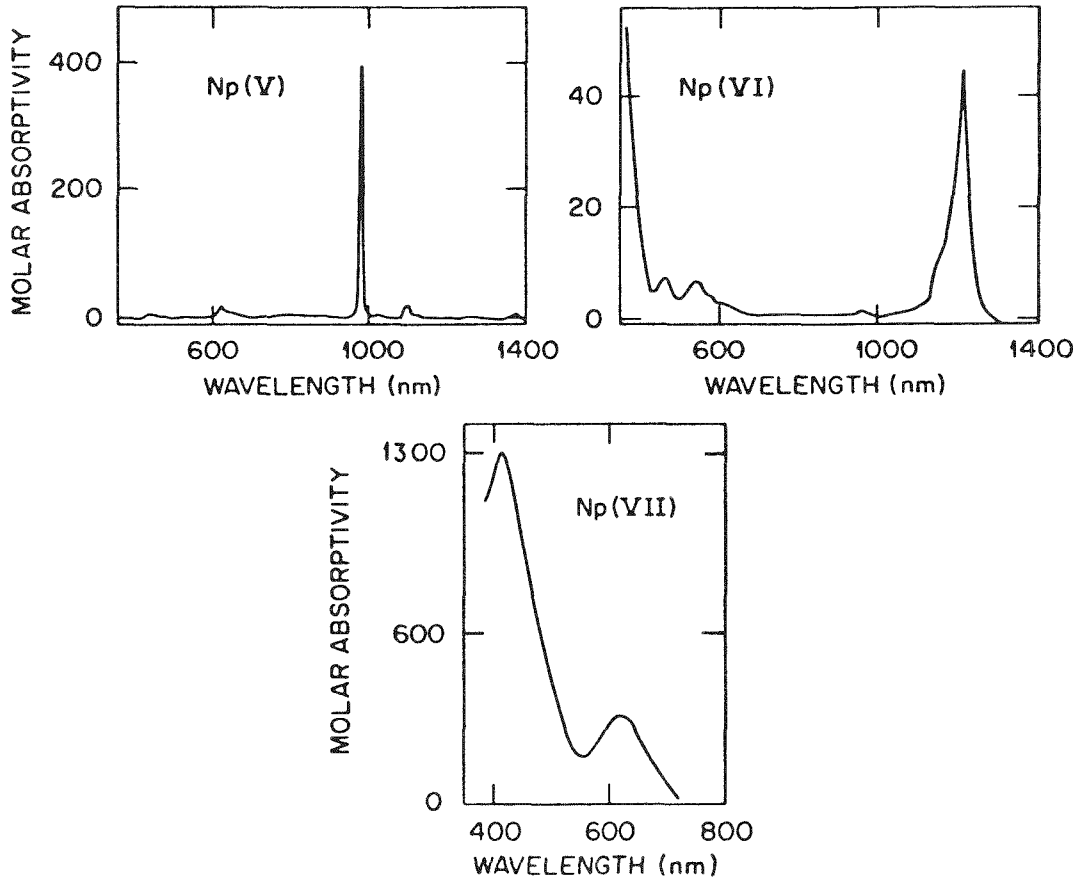

Figure 32. Solution absorption spectra of Np(V) and Np(VI) in 1 M $HClO_4$ and Np(VII) in 1 M LiOH.

values of applied potential. These spectra are shown in Figure 33. Spectrum A is that of the initial Np(VI) solution with its main absorbance peak at about 1210 nm. As reduction proceeded, Np(V) absorption peaks (main absorbance peak at 980 nm) appeared as shown in spectra B through E. Following complete reduction the product was exclusively Np(V), as determined from spectrum F. The data derived from the peak at 980 nm for the spectropotentiostatic determinations of $E^{o'}$ and n are collected in Table VIII.

The Nernstian plot for the Np(VI)/Np(V) redox couple in 1 M $HClO_4$ is shown in Figure 34. The $E^{o'}$ value was determined to be 1.140 $\pm$ 0.005 V (n = 0.93) in excellent agreement with the 1.137 V value from the literature.[69] This result verifies the usefulness of the spectropotentiostatic method with the RVC-OTE in a gloved box experiment.

The stock solution of yellow-green Np(VI) in 2 M Na_2CO_3 was reduced at a platinum screen large surface electrode to Np(V) at -0.2 V. The solution absorption spectra of the starting solution and of the product Np(V) were recorded. The spectrum of green Np(V) in 2 M Na_2CO_3 is shown in Figure 35. The completely different appearance of the spectrum of Np(V) in 2 M Na_2CO_3 as compared to that in 1 M $HClO_4$ (see Figure 32) indicates strong complexation of the Np(V) by the carbonate ion.

b. Np(VII)/Np(VI) redox couple. Neptunium has been reported to be stable in the heptavalent state in carbonate solution.[99] The Np(VII)/Np(VI) redox couple was studied in 2 M Na_2CO_3 by electrolysis of the Np(VI) stock solution.

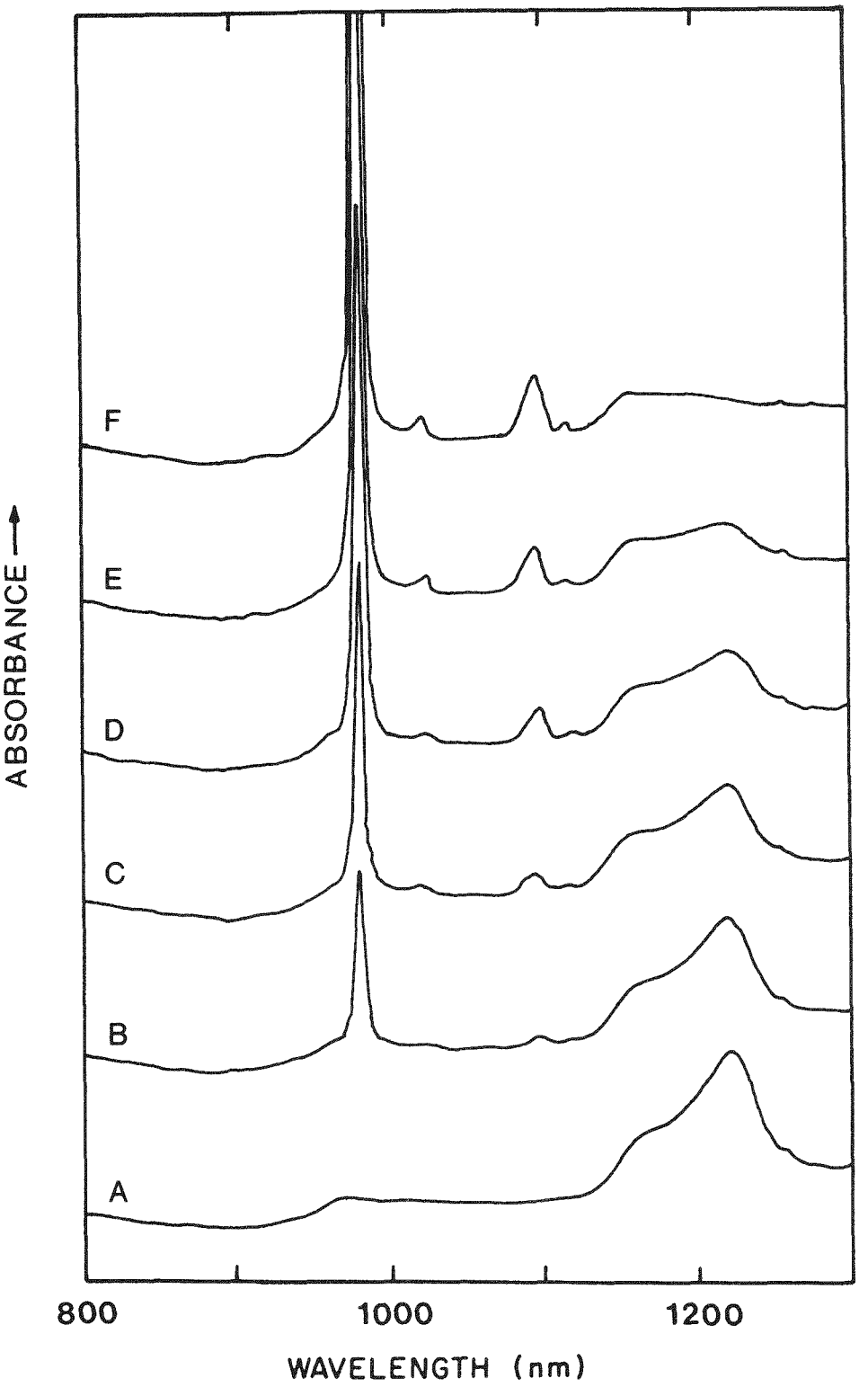

Figure 33. Solution absorption spectra of Np(VI) and Np(V) at various values of applied potential in 1 M $HClO_4$. 1.34 V (A), 1.18 V (B), 1.16 V (C), 1.14 V (D), 1.12 V (E), and 1.04 V (F), RVC-OTE: 100 ppi, 1 mm path length, [Np(VI)] = 2.0×10^{-2} M.

TABLE VIII

DATA FOR SPECTROPOTENTIOSTATIC DETERMINATION OF THERMODYNAMIC PARAMETERS FOR THE Np(VI)/Np(V) REDOX COUPLE

Potential (volts vs SCE)	Absorbance A_2	A_2-A_1	A_3-A_2	A_2-A_1/A_3-A_2	log (A_2-A_1/A_3-A_2)
1.10	$(0.0060)=A_1$				
1.00	0.0280	0.0220	1.5220	0.0145	-1.839
0.98	0.0575	0.0515	1.4925	0.0345	-1.462
0.96	0.1160	0.1100	1.4340	0.07671	-1.115
0.94	0.2420	0.2360	1.3080	0.1804	-0.7438
0.92	0.4650	0.4590	1.0850	0.4230	-0.3737
0.90	0.7701	0.7641	0.7799	0.9797	-0.08907
0.88	1.0883	1.0823	0.4617	2.344	0.3700
0.86	1.2852	1.2792	0.2648	4.831	0.6840
0.84	1.4280	1.4220	0.1220	11.66	1.0667
0.82	1.4941	1.4881	0.0559	26.6	1.425
0.80	$(1.5500)=A_3$				

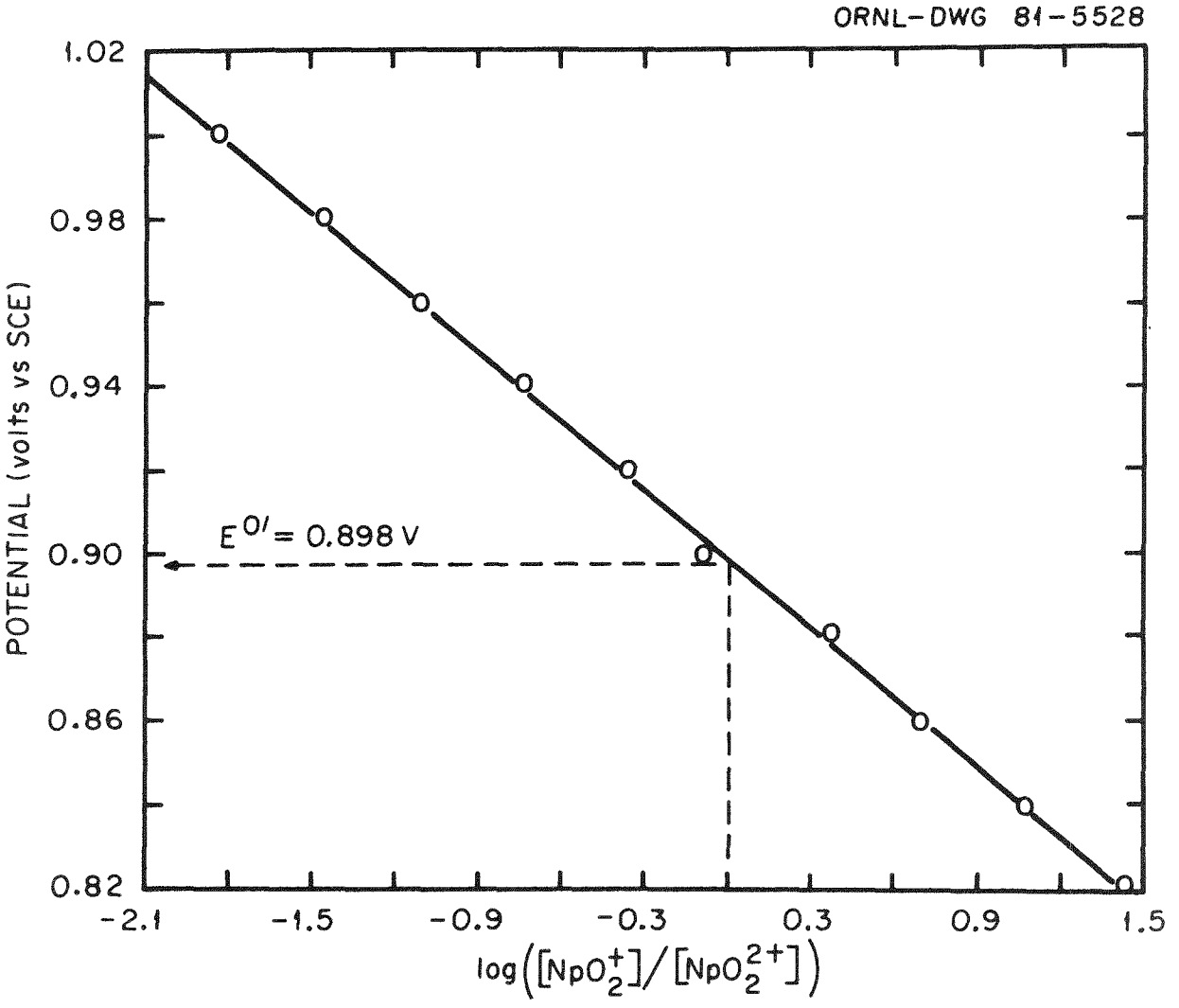

Figure 34. Nernstian plot for the Np(VI)/Np(V) redox couple in 1 M $HClO_4$.

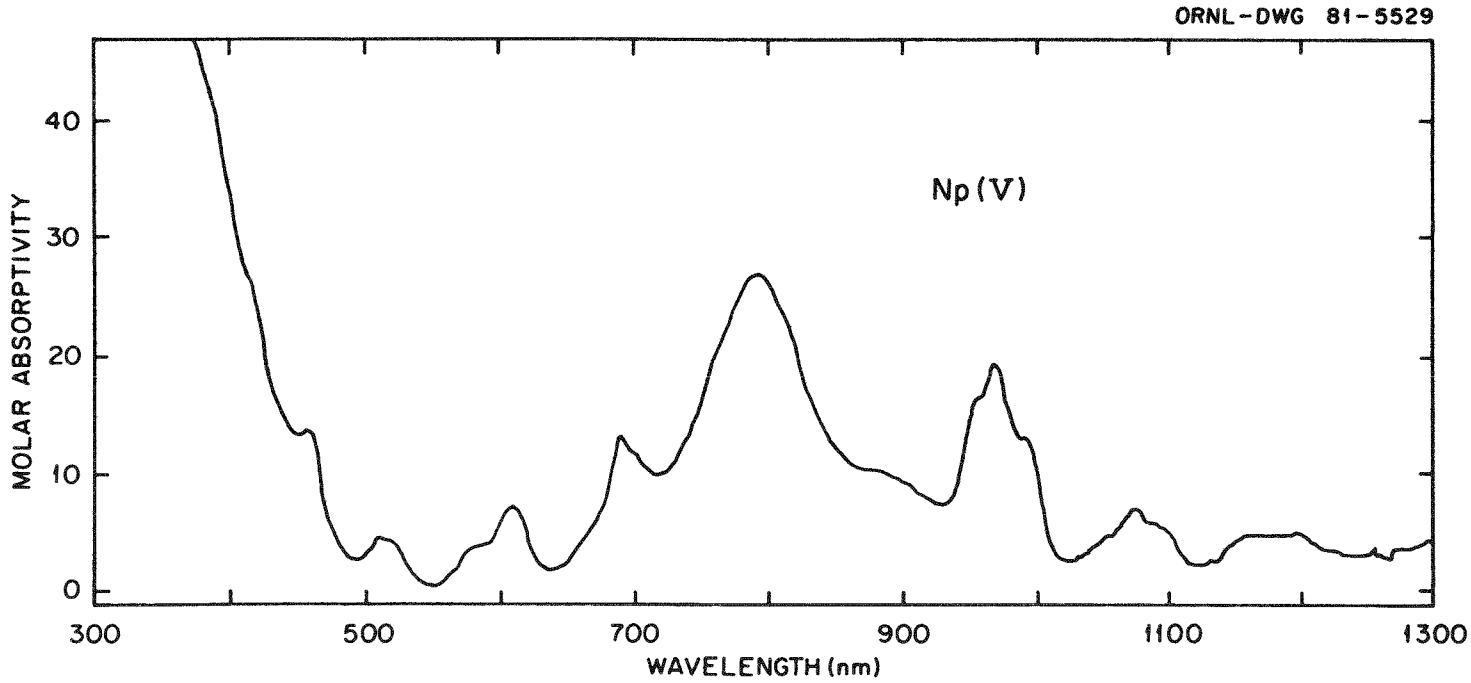

Figure 35. Solution absorption spectrum of Np(V) in 2 M Na_2CO_3.

Voltammograms of Np(VI) in 2 M Na_2CO_3 at pH 13 were recorded at a platinum wire microelectrode. A representative voltammogram is shown in Figure 36. The voltammogram indicates a reversible reaction for the Np(VII)/Np(VI) redox couple. Successive potential sweeps were reproducible, and an $E^{o'}$ value was determined from the voltammogram to be 0.46 ± 0.01 V.

Bulk solution electrolysis at 0.80 V of the yellow-green Np(VI) species in 2 M Na_2CO_3 at pH 13 results in the formation of a dark green solution of Np(VII). The solution absorption spectra of Np(VI) and Np(VII) in this medium are shown in Figure 37. The Np(VI) spectrum exhibits no features other than an UV cut-off at about 400 nm. The Np(VII) spectrum is nearly identical to that in 1 M LiOH (see Figure 32, page 97).

The Raman spectra of the Np(VI) and electrogenerated Np(VII) species in carbonate solution were recorded in an effort to further characterize these ions. The 514.5 nm line of the argon ion laser was used at 100 mW output for Raman excitation. The Raman spectra of Np(VI) and Np(VII) in 2 M Na_2CO_3 are shown in Figure 38. The observed vibration frequencies of the Np(VI) and Np(VII) ions in this medium are in close agreement with those reported by Basile et al.[100,101] which suggests that the structure of the Np(VII) species is at least very similar to that which it exhibits in molar hydroxide solutions, where it is in the linear NpO_2^{3+} form. The fact that the same number of oxygen atoms surround the Np(VI) and Np(VII) ions in this medium is also evidenced by the similarity of their absorption spectra and the reversibility of the Np(VII)/Np(VI) redox couple.

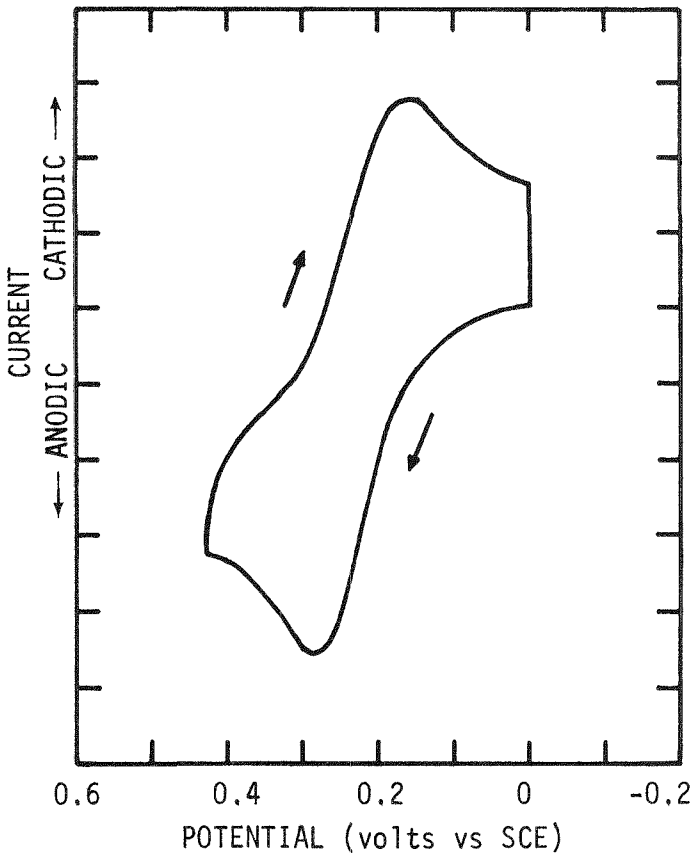

Figure 36. Cyclic voltammogram of Np(VI) in 2 M Na_2CO_3 at pH 13. Pt electrode, sweep rate: 50 mV/s, [Np(VI)] = 10^{-3} M.

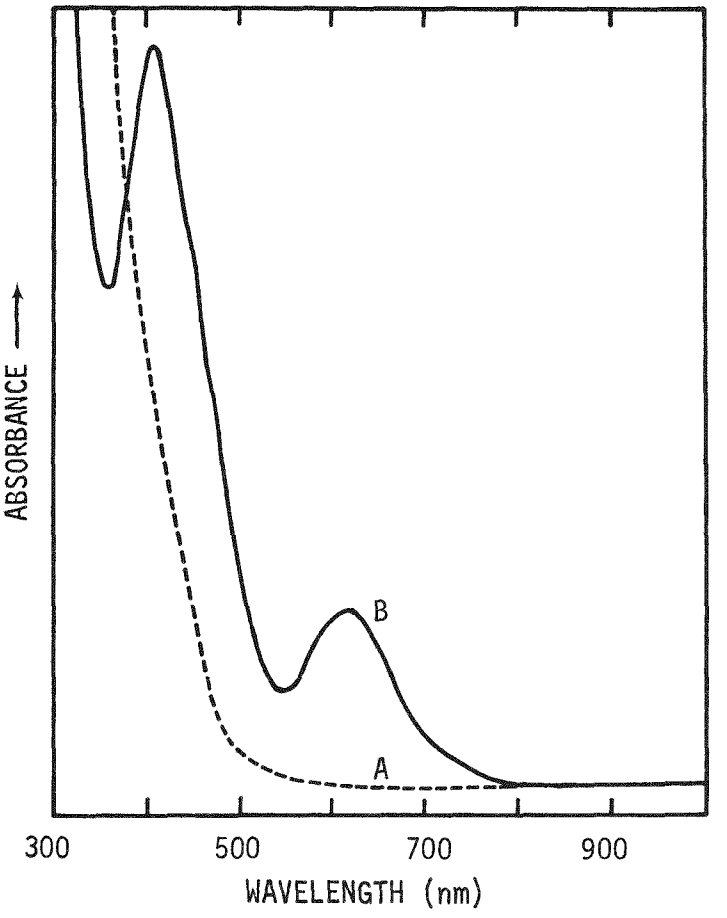

Figure 37. Solution absorption spectra of Np(VI) (A) and Np(VII) (B) in 2 M Na_2CO_3 at pH 13.

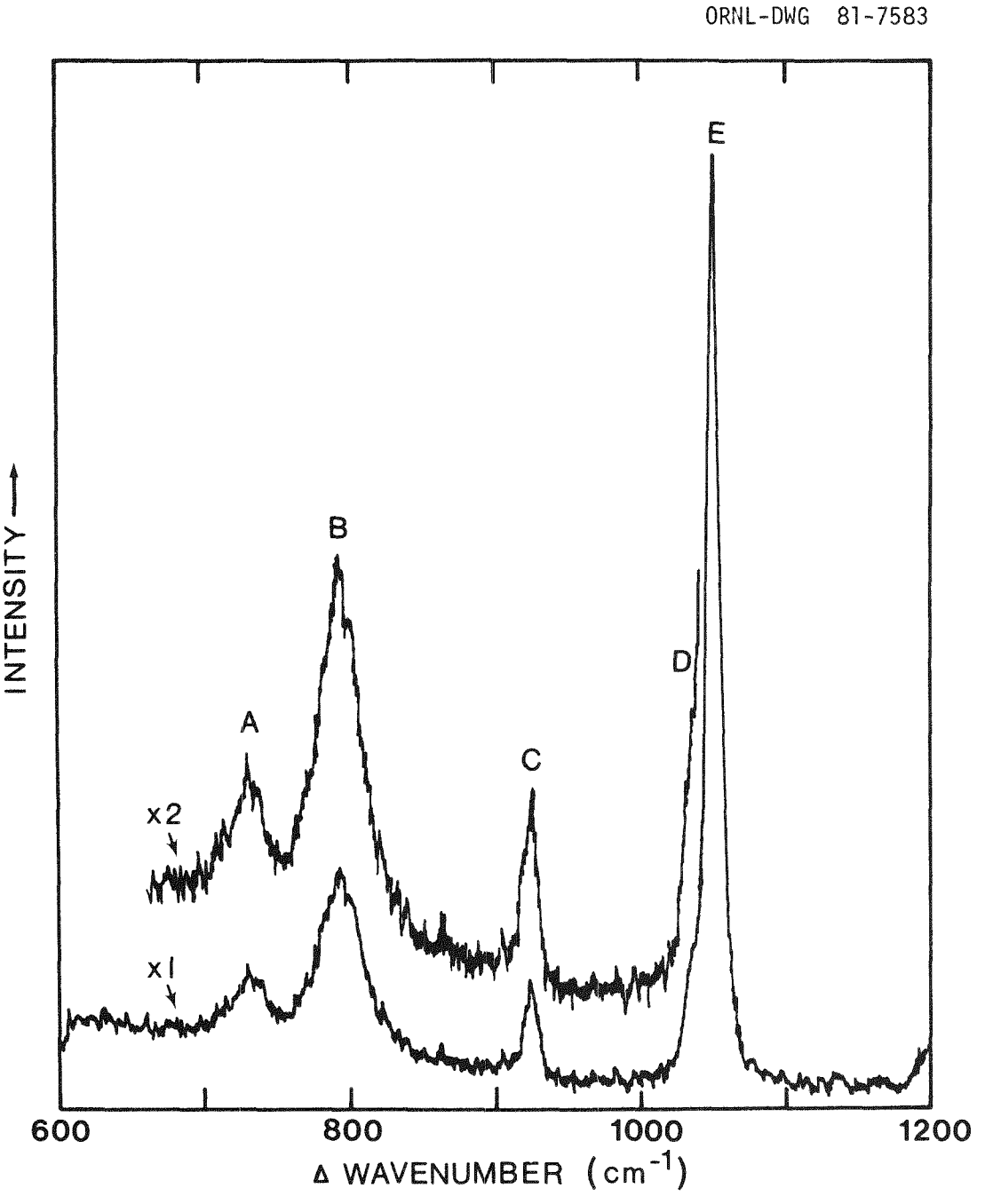

Figure 38. Raman spectra of Np(VI) and Np(VII) in 2 M Na_2CO_3 at pH 13. NpO_2^{3+} (A), NpO_2^{2+}, (B), ClO_4^- (C), complexed CO_3^{2-} (D), and free CO_3^{2-} (E).

3. Americium

The oxidation states of americium are reasonably stable in aqueous media, with the exception of Am(IV), which tends to disproportionate. It is possible to stabilize Am(IV) in strongly complexing aqueous solutions. Previous work, presented earlier in this report, concerning the stabilization of Pr(IV) and Tb(IV) in concentrated carbonate solution suggested the possibility of generating and stabilizing Am(IV) in the same medium.[87]

The study of Am(IV) in concentrated fluoride solutions is also of interest because of the stability provided by fluoride ion complexation[61] and the possibility of ataining higher oxidation states in this medium by electrochemical means.

a. Am(IV)/Am(III) redox couple. The oxidation of Am(III) was studied in 2 M $(NH_4)_2CO_3$, 2 M Na_2CO_3, 5.5 M K_2CO_3, and 5 M Cs_2CO_3. The pH of these solutions was adjusted to various values, with the exception of the ammonium carbonate solution, which is self-buffered at pH 9.5.

Cyclic voltammograms of the Am(IV)/Am(III) redox couple were recorded in 2 M Na_2CO_3 and 5.5 M K_2CO_3 at various pH values. Cyclic voltammograms recorded in the sodium carbonate solution are shown in Figure 39. Voltammogram A was recorded at pH 12.5 in 2 M Na_2CO_3; the oxidation wave is partially obscured by the oxygen gas discharge wave. There is no evidence for a corresponding reduction wave, so the electrochemical reaction is irreversible under these conditions. In an attempt to separate the two oxidation waves, the pH of the carbonate solution was lowered by bubbling CO_2 gas through it. This generated a mixture of carbonate-bicarbonate species in the solution.

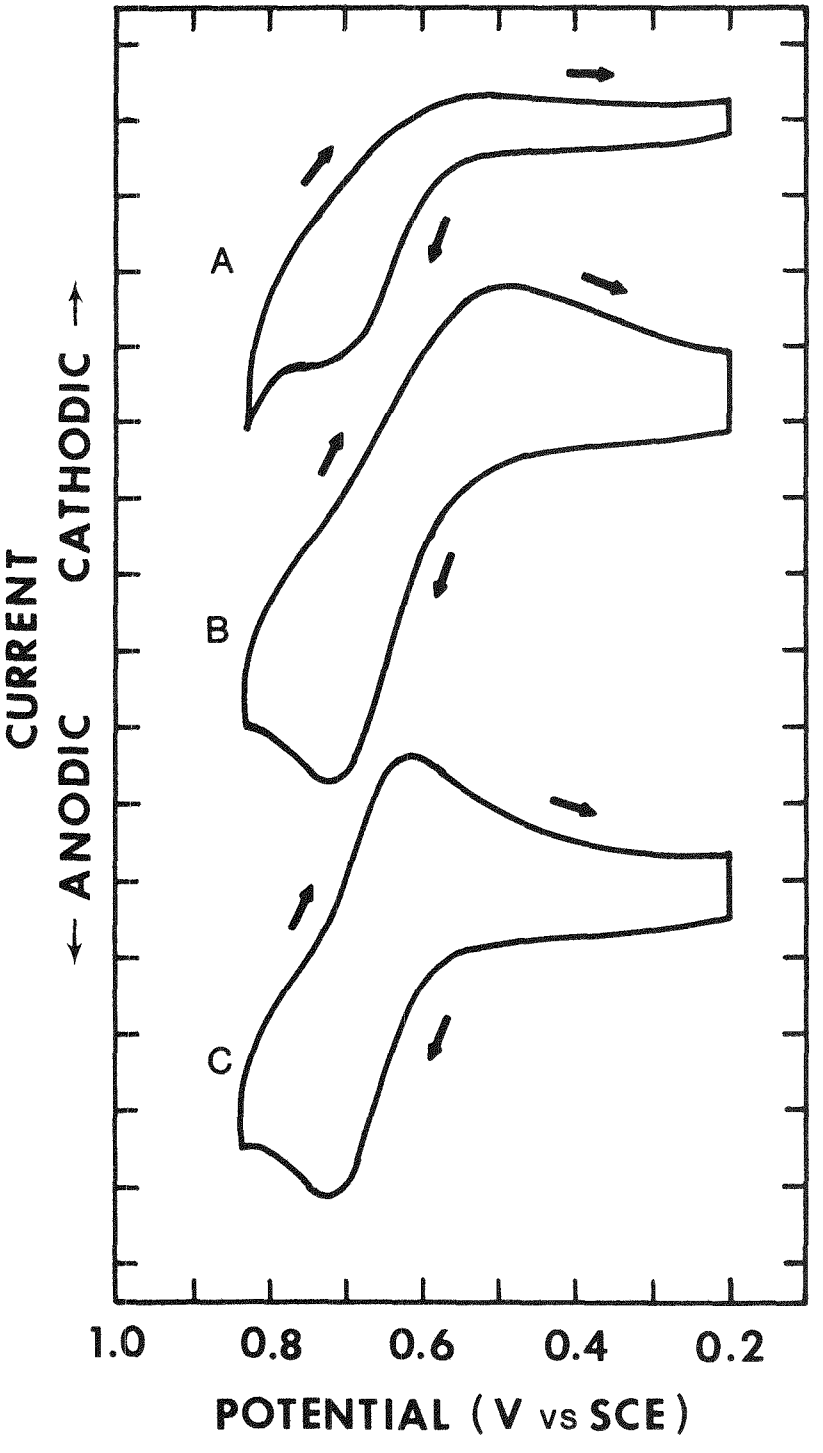

Figure 39. Cyclic voltammograms of Am(III) in 2 M Na_2CO_3 at various pH values. pH 12.5 (A), pH 10.2 (B), and pH 9.7 (C), Pt electrode, sweep rate: 50 mV/s, [Am(III)] = 1.0×10^{-3} M.

The voltammogram (B in Figure 39) recorded at pH 10.2 following the CO_2 treatment exhibited the Am oxidation wave more clearly because of the shift of the oxygen discharge wave to a more anodic potential. In addition, a reduction wave was also visible. Following a second CO_2 treatment, yielding a solution of pH 9.7, the voltammogram (C in Figure 39) indicated that the Am(IV)/Am(III) redox couple became more reversible. The limit of this experimental approach was reached at pH 8 where Am precipitated as $Am(OH)_3$. A formal reduction potential for the Am(IV)/Am(III) redox couple was estimated from the reversible cyclic voltammogram to be 0.92 $\pm$ 0.01 V. Assuming the same shift in potential for the Am(IV)/Am(III) couple as was observed for the Ce(IV)/Ce(III) redox couple in this medium, a standard reduction potential (E°) for the Am couple was estimated to be 2.62 $\pm$ 0.01 V.

Cyclic voltammograms of the Am(III) species in 5.5 $\underline{M}$ K_2CO_3 (pH 12.7) were not very useful because the oxygen gas discharge wave obscured the Am(III) oxidation wave. The K_2CO_3 solution was adjusted to pH 14 in an effort to reproduce the conditions under which Pr(IV) and Tb(IV) were generated. Since cyclic voltammetry was not useful at this high pH, bulk solution electrolysis followed by spectrophotometry was performed at constant potential in a Teflon spectroelectrochemical cell holder. The conventional three electrode system was used without separate compartments for the counter and reference electrodes. This was necessary because of the limited quantity of Am which was available for the first experiments. A platinum screen was used as the working anode. RVC was used for some experiments where the potential at which RVC is destroyed was not approached. [RVC can be

oxidized at potentials in excess of 1 V in strong carbonate solutions resulting in a yellow discoloration of the solution.]

Solution absorption spectra were recorded prior to and after bulk electrolysis. The solution absorption spectra of Am(III, IV, V, and VI) are shown in Figure 40. These spectra were adapted from the work of Schulz[102] and were taken in 1 M $HClO_4$, with the exception of Am(IV) which was in 10 M H_3PO_4. The solution absorption spectrum of Am(III) in 5.5 M K_2CO_3, prior to electrolysis, is shown in Figure 41. A potential was applied to the cell and was increased to more positive values until a change was noted visually or in the recorded spectrum. At 0.94 V the initially pink-tan solution of Am(III) became golden-brown and exhibited the spectrum shown in Figure 41. Since oxygen gas was generated simultaneously at the platinum working anode, the oxidation of Am(III) was slow; only partial oxidation to Am(IV) is indicated by the spectrum in Figure 41.

A value for the formal reduction potential of the Am(IV)/Am(III) redox couple was approximated from the potential (0.94 V) at which Am(IV) was first observed. Assuming the shift in potential provided by carbonate ion complexation to be 1.7 V, a value for E° of the Am(IV)/Am(III) couple of 2.65 $\pm$ 0.05 V was calculated.[103] This value agrees well with that derived from the results of cyclic voltammetry discussed above and with the 2.62 $\pm$ 0.05 V value reported by Morss and Fuger.[104]

Bulk solution electrolysis of Am(III) in 2 M Na_2CO_3 was performed using larger volumes of solution and separate (Vycor frits) cell compartments for the reference and counter electrodes. A potential

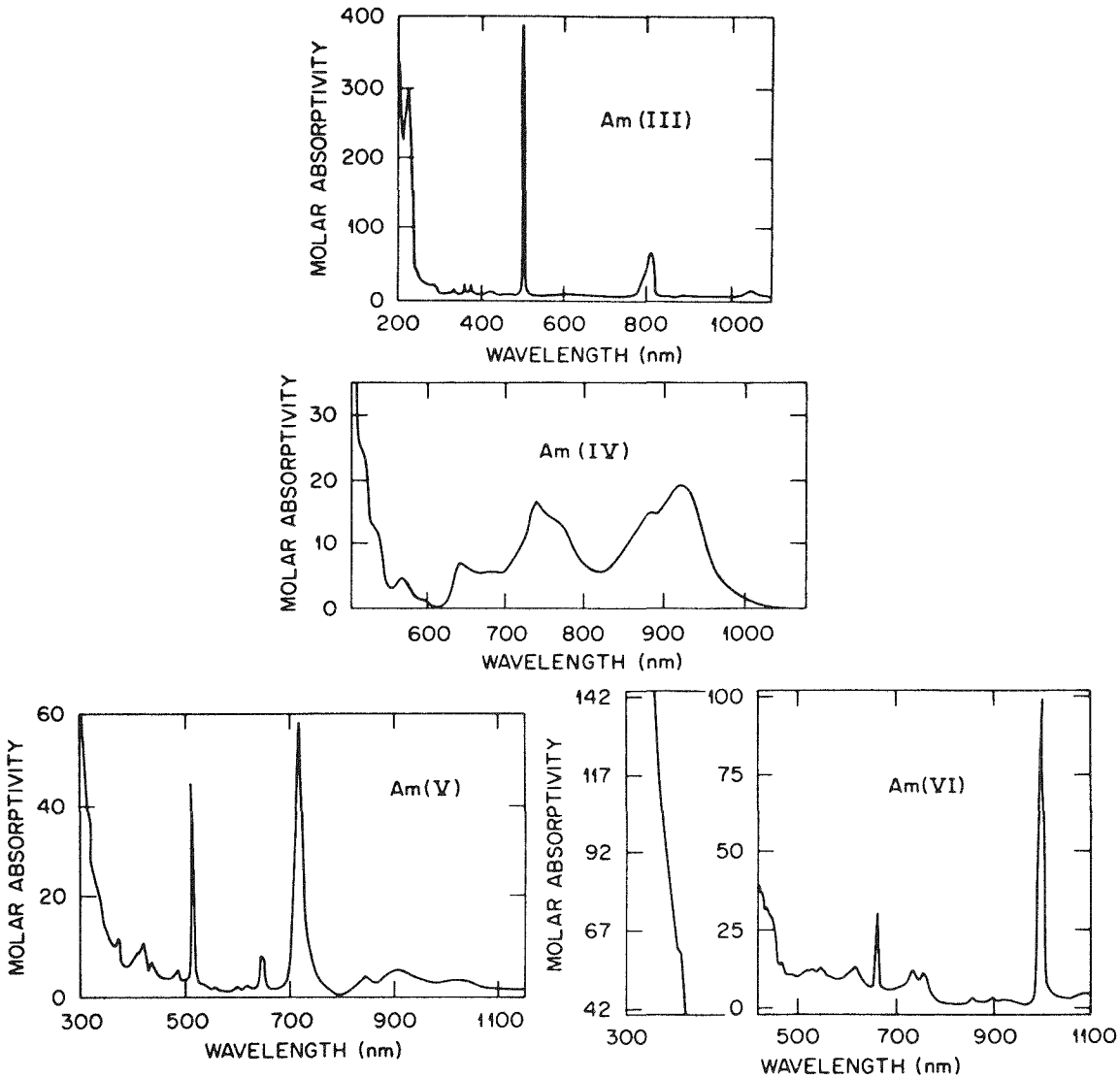

Figure 40. Solution absorption spectra of Am(III, IV, V, and VI). Am(IV) in 10 M H_3PO_4, others in 1 M $HClO_4$.

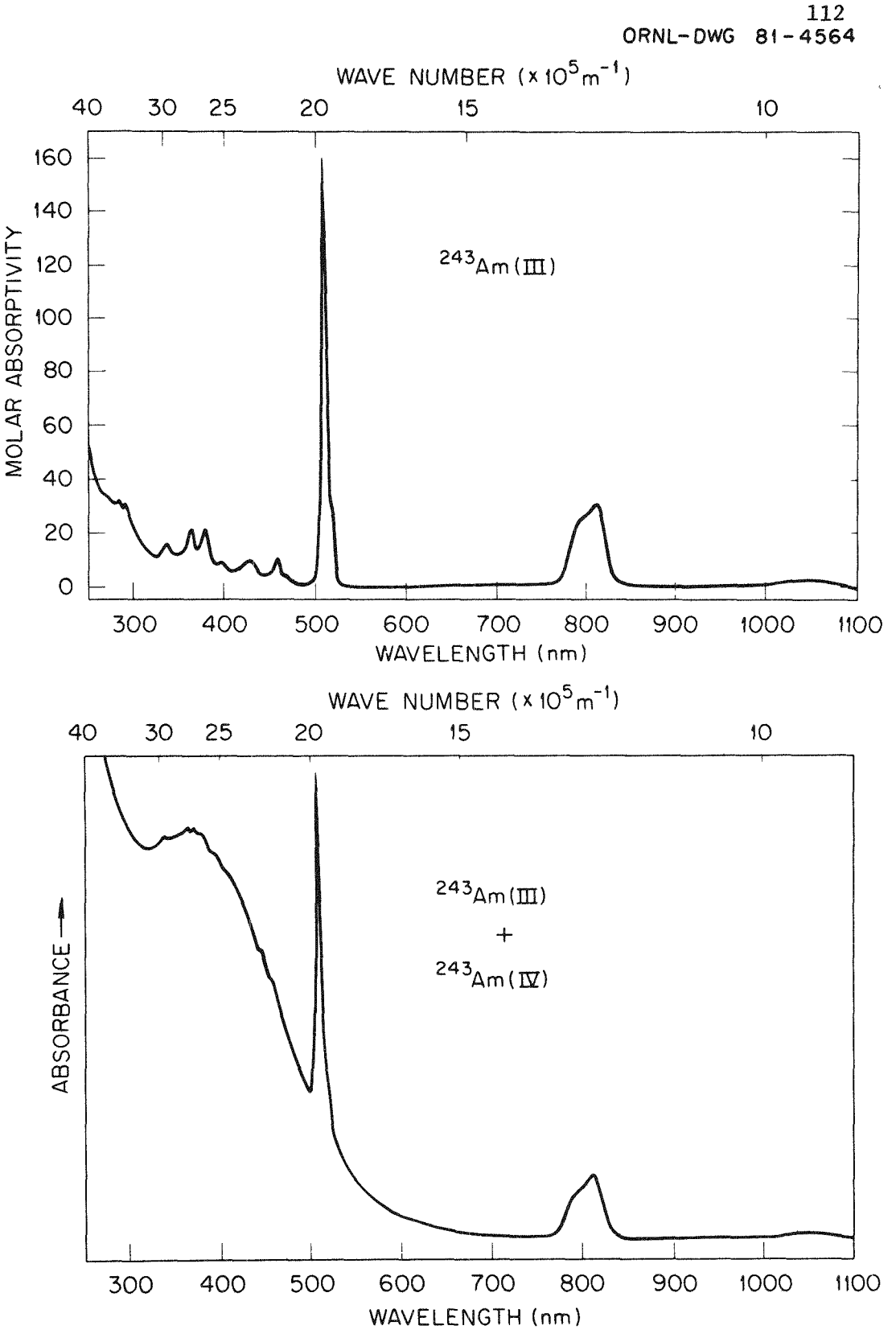

Figure 41. Solution absorption spectra of Am(III) and Am(III) plus Am(IV) in 5.5 M K_2CO_3.

of 1 V was applied to the cell, corresponding to a potential just beyond the anodic peak potential observed in the cyclic voltammogram. Stirring was provided by bubbling N_2 gas through the solution. Within a few minutes, the pink-tan solution turned golden yellow and then dark orange-brown. The spectra of the initial Am(III) solution and the Am(IV) oxidation product in 2 M Na_2CO_3 are shown in Figure 42. The absorption peak of Am(IV) at about 360 nm was determined to have a molar absorptivity near 2200. This value was based on a determination of the Am concentration by alpha counting techniques.

Am(III) was also oxidized at 1.0 V at a Pt screen anode in 2 M $(NH_4)_2CO_3$ and in 5 M Cs_2CO_3 with the same results as described above. A difference was noted, however, in the solubility of the Am chloride and hydroxide solids in the various carbonate solutions. The solubility was good and dissolution was rapid in the 5.5 M K_2CO_3 and in the 5 M Cs_2CO_3. The solubility was reduced in 2 M Na_2CO_3 and 2 M $(NH_4)_2CO_3$. It is evident that the solubility of the Am compounds is a function of the pH of the carbonate solution.

The Am(IV)/Am(III) redox couple was also studied in concentrated fluoride solution. Solid AmF_4 and Cs_3AmF_7 (2 to 3 mg), prepared under anhydrous conditions, were dissolved in concentrated HF saturated with CsF (about 12 M HF and 15 M CsF). The solids dissolved readily at room temperature. The resultant solution was placed in a plastic cuvet, and the absorption spectrum was recorded. The spectrum, shown in Figure 43, exhibited absorbances due only to Am(IV) and was nearly identical to that of Am(IV) in the solid state (as AmF_4)[105] and in 13 M NH_4F solution.[106] With time, the Am(IV) solution was reduced to Am(III) by

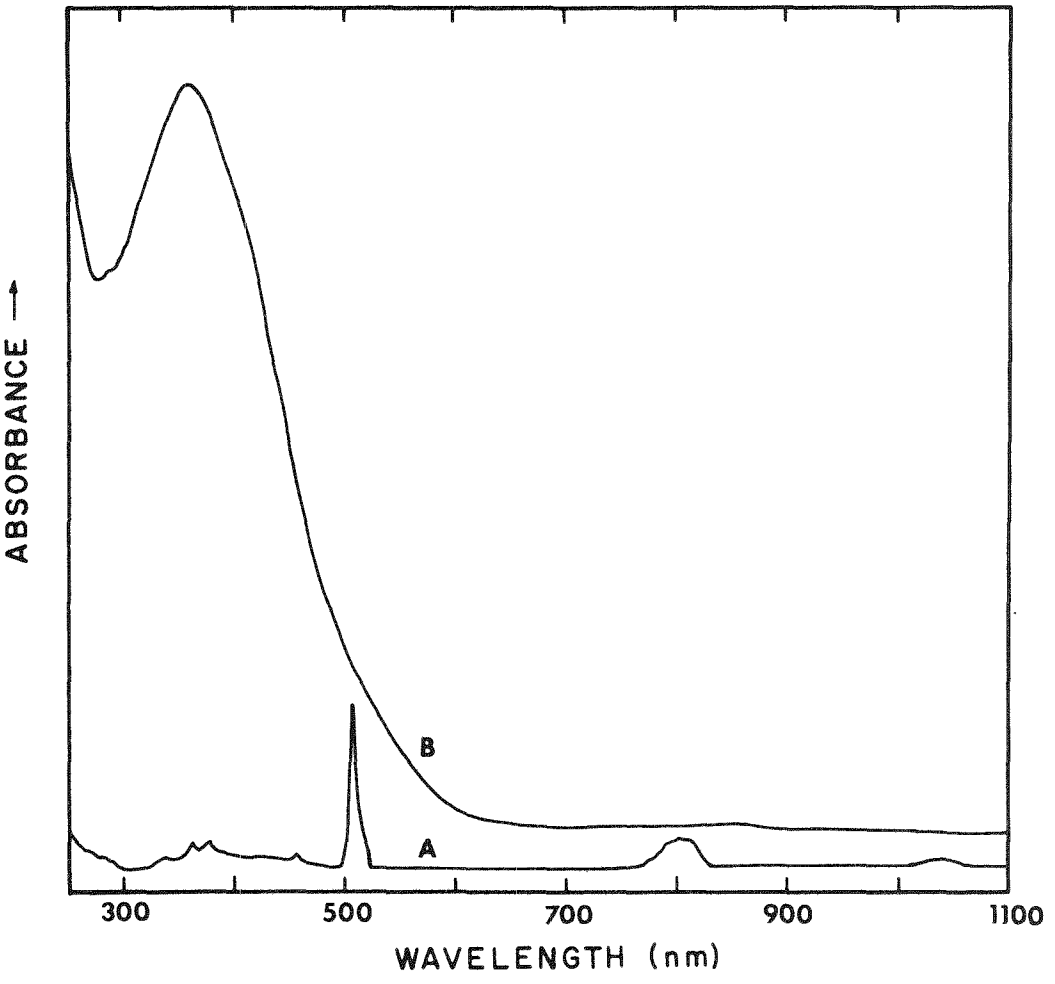

Figure 42. Solution absorption spectra of Am(III) (A) and Am(IV) (B) in 2 M Na_2CO_3. pH 9.5.

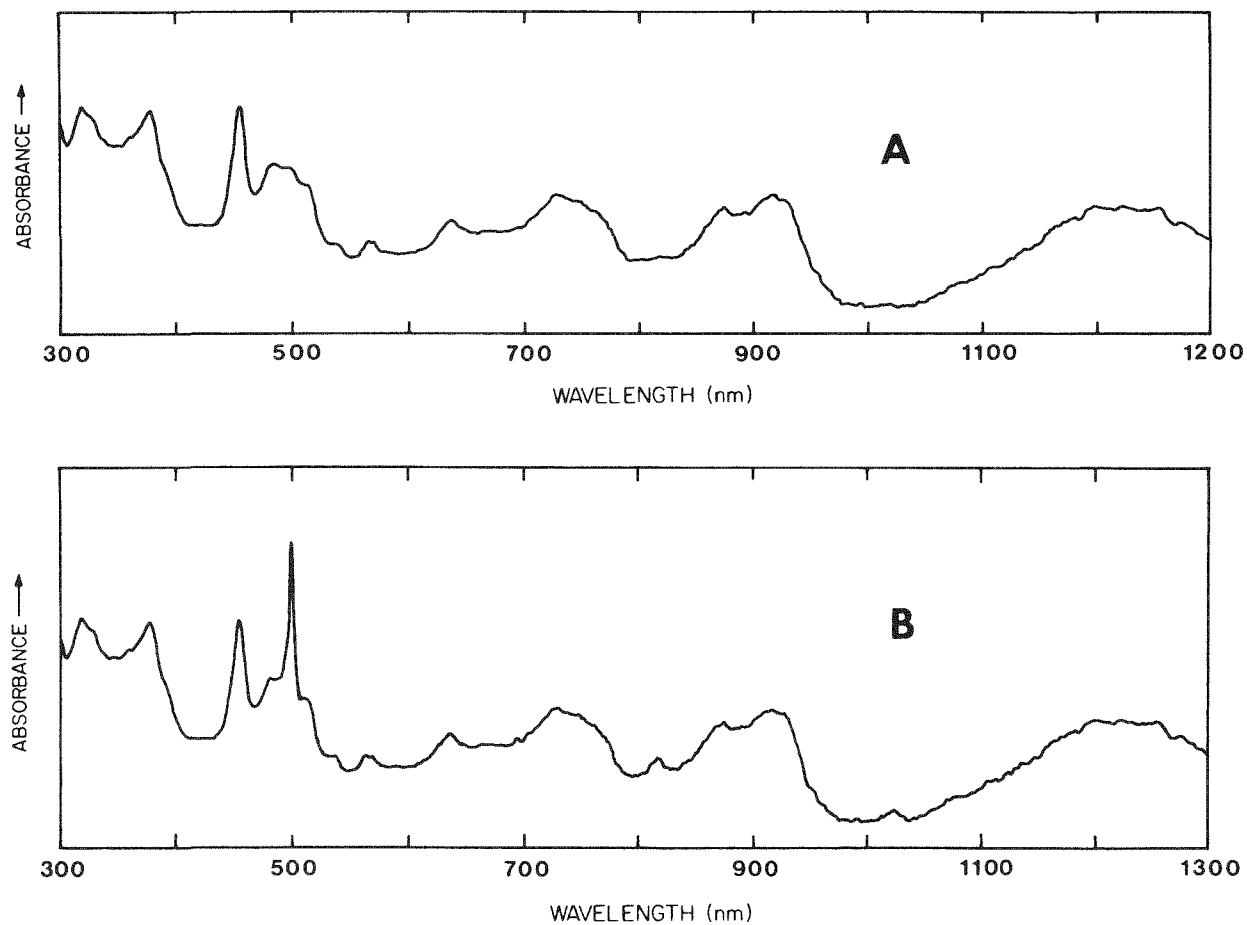

Figure 43. Solution absorption spectra of Am(IV) (A) and Am(IV) plus Am(III) (B) in concentrated HF saturated with CsF.

radiolysis products. Am(III) was, for the most part, insoluble in HF-CsF solution; however, a sufficient quantity was soluble to exhibit the characteristic Am(III) absorption peak at 500 nm. The spectrum of this mixture of Am(IV) and reduction product Am(III) in HF-CsF is shown in Figure 43.

Voltammetric study of the Am(IV) species in HF-CsF solution was not useful because of the large background currents at the RVC and Pt working electrodes. Therefore, bulk solution electrolysis was performed in an effort to oxidize the Am(IV) species to higher oxidation states. Electrolysis experiments were conducted from 30 min to 1 hr from 0.95 to 2.34 V at RVC and Pt electrodes. The absorption spectra recorded after electrolysis show a significant decrease in the Am(IV) present and an increase in the absorption peak of Am(III) at 500 nm; in addition, more solid AmF_3 was formed than that present at the start of electrolysis which indicated a reduction rather than an oxidation. At the potential applied Am(IV) was reduced to Am(III). Therefore, the $E^{\circ\prime}$ for the Am(IV)/Am(III) redox couple in this medium is probably more positive than the anodic potential limit of RVC and Pt in HF-CsF solution, i.e., more positive than 2.34 V vs NHE.

Chemical oxidation of Am(IV) in HF-CsF solution was performed with ozone and peroxydisulfate-silver(I) oxide. The Am(IV) was oxidized quantitatively, but the initial solid AmF_3 present in the solution was unaffected. The oxidation of Am(IV) to Am(VI) has been reported in 13 M NH_4F,[105] in which the spectrum of Am(VI) was obtained. No spectrum attributable to Am(VI) was observed in the present work; however, additional solid may have been formed, reflecting a reduced solubility of Am(VI) in HF-CsF solution as compared to that in 13 M NH_4F.

b. Am(V)/Am(IV)/Am(III) redox couples. As previously stated, Am(III) is oxidized to soluble Am(IV) at a potential of 0.94 V in 5.5 M K_2CO_3. Increasing the potential applied to 1.10 V resulted in the formation of a dark tan precipitate. A portion of this precipitate was collected and dissolved in 1 M $HClO_4$. The spectrum of the resultant solution was that of Am(V), identical to the spectrum shown in Figure 40, page 111. A portion of the dark tan solid was collected, rinsed with alcohol, dried in air, and placed in a capillary tube for X-ray powder diffraction and microscope spectrophotometric analyses. The compound was identified as a potassium AmO_2^+ double-carbonate salt [$K_3AmO_2(CO_3)_2$ or $K_5AmO_2(CO_3)_3$ depending on the pH of the carbonate solution and the time of standing of the precipitate in contact with the solution]. Similar results were obtained in 5 M Cs_2CO_3 at potentials exceeding 1.10 V except that the solid was a cesium AmO_2^+ double-carbonate salt. No solid formation was detected when the oxidation was performed in 2 M Na_2CO_3 solution. At potentials higher than 1.10 V the Am(V) was generated as a soluble species in 2 M Na_2CO_3. No characteristic Am(V) spectrum was observed in the Na_2CO_3 solution. However, upon addition of KOH to a mixture of Am(IV) and Am(V) in carbonate solution, the orange-brown color, due to Am(IV), disappeared, and a colorless solution resulted. The spectrum of this colorless solution is shown in Figure 44, spectrum A. The solution was acidified with HNO_3 and spectrum B in Figure 44 was recorded. Both spectra are probably those of Am(V). The shifts in the absorbance peaks of Am(V) in the carbonate solution compared to those in the acid medium can be

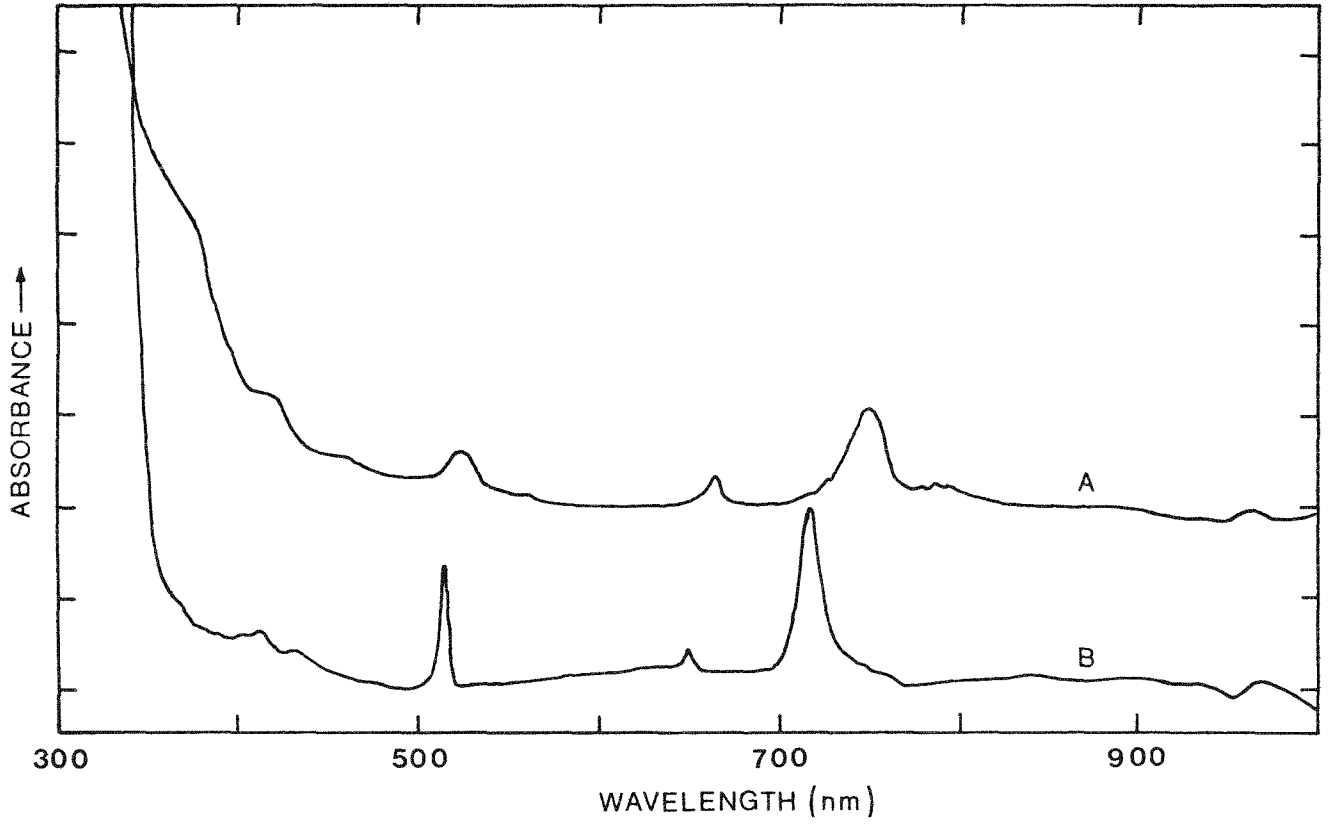

Figure 44. Solution absorption spectra of Am(V) in 2 M Na_2CO_3-KOH (A) and in 1 M HNO_3 (B).

attributed to strong complexation by carbonate and/or hydroxide ions. Although the solution yielding spectrum B was more dilute in Am(V), the peaks are more intense due to the higher molar absorptivity of Am(V) in acid solution.

It is not clear if Am(V) was produced by direct oxidation of Am(III) or by the oxidation of stable Am(IV) in carbonate media. The potential at which Am(V) was generated was well beyond the useful range of the RVC or Pt electrode. Therefore, no voltammetric measurements could be made to aid in the elucidation of the redox reaction mechanism. It is obvious, however, that Am(V) production in carbonate media was not the result of the disproportionation of Am(IV), since no Am(V) was produced at potentials less than 1.0 V.

c. Am(VI)/Am(V)/Am(IV)/Am(III) redox couples. In an effort to further characterize the oxidation products of americium in carbonate solutions, and in particular to substantiate the identity of the stable Am(IV) species, chemical oxidations of the Am(III) solutions were performed. Am(III) solutions in 2 M Na_2CO_3 were oxidized to Am(VI) by sodium peroxydisulfate-silver(I) oxide, as described elsewhere.[105] The resulting red-brown solution closely resembled (by eye) the coloration of the Am(IV) solution which was electrochemically generated. The spectrum of the Am(VI) solution was recorded and compared directly to that of Am(IV) in the same medium. The spectra exhibited only insignificant differences in the position and slope of the UV cut-off shoulders.

A stock solution of Am(III) in 2 M Na_2CO_3 was divided in half. One half was oxidized electrochemically at 0.98 V for 2 to 3 hours to generate Am(IV). The other half was oxidized by peroxydisulfate-silver(I) oxide to Am(VI) and the two solutions, equal in Am concentration, were compared. The Am(VI) solution was darker than the Am(IV) solution, and there was a subtle difference in the shades of the red-orange to red-brown solutions. The spectra of these two solutions were quite similar except for the low-intensity absorption peak of Am(VI) at about 1000 nm.

Since spectral evidence was not particularly conclusive in distinguishing between Am(IV) and Am(VI) in carbonate solutions, other chemical methods were utilized. The two previously mentioned solutions with equal concentrations of Am(IV) and Am(VI) were both acidified with HNO_3, and their absorption spectra recorded. The solution containing Am(VI) in Na_2CO_3 yielded only the spectrum of Am(VI) in acid medium (see Figure 40, page 111). Upon acidification of the Am(IV) species in Na_2CO_3 medium, no spectrum of acidic Am(IV) was evident, but equal quantities of Am(III) and Am(V) were observed. These species result from the disproportionation of Am(IV).

Additional characterization of Am(IV) in carbonate solution included spectrophotometric and potentiometric titrations with $K_4Fe(CN)_6$ in 2 M Na_2CO_3. The $[Fe(CN)_6]^{3-}/[Fe(CN)_6]^{4-}$ redox couple was determined[107] to be reversible in 2 M Na_2CO_3 and have an E°' value of 0.50 ± 0.01 V. Stock solutions of Am(IV) in 2 M Na_2CO_3 at pH 9.7 were prepared by bulk solution electrolysis at a constant potential of

0.95 V. The electrolysis was continued until the current was constant. Aliquots of these solutions were removed and diluted for alpha counting analysis. A known volume of the Am(IV) stock solution was placed in a quartz cuvet, and an initial spectrum was recorded. The spectra of Am(IV) and Am(III) as a function of titrant added are displayed in Figure 45. Spectrum A is exclusively that of Am(IV). As titrant was added (spectra B through E), additional Am(III) was produced until all of the Am(IV) was reduced to Am(III) (spectrum F). The data obtained from the spectrophotometric titration are listed in Table IX. The absorbance of the 508 nm peak of Am(III) was used and a dilution factor was accounted for during the titration. A plot of the Am(III) absorbance vs volume of titrant added is given in Figure 46.

It was found from the data obtained in the spectrophotometric titration that 0.88 equivalent of $Fe(CN)_6^{4-}$ was required to reduce one equivalent of the higher-oxidation-state Am species to Am(III). Although this determination yielded a value less than the one equivalent required to reduce Am(IV) to Am(III), it does support a one-electron reduction rather than the two- or three-electron reduction required for Am(V) and Am(VI), respectively. The results of the spectrophotometric titration were checked and verified by alpha counting the samples again and submitting the ferrocyanide solution to ORNL Analytical Chemistry Division for quantitative analysis.

Potentiometric titrations of the Am(IV)-Na_2CO_3 solution were also performed to obtain additional verification of the identity of the higher oxidation state of americium. The results of two separate

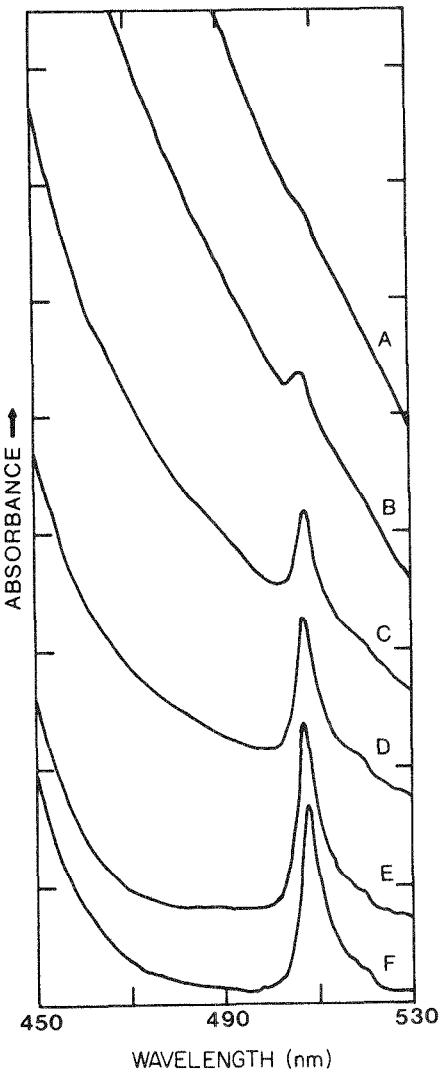

Figure 45. Solution absorption spectra of Am(IV) and Am(III) as a function of titrant added during a spectrophotometric titration of Am(IV) with ferrocyanide solution. 0 L (A), 50 L (B), 100 L (C), 150 L (D), 175 L (E), and 200 L (F).

TABLE IX

DATA FROM THE SPECTROPHOTOMETRIC TITRATION OF Am(IV) WITH FERROCYANIDE SOLUTION[a]

Volume of titrant (μL)	Am(III) absorbance	Dilution factor	Am(III) absorbance (corrected)
0	0.0075	1.000	0.0075
50	0.0280	1.100	0.0308
100	0.0825	1.200	0.0990
150	0.1250	1.300	0.1625
175	0.1575	1.350	0.2130
200	0.1600	1.400	0.2240
225	0.1600	1.450	0.2320
250	0.1540	1.500	0.2310
275	0.1500	1.550	0.2325
325	0.1470	1.650	0.2426

[a]Concentration of titrant: 5.34×10^{-3} M. Volume of titrant required: 203 μL. Initial volume of Am: 500 μL. Concentration of Am: 2.46×10^{-3} M (from alpha counting). Equivalents of titrant per equivalent of Am: 0.88.

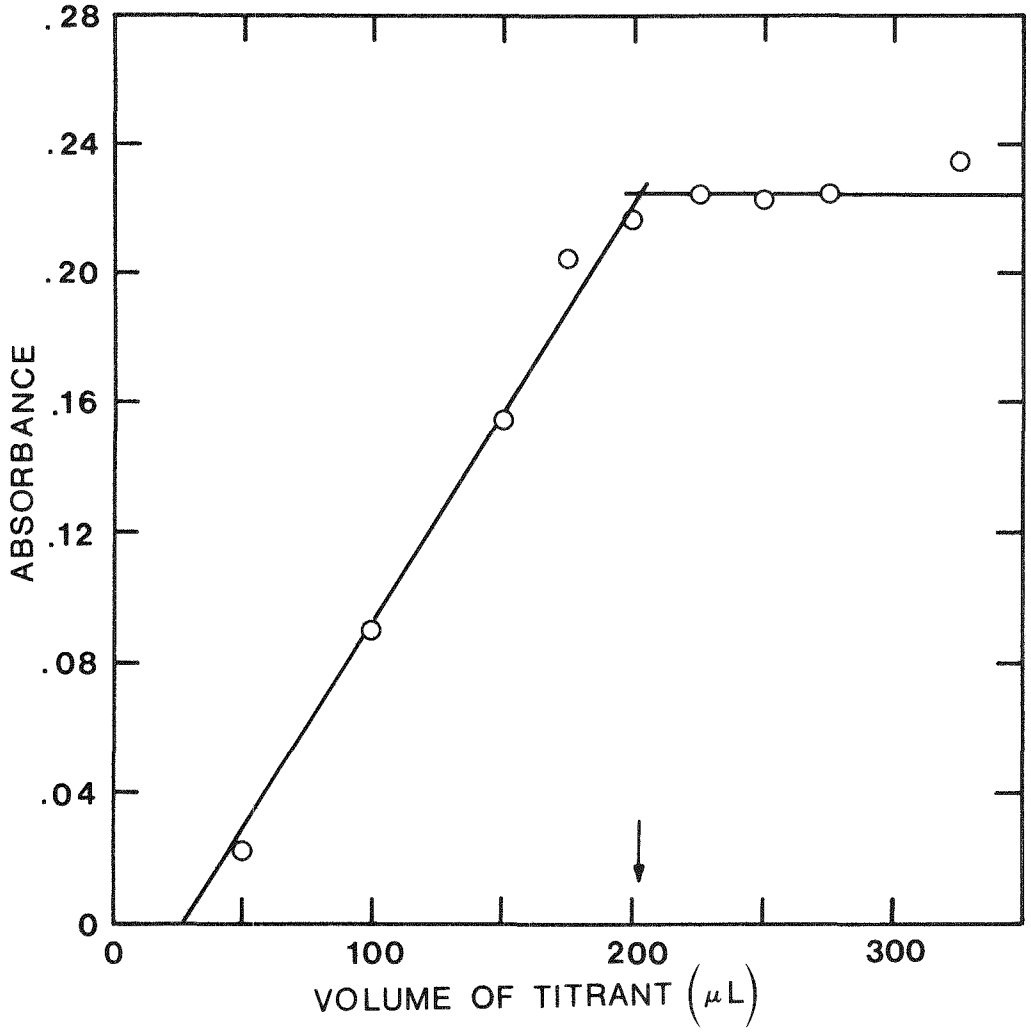

Figure 46. Absorbance vs volume of titrant added in the spectrophotometric titration of Am(IV) with ferrocyanide solution. Absorbance constant at 508 nm.

experiments yielded 0.94 and 0.62 equivalents of ferrocyanide to reduce one equivalent of the Am to Am(III). The data for one potentiometric titration are presented in Table X, and the titration curve is shown in Figure 47. Both titration experiments suggest a one-electron reaction, indicating reduction of Am(IV) to Am(III). The reason why all the determinations yielded a lower number of equivalents than expected for a one-electron reduction is not immediately clear. No complications were indicated by the results of the cyclic voltammetry experiments within the potential range of the electrodes in this solution. The reversibility of the voltammetric wave indicates that only the Am(IV)/Am(III) redox couple is involved, since the higher oxidation states of Am involve the dioxo-cation species AmO_2^+ and AmO_2^{2+}. The exchange of oxygen is required in any redox couple involving Am(III) and Am(V) or Am(VI), and these reactions are not reversible at an electrode.

The spectroscopic and electrochemical results combined with those of the chemical tests and the spectrophotometric and potentiometric titrations support the evidence for a reversible Am(IV)/Am(III) redox couple in concentrated carbonate solution. The stable Am(IV) species may be oxidized electrochemically to Am(V) or to Am(VI). The existence of stable Am(IV) in concentrated carbonate solution has not, to the knowledge of this author, been reported previously.

4. Curium

Because of its lower specific activity and its current availability in milligram quantities, curium-248 is the Cm isotope

TABLE X

DATA FROM THE POTENTIOMETRIC TITRATION OF Am(IV) WITH FERROCYANIDE SOLUTION[a]

Volume of titrant (μL)	Potential (mV vs SCE)	Volume of titrant (μL)	Potential (mV vs SCE)
0	691	700	311
50	676	750	295
100	668	800	285
150	658	850	278
200	650	900	273
250	641	950	268
300	633	1000	264
350	624	1050	264
400	615	1100	261
450	602	1150	258
500	592	1200	255
550	578	1250	253
600	548	1300	251
650	356		

[a]Concentration of titrant: 5.34×10^{-3} M. Volume of titrant required: 650 μL. Initial volume of Am: 1500 μL. Concentration of Am: 2.46×10^{-3} M (from alpha counting). Equivalents of titrant per equivalent of Am: 0.94.

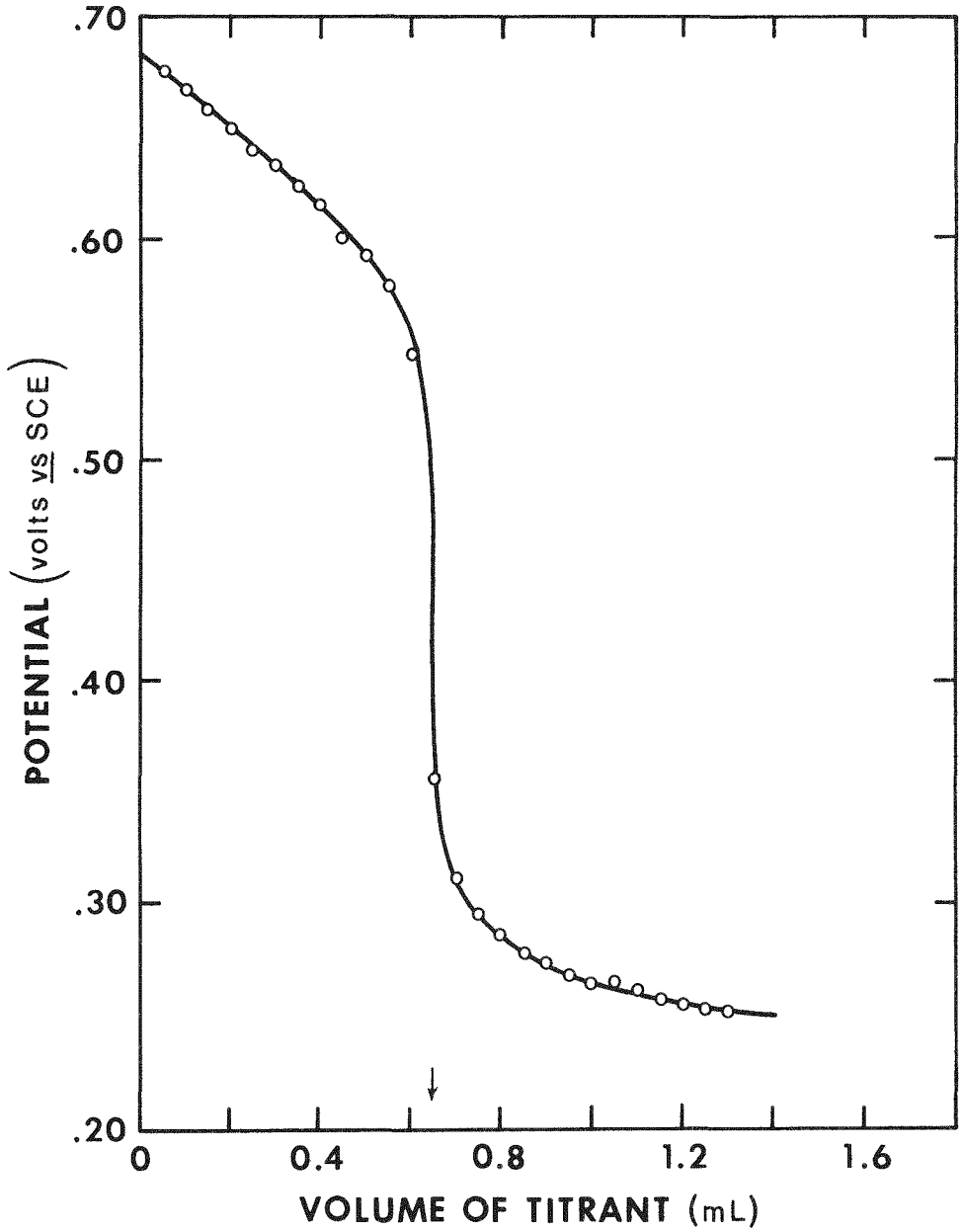

Figure 47. Potential vs volume of titrant added for the potentiometric titration of Am(IV) with ferrocyanide solution.

best suited for electrochemical and spectroscopic studies. Curium is known in two oxidation states, Cm(III) and Cm(IV), in aqueous solution as well as in the solid state. Although Peretrukhin *et al.*[108] reported the existence of Cm(VI), based on results of beta-decay of a short-lived isotope of Am as AmO_2^+, this work has not been confirmed. Aqueous solutions of Cm(III) are very stable. Solutions of Cm(IV), unstable in noncomplexing aqueous media, can be prepared in concentrated fluoride solution by dissolution of CmF_4 or Cs_3CmF_7. No one has yet succeeded in preparing Cm(IV) in solution by direct oxidation of Cm(III).[53] Based on an estimated standard reduction potential of the Cm(IV)/Cm(III) redox couple,[69] it was expected that Cm(IV) could be prepared by oxidation of Cm(III) in concentrated aqueous carbonate solution.

Solution absorption spectra of Cm(III) in 1 M $HClO_4$ and Cm(IV) in 15 M CsF at 10.5°C, adapted from the literature,[53] are displayed in Figure 48. Multimilligram quantities of solid yellow-green $CmCl_3.nH_2O$ were converted to light green $Cm(OH)_3$ and dissolved separately in 5.5 M K_2CO_3 and 5 M Cs_2CO_3. Initial spectra were recorded prior to electrochemical oxidation. The solution spectrum of colorless Cm(III) in 5.5 M K_2CO_3 is shown in Figure 49. The similarity of the trivalent curium species in $HClO_4$ to that in K_2CO_3 is indicated by the similarity in their solution absorption spectra; however, minor differences between the two spectra indicate a certain degree of complexation provided by the carbonate ions.

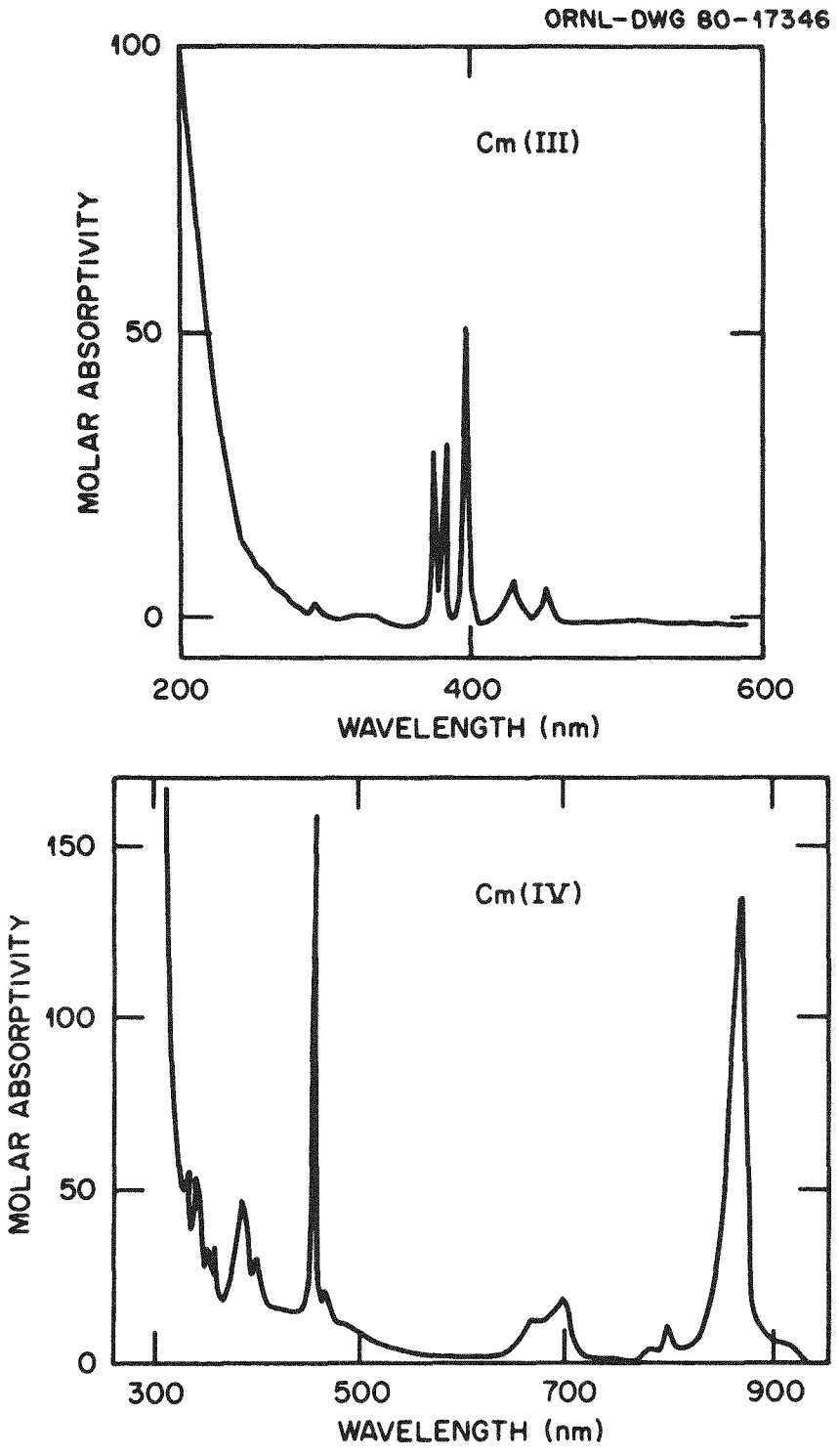

Figure 48. Solution absorption spectra of Cm(III) in 1 M $HClO_4$ and Cm(IV) in 15 M CsF at 10.5°C.

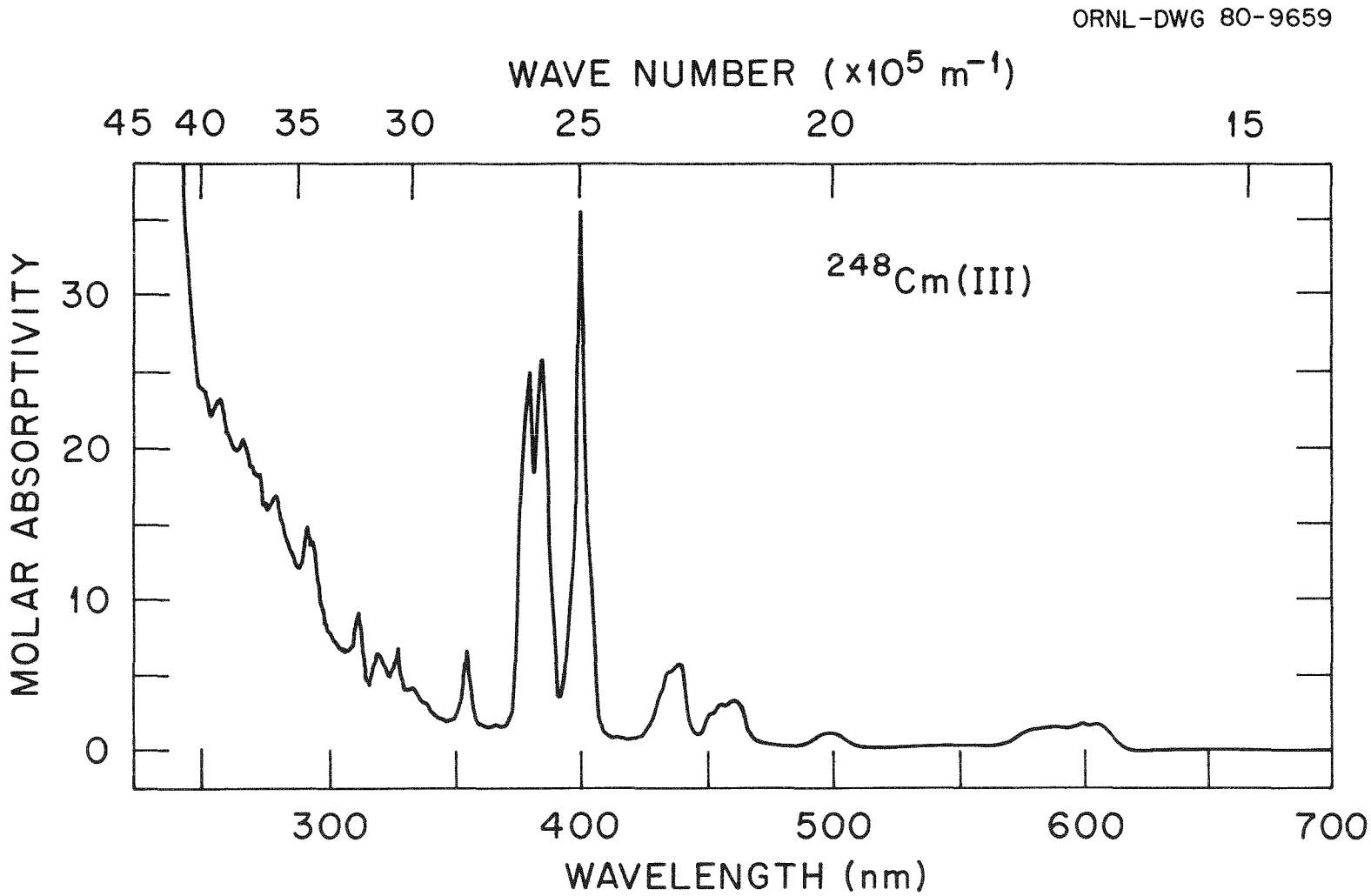

Figure 49. Solution absorption spectrum of Cm(III) in 5.5 M K_2CO_3.

The Cm(III)-K_2CO_3 solution was placed in a quartz cuvet in a Teflon cell holder. Cyclic voltammetry at Pt and RVC working electrodes indicated no oxidation wave within the potential range of either of the electrodes. Bulk solution electrolysis was then performed by placing RVC working, Pt counter, and SCE reference electrodes directly in contact with the solution in the cuvet. Increasingly more positive potentials were applied to the cell until a change was noted visually or by examination of the recorded solution absorption spectra. At 1.1 V the initially colorless solution turned light yellow. The solution absorption spectrum showed only characteristic Cm(III) peaks with an additional broad-band absorption starting at about 400 nm and increasing to an UV cut-off. The same experiment was repeated using a platinum screen working electrode. At potential values exceeding 2.0 V, no discoloration of the solution was noted; only oxygen gas was evolved from the anode. It was later determined that the RVC electrode material was being oxidized in this carbonate medium and that it was this oxidized electrode material which gave rise to the yellow color of the solution.

Experiments performed with Cm(III) in both K_2CO_3 and Cs_2CO_3 indicate no evidence for oxidation of Cm(III) to higher oxidation states. An estimated E° of the Cm(IV)/Cm(III) redox couple has been reported as 3.1 V which is the same as the values reported for the M(IV)/M(III) redox couples of both Pr and Tb, i.e., 3.2 and 3.1 V, respectively. The tetravalent states of both Pr and Tb have been prepared successfully in concentrated aqueous carbonate solution, as reported previously in this dissertation. It is not presently known

why the above-mentioned experiments did not result in the oxidation of Cm(III) to Cm(IV), unless the E° of the Cm(IV)/Cm(III) redox couple is more positive than the estimated 3.1 V.[69]

CHAPTER IV

SUMMARY AND CONCLUSIONS

A. Optically Transparent Electrodes

Of the various types of optically transparent electrodes utilized in this research project, the RVC and PMF OTE's were found to be superior to the screen type OTE's for spectroelectrochemical investigation of the lanthanides and actinides. [This document constitutes the first report of the application of porous metal foam for use as an optically transparent electrode.[76]] The relatively long path length (>1 mm) and large electrode surface area combined with a relatively small electroactive sample volume (< 1 mL) provided by the RVC and PMF OTE's made these electrodes particularly well suited to the study of the transplutonium elements, many of which are available only in limited quantities and exhibit relatively low molar absorptivities.

The RVC-OTE was found to exhibit an extensive potential range in aqueous solution of from 1.4 to -1.0 V at pH 6. This potential range could be exceeded for applications other than voltammetry to the limits where gross interference from evolution of hydrogen gas (cathodic) or oxygen gas (anodic) occurred. The RVC-OTE was found to exhibit good optical transparency (52% T for 0.5 mm and 27% T for 1.0 mm of 100 ppi RVC) throughout the UV-VIS-near IR spectral region. RVC was found to be inert in most aqueous solvents studied. Only in

concentrated phosphoric acid and concentrated carbonate solutions, at potentials exceeding 1 V, was it noted that RVC was destroyed by oxidation, imparting a yellowish coloration to the solution. RVC seemed to be unaffected by contact with radioactive actinide solutions. If adsorption of the radioactive actinides on the RVC electrode occurred, it did not affect the results of voltammetric or spectroelectrochemical experiments with these solutions.

PMF is a three-dimensional network of metal struts very similar in structure and appearance to RVC. The PMF-OTE has many of the advantages of the RVC-OTE including good optical transparency and allowing for a reasonably long optical path length while maintaining a small sample volume. The PMF-OTE also has a large electrode surface area within a small volume of the material, and since it is nickel or copper, it has a much higher electrical conductivity than does the RVC glassy carbon. Additionally, the effective potential range of PMF is only limited by the electrode material which is plated on the foam substrate. Platinum was plated on nickel foam substrate for anodic use, and mercury was deposited on the substrate for extended cathodic applications. The mercury coated PMF did not have the same cathodic range as pure mercury, but an intermediate range between that of pure nickel and pure mercury (0 to -1.6 V if used immediately after electrodeposition).

Another consideration in direct comparison between the RVC and PMF OTE's is the cost. For example, an RVC-OTE was made with glass microscope slides; the total cost was just under one dollar. A comparable PMF-OTE was made using nickel foam; the total cost was

about ten dollars. The expense of plating a noble metal on the PMF substrate should be added to the cost given above.

B. Lanthanide Elements

1. M(III)/M(II) Redox Couples

The M(III)/M(II) redox couples of Eu, Yb, and Sm, the only lanthanide elements known to exist in the divalent state in aqueous solution, were investigated by cyclic voltammetry, solution absorption spectrophotometry, and spectroelectrochemistry. The E°' values obtained from cyclic voltammetry [-0.34 ± 0.01 V for Eu(III)/Eu(II), -1.18 ± 0.01 V for Yb(III)/Yb(II), and -1.50 ± 0.01 V for Sm(III)/Sm(II)] were found to agree with literature values.[69] The spectropotentiostatic method for determinations of E°' and n was applied to the Eu(III)/Eu(II) redox couple using an RVC-OTE. The E°' value so determined [-0.391 ± 0.005 V for n = 1.007] was slightly higher than that derived from voltammetry but still in agreement with reported values.[85,86]

The M(III)/M(II) redox couples of Yb and Sm were not amenable to spectropotentiostatic analysis because of the instability of their divalent ions and the limited cathodic range of the OTE's in aqueous solution. Yb(II) was electrochemically generated and spectrally identified in a silver amalgam screen OTE, but Sm(II) could not be prepared using any OTE but was generated by dissolution of Sm metal in dilute HCl.

2. M(IV)/M(III) Redox Couples

Since Ce(IV) was the only tetravalent lanthanide ion found to be sufficiently stable to exist in aqueous solution prior to this work, the

Ce(IV)/Ce(III) redox couple was used as a reference couple to study the shift in reduction potential provided by various complexing aqueous solutions. A complexing medium which could provide a substantially less positive shift in the reduction potential of the cerium couple may also be used to generate and stabilize other less stable M(IV) states of the lanthanides and actinides.

It was found that in 15 M H_3PO_4 the shift in the potential for the cerium couple was insufficient to allow for generation of any other lanthanide M(IV) species. Difficulty with the solubility of M(III) ions of the lanthanides was experienced in concentrated CsF solution and the insolubility of alkali metal oxalates prevented preparation of complexing solutions in concentrations greater than 2 M.

Ce(III) was found to be quite soluble in 5.5 M K_2CO_3 and was oxidized to Ce(IV) by oxygen in the atmosphere. Since voltammetric methods were not particularly useful because of high background currents in concentrated carbonate solution, spectropotentiometric determinations of E°' and n were applied to the Ce(IV)/Ce(III) redox couple in order to quantify the shift in the reduction potential provided by carbonate ion complexation. The E°' value was found to be 0.051 $\pm$ 0.005 V (n = 0.95) reflecting a substantial shift in the potential from the 1.7 V value reported in $HClO_4$.[69] Assuming a similar shift in potential across the lanthanide series, it was expected that both Pr(IV) and Tb(IV) may also be generated and stabilized in this same medium.

Pr(III) and Tb(III) salts were separately dissolved in 5.5 M K_2CO_3 and electrolyzed at Pt and RVC electrodes. The appearance of new spectral bands and changes in the colors of the carbonate solutions

confirmed the generation of Pr(IV) and Tb(IV). These results were reproduced in 2 M Na_2CO_3 and 5 M Cs_2CO_3; however, Pr(IV) and Tb(IV) could not be stabilized in bulk solution in 2 M $(NH_4)_2CO_3$ since pH 14 was required; $(NH_4)_2CO_3$ is self-buffered at pH 9. Pr(IV) and Tb(IV) were also prepared by oxidation by ozone in 5.5 M K_2CO_3 adjusted to pH 14.

Assignment of oxidation state IV to the oxidized Pr and Tb species was based on (a) correlations of the known M(IV)/M(III) redox potentials in noncomplexing media[69] with the significantly less positive formal reduction potential of the Ce(IV)/Ce(III) redox couple in concentrated carbonate solution and (b) prediction of the approximate position and intensity of the electron-transfer bands of these M(IV) species in chloride ion complexes.[109]

The electrochemical generation of soluble tetravalent species of Pr and Tb in aqueous solution has not, to the knowledge of this author, been reported previously.

A solid compound prepared by electrochemical oxidation of carbonate solutions of Tb(III) has been analyzed by TGA-MS, X-ray powder diffraction, and X-ray fluorescence and reflectance spectroscopies and was shown to be a compound consisting of mixed Tb(III)-Tb(IV) oxidation states. The preparation of this solid compound suggests the possibility of generating similar compounds of the actinides, which may have important applications in the recovery and reprocessing of the transuranium elements.

C. Actinide Elements

1. Uranium

Uranium redox couples were used as substitutes for the heavier, more radioactive actinides in preliminary experiments because of the well-known reduction potentials for uranium redox couples and the well-characterized absorption spectra of their ions in solution.

The U(VI)/U(V)/U(IV) redox couples were studied in 1 M KCl at different pH values. Cyclic voltammetry and spectroelectrochemistry were employed to study the stability of U(V) in aqueous solution. U(VI) was reduced to U(V) in a pH range between 2 and 4. Below pH 2 U(VI) was reduced to unstable U(V) which disproportionated to U(IV) and U(VI); the net effect was reduction to U(IV). U(V) was generated electrochemically in KCl-D_2O at -0.26 V while the absorption spectrum was recorded in an RVC-OTE.

The U(IV)/U(III) redox couple was studied in 1 M KCl at different pH values. The couple was found to be reversible in deoxygenated solvent at pH 0 with an $E^{\circ\prime}$ value of -0.65 ± 0.01 V, in good agreement with the reported -0.631 V value.[69] U(III) was generated electrochemically using silver amalgam screen and porous nickel amalgam foam OTE's and absorption spectra were recorded as a function of time.

The simultaneous electrochemical generation and spectral characterization of U(V) and U(III) in optically transparent electrodes has demonstrated the usefulness of spectroelectrochemical techniques in the study of less stable oxidation states of the actinide elements.

2. Neptunium

Electrochemical and spectroscopic studies of neptunium-237 as well as heavier actinides were carried out in containment gloved box facilities.

The Np(VI)/Np(V) redox couple was studied in 1 M $HClO_4$ and 2 M Na_2CO_3. Cyclic voltammetry of the Np(VI)-$HClO_4$ solution showed the Np(VI)/Np(V) couple to be reversible with an E°' value of 1.11 ± 0.01 V as compared to the 1.137 V literature value.[69] The solution absorption spectra were recorded during the spectropotentiostatic determinations of E°' and n in an RVC-OTE. The values so derived [E°' = 1.140 ± 0.005 V and n = 0.93] were in excellent agreement with reported values. A solution of Np(VI) in 2 M Na_2CO_3 was reduced to Np(V), and the spectrum of Np(V) was recorded in this medium.

The Np(VII)/Np(VI) redox couple was investigated in 2 M Na_2CO_3 at pH 13. Cyclic voltammograms at a Pt electrode showed a reversible couple with an E°' value of 0.46 ± 0.01 V as compared to the reported 0.582 V in 1 M OH^- solution.[45,53] Bulk quantities of Np(VII) were prepared by electrolysis of Np(VI) in 2 M Na_2CO_3 at pH 13. Solution absorption and Raman spectra of the initial Np(VI) solution and the resultant dark green Np(VII) solution were recorded. The Raman spectrum of Np(VII) in carbonate media was quite similar to that reported in 1 M LiOH solution [100,101] which suggests that the structure of Np(VII) is at least similar in both solutions. To the knowledge of this author, this constitutes the first report of the Raman spectrum of Np(VII) in carbonate solution.

The above-mentioned experiments using neptunium-237 demonstrate the usefulness of spectroelectrochemistry at optically transparent electrodes in containment gloved box facilities and also suggest the use of laser Raman spectroscopy-spectroelectrochemistry to study radioactive actinide elements.

3. Americium

Although Am(IV) is reported to be unstable with respect to disproportionation in mineral acid solutions, it was expected that, like Pr(IV) and Tb(IV), it could be generated and stabilized in concentrated aqueous carbonate solution.

The oxidation of $^{243}Am(III)$ was studied in $(NH_4)_2CO_3$, Na_2CO_3, K_2CO_3, and Cs_2CO_3. Cyclic voltammetry showed the reversibility of the Am(IV)/Am(III) redox couple to be dependent on pH. A reversible voltammogram at pH 9.7 in 2 M Na_2CO_3 yielded an E°' value of 0.92 ± 0.01 V. This value was used to calculate a predicted E° value in noncomplexing media by assuming the same shift in the potential as that observed for the Ce(IV)/Ce(III) couple. The value so derived was 2.62 ± 0.01 V in excellent agreement with the work of Morss and Fuger.[104]

Bulk solution electrolysis in Teflon spectroelectrochemical cell holders [specially designed for this work] using RVC and Pt screen OTE's allowed for complete electrolysis of Am(III) to stable Am(IV). The solution absorption spectrum of Am(IV) in carbonate solution is reported here for the first time. An approximate E° value calculated from results of bulk solution electrolysis of Am(III) to Am(IV) was reported to be 2.65 ± 0.01 V.[103] [This value was cited by Morss and Fuger in their recent work.[104]]

The assignment of oxidation state IV to the oxidized americium species was based on (a) correlation of the known Am(IV)/Am(III) redox potential in noncomplexing media[69,102,104] with the measured shift in the Ce(IV)/Ce(III) reduction potential in concentrated carbonate solution versus that in noncomplexing media, (b) prediction of the approximate position and intensity of the electron-transfer band of Am(IV) in chloride ion complexes,[109] (c) direct spectrophotometric comparison of Am(IV) with known Am(VI) carbonate solutions, (d) generation of Am(V) solutions and compounds at potentials exceeding that for generation of Am(IV), and (e) spectrophotometric and potentiometric titrations which showed a one-electron exchange upon reduction of Am(IV) to Am(III).

The conditions under which Am(IV) was generated in this work [0.92 V, pH 9-14] correlate well with a recently prepared potential vs pH diagram for the predicted oxidation state species of Am in aqueous solution (see Figure 50). This diagram, which is based on reported literature data, and was prepared by Allard,[110] predicts a stable Am(IV) species in a potential range between 0.4 and 0.75 V and a pH range between 9.5 and 14.

This dissertation research constitutes the first report of the generation and stabilization of Am(IV) in aqueous carbonate solution including its solution absorption spectrum and reversible cyclic voltammograms and formal reduction potential of the Am(IV)/Am(III) redox couple.[103]

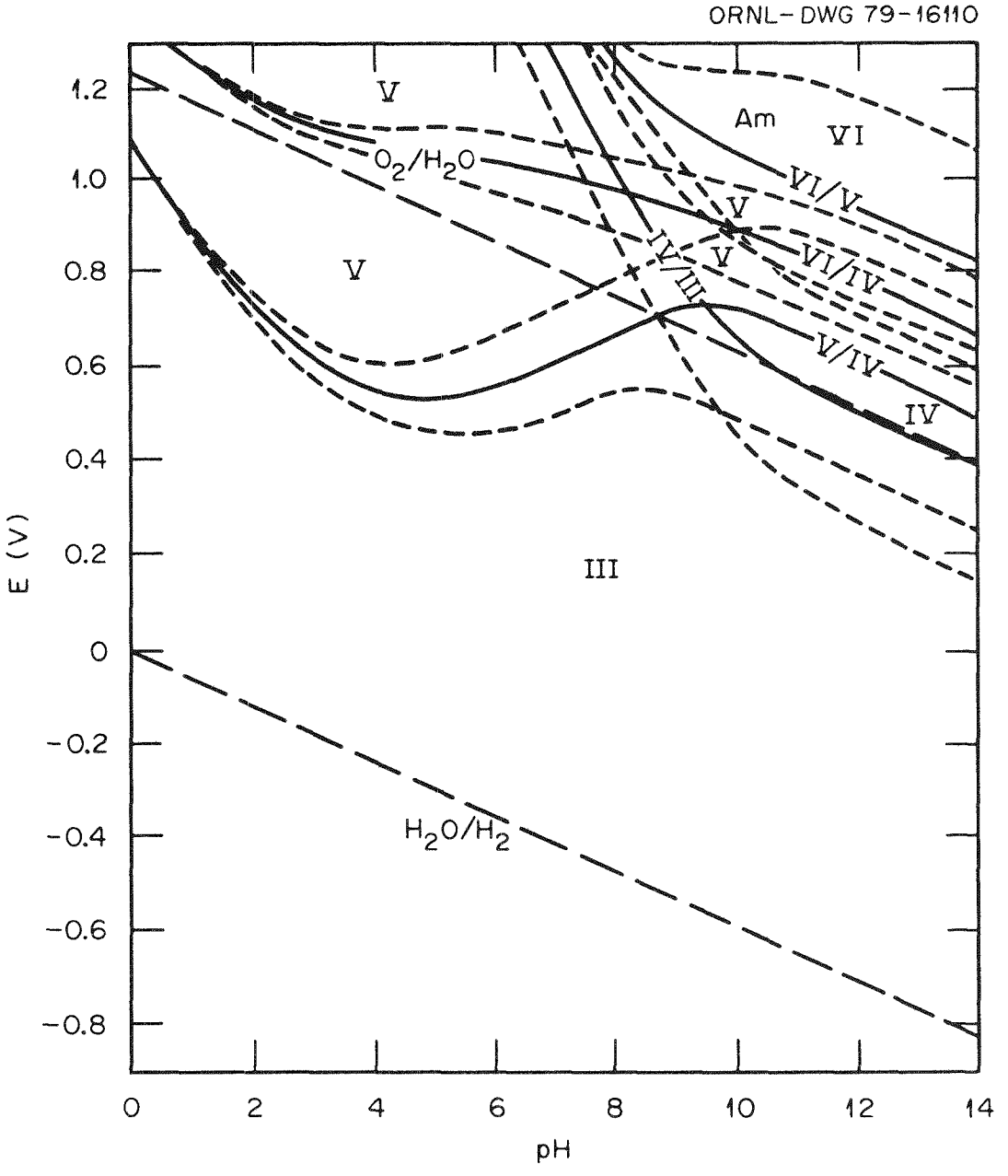

Figure 50. Potential vs pH diagram for the predicted oxidation state species of Am in aqueous solution. Potential in V vs NHE.

4. Curium

Based on an estimated standard reduction potential for the Cm(IV)/Cm(III) redox couple of 3.1 V,[69] it was expected that Cm(IV) could be prepared by oxidation of Cm(III) in concentrated aqueous carbonate media. The solution absorption spectrum of Cm(III) in 5.5 M K_2CO_3 was recorded prior to electrochemical oxidation in a spectro-electrochemical cell at RVC and Pt screen electrodes. Increasing the electrode potential to the anodic limit in this solution did not cause the oxidation of Cm(III), since no new spectrum was observed. It was therefore determined that the estimated E° value for the Cm(IV)/Cm(III) redox couple is probably too low, based on the behavior of the Tb(IV)/Tb(III) redox couple; Tb(IV) can be prepared in concentrated aqueous carbonate solution, and the Tb couple has the same E° value as that estimated for the Cm couple.

Additional experiments with Cm(III) in carbonate solution at different pH values and at below room temperature are needed to confirm the above-mentioned conclusions. Due to the lack of additional quantities of purified curium-248, it was not possible to pursue this direction in the present work.

D. Suggested Future Research

The use of complexing aqueous solutions as a means to stabilize less stable oxidation states should be further exploited. It is expected, for example, that concentrated aqueous carbonate solution can provide stability to Cf(IV) and possibly allow for the oxidation to Cf(V). Concentrated fluoride solutions, known to stabilize Cm(IV),

may permit oxidation to Cm(V). The alkali metal oxalates and oxalic acid should be studied as a complexing aqueous solution to find a way to increase the oxalate ion concentration.

The electrochemical and spectroscopic study of less stable oxidation states in aqueous solution is, of course, limited by the redox and spectral properties of water. The use of nonaqueous organic and molten salt solvent systems, with extended potential limits and spectral transparencies, may provide a substantial advantage in the study of less stable and unusual oxidation states of the lanthanide and actinide elements. Dimethylsulfoxide (DMSO), acetonitrile, and dimethylformamide (DMF) are a few nonaqueous organic solvents which should be considered, since they are commonly used solvents for electrochemical studies.

Some molten salt systems of promise for the stabilization of higher oxidation states of the lanthanides and actinides are CsOH-RbOH eutectics, molten alkali metal carbonates and low melting oxide eutectics.

It is the use of such nonaqueous solvent systems in conjunction with compatible spectroelectrochemical cells and electrode materials in a gloved box environment that should result in the characterization of some new oxidation states like Cm(V), Bk(II), Cf(V), and Es(IV).

It is anticipated that the continued development of improved cell designs and new electrode materials will enhance the applications of spectroelectrochemistry to the investigation of the oxidation state behavior of the transuranium elements.

LIST OF REFERENCES

LIST OF REFERENCES

1. K. W. Bagnall, "Lanthanides and Actinides," Inorganic Chemistry, Series I, Vol. 7, K. W. Bagnall, Ed., University Park Press, Baltimore, MD, 1972.

2. D. T. Sawyer and J. L. Roberts, Jr., "Experimental Electrochemistry for Chemists," John Wiley and Sons, New York, NY, 1974, p. 2.

3. T. Kuwana, R. K. Darlington, and D. W. Leedy, Anal. Chem., 36, 2023 (1964).

4. T. Kuwana and W. R. Heineman, Acc. of Chem. Res., 9, 241 (1976), and references therein.

5. N. Winograd and T. Kuwana, in "Electroanalytical Chemistry," Vol. 7, A. J. Bard, Ed., Marcel-Dekker, New York, NY, 1974.

6. W. R. Heineman, Anal. Chem., 50, 390A (1978).

7. H. N. Blount, N. W. Winograd, and T. Kuwana, J. Phys. Chem., 74, 3231 (1970).

8. N. Winograd and T. Kuwana, Anal. Chem., 43, 252 (1971)

9. C. E. Baumgartner, G. T. Marks, D. A. Aikens, and H. H. Richtol, Anal. Chem., 52, 267 (1980).

10. W. N. Hansen, R. A. Osteryoung, and T. Kuwana, J. Am. Chem. Soc., 88, 1062 (1966).

11. W. N. Hansen, T. Kuwana, and R. A. Osteryoung, Anal. Chem., 38, 1910 (1966).

12. T. Kuwana, Ber. Bunsenges. Phys. Chem., 77, 858 (1973) and references therein.

13. T. P. DeAngelis and W. R. Heineman, J. Chem. Ed., 53, 594 (1976).

14. D. E. Albertson, H. N. Blount, and F. M. Hawkridge, Anal. Chem., 51, 556 (1976).

15. M. Petek, T. E. Neal, and W. R. Murray, Anal. Chem., 43, 1069 (1971).

16. E. A. Blubaugh, A. M. Yacynych, and W. R. Heineman, Anal. Chem., 51, 561 (1979).

17. B. S. Pons, J. S. Mattson, L. O. Winstrom, and H. B. Mark, Jr., Anal. Chem., 39, 685 (1967).

18. A. Yilding, P. T. Kissinger, and C. N. Reilley, Anal. Chem., 40, 1018 (1968).

19. R. Cieslinski and N. R. Armstrong, Anal. Chem., 51, 565 (1979).

20. T. P. DeAngelis, R. W. Hurst, A. M. Yacynych, H. B. Mark, Jr., W. R. Heineman, and J. S. Mattson, Anal. Chem., 49, 1395 (1977).

21. J. S. Mattson and C. A. Smith, Anal. Chem., 47, 1122 (1975).

22. W. J. Blaedel and G. A. Mabbott, Anal. Chem., 50, 933 (1978).

23. R. W. Murray, W. R. Heineman, and G. W. O'Dom, Anal. Chem., 39, 1666 (1967).

24. D. Lexa, J. M. Saveant, and J. Zickler, J. Am. Chem. Soc., 99, 2786 (1977).

25. W. R. Heineman and T. Kuwana, Anal. Chem., 43, 1075 (1971).

26. M. L. Meyer, T. P. DeAngelis, and W. R. Heineman, Anal. Chem., 49, 602 (1977).

27. W. R. Heineman, T. P. DeAngelis, and J. F. Goelz, Anal. Chem., 47, 1364 (1975).

28. V. E. Norvell and G. Mamantov, Anal. Chem., 49, 1470 (1977).

29. V. S. Srinivasan and C. F. Anson, J. Electrochem. Soc., 120, 1359 (1973).

30. W. R. Heineman, J. N. Burnett, and R. W. Murray, Anal. Chem., 40, 1974 (1968).

31. I. Piljac, M. Tkalcec, and B. Grabaric, Anal. Chem., 47, 1369 (1975).

32. R. M. Wightman, J. R. Cockrell, R. W. Murray, J. N. Burnett, and S. B. Jones, J. Am. Chem. Soc., 98, 2562 (1976).

33. W. R. Heineman, J. N. Burnett, and R. W. Murray, Anal. Chem., 40, 1970 (1968).

34. F. M. Hawkridge and B. Ke, Anal. Biochem., 78, 76 (1977).

35. D. F. Rohrbach, E. Deutsch, and W. R. Heineman, in "Characterization of Solutes in Nonaqueous Solvents," G. Mamantov, Ed., Plenum Press, New York, NY, 1978.

36. W. R. Heineman, B. J. Norris, and J. F. Goelz, Anal. Chem., 47, 79 (1975).

37. D. F. Rohrbach, E. Deutsch, W. R. Heineman, and R. F. Pasternack, Inorg. Chem., 16, 2650 (1977).

38. W. R. Heineman and P. T. Kissinger, Anal. Chem., 50, 166R (1978).

39. D. Cohen and W. T. Carnall, J. Phys. Chem., 64, 1933 (1960).

40. B. F. Myasoedov, V. M. Mikhailov, I. A. Lebedev, O. E. Koiro, and V. Ya. Frenkel, Radiochem. Radioanal. Letters, 14, 17 (1973).

41. E. Yanir, M. Givon, and Y. Marcus, Inorg. Nucl. Chem. Letters, 6, 415 (1970).

42. R. D. Baybarz, J. R. Stokely, and J. R. Peterson, J. Inorg. Nucl. Chem., 34, 739 (1972).

43. J. P. Young, G. Mamantov, and F. L. Whiting, J. Phys. Chem., 71, 782 (1967).

44. T. Moeller, "The Chemistry of the Lanthanides," Reinhold Publ., New York, NY, 1963.

45. F. A. Cotton and G. Wilkinson, "Advanced Inorganic Chemistry," 4th ed., Interscience, New York, NY, 1980, Chap. 24, and references therein.

46. N. B. Mikeev, V. I. Spitsyn, A. N. Kamenskaya, I. A. Rumer, B. A. Gvozdev, N. A. Rozenkevich, and L. N. Auerman, Dokl. Akad. Nauk SSSR, 208, 1146 (1973).

47. E. K. Hulet, R. W. Lougheed, P. A. Baisden, J. H. Landrum, J. F. Wild, and R. F. Lundqvist, J. Inorg. Nucl. Chem., 41, 1743 (1979).

48. K. Samhoun, F. David, R. L. Hahn, G. D. O'Kelley, J. R. Tarrant, and D. E. Hobart, J. Inorg. Nucl. Chem., 41, 1749 (1979).

49. F. David, K. Samhoun, E. K. Hulet, P. A. Baisden, R. W. Lougheed, J. H. Landrum, G. D. O'Kelley, and J. F. Wild, J. Inorg. Nucl. Chem. (in press).

50. K. Samhoun and F. David, in "Transplutonium Elements," W. Müller and R. Lindner, Eds., North-Holland, Amsterdam, 1976, p. 297; K. Samhoun and F. David, J. Inorg. Nucl. Chem., 41, 357 (1979).

51. F. David, K. Samhoun, and R. Guillaumont, Rev. Chim. Minerale, 14, 199 (1977).

52. T. Moeller, "The Chemistry of the Lanthanides," Reinhold Publishers, New York, NY (1963).

53. C. Keller, "The Chemistry of the Transuranium Elements," Verlag Chemie, GmbH, Germany, 1971 and references therein.

54. R. D. Baybarz, J. Inorg. Nucl. Chem., 35, 483 (1973).

55. R. D. Baybarz, L. B. Asprey, C. E. Strouse, and E. Fukushima, J. Inorg. Nucl. Chem., 34, 3427 (1972).

56. L. J. Mullins, A. J. Beamont, and J. A. Leary, J. Inorg. Nucl. Chem., 30, 147 (1968).

57. V. Scherrer, F. Weigel, and M. Van Ghemen, Inorg. Nucl. Chem. Letters, 3, 589 (1967).

58. L. B. Asprey and B. B. Cunningham, in "Progress in Inorganic Chemistry," F. A. Cotton, Ed., Vol. 2, Interscience, NY, 1960, p. 270.

59. R. Hoppe, Israel J. Chem., 17, 48 (1978).

60. G. Brauer and H. Kristen, Z. Anorg. Allg. Chem., 456, 41 (1979).

61. L. B. Asprey and R. A. Penneman, J. Am. Chem. Soc., 83, 2200 (1961).

62. E. Yanir, M. Givon, and Y. Marcus, Inorg. Nucl. Chem. Letters, 5, 369 (1969).

63. J. R. Stokely, Analytical Chem. Div. Annual Prog. Report for period ending Sept. 30, 1971, ORNL-4749, p. 7.

64. T. K. Keenan, J. Am. Chem. Soc., 83, 3719 (1961).

65. O. L. Keller, Radiochimia Acta, 25, 211 (1978).

66. J. Selbin and J. D. Ortega, Chem. Rev., 69, 657 (1969), and references therein.

67. N. N. Krot and A. D. Gelman, Dokl. Akad. Nauk. SSSR, 177, 124 (1967).

68. N. N. Krot, V. P. Shilov, V. B. Nikolaevskii, A. K. Nikaev, A. D. Gelman, and V. I. Spitsyn, Dokl. Akad. Nauk. SSSR, 217, 589 (1974); USAEC Report ORNL-tr-2828 (1974).

69. L. J. Nugent, R. D. Baybarz, J. L. Burnett, and J. L. Ryan, J. Phys. Chem., 77, 1528 (1973).

70. C. K. Jórgensen, Molec. Phys., 5, 271 (1962).

71. J. R. Stokely, R. D. Baybarz, and J. R. Peterson, J. Inorg. Nucl. Chem., 34, 392 (1972).

72. L. J. Nugent, in "Lanthanides and Actinides," Inorganic Chemistry, Series II, K. W. Bagnall, Ed., Univ. Park Press, Baltimore, MD, 1975, Vol. 7, p. 195.

73. J. Fuger, Univ. of Liège, Radiochem. Lab., personal communication, 1980.

74. L. N. Klatt, J. Chromatogr. Sci., 17, 225 (1979).

75. J. P. Young, R. G. Haire, R. L. Fellows, and J. R. Peterson, J. Radioanal. Chem., 43, 479 (1978).

76. D. E. Hobart, V. E. Norvell, and S. A. Morris, unpublished work.

77. B. Guillaume, CEN-FAR, Fontenay-aux-Roses, France, private communication, 1980.

78. B. Guillaume, G. M. Begun, and R. L. Hahn, "Raman Spectrophotometric Studies of 'Cation-Cation' Complexes of Pentavalent Actinides in Aqueous Solutions," to be published.

79. R. D. Baybarz, J. B. Knauer, and P. B. Orr, Oak Ridge National Laboratory Report ORNL-4672 (1973).

80. Z. Borkowska and H. Elzanowska, J. Electroanal. Chem., 76, 287 (1977).

81. A. J. Bard and L. R. Faulkner, "Electrochemical Methods: Fundamentals and Applications," John Wiley and Sons, New York, NY, 1980.

82. H. B. Herman and J. R. Rairden in "The Encyclopedia of Electrochemistry of the Elements," A. J. Bard, Ed., Marcel-Dekker, New York, NY, 1973, Chapter VI-2, and references therein.

83. R. N. Adams, "Electrochemistry at Solid Electrodes," Marcel Dekker, New York, NY, 1969, Chapter 3-6.

84. W. T. Carnall,in "Handbook on the Physics and Chemistry of Rare Earths," K. A. Gschneidner, Jr. and L. Eyring, Eds., North-Holland, Amsterdam, 1979, Vol. 3, Chap. 24, p. 171.

85. L. R. Morss and H. Haug, J. Chem. Thermo., 5, 513 (1973).

86. G. Biedermann and H. B. Silber, Acta Chem. Scand., 27, 3761 (1973).

87. D. E. Hobart, K. Samhoun, J. P. Young, V. E. Norvell, G. Mamantov, and J. R. Peterson, Inorg. Nucl. Chem. Letters, 16, 321 (1980).

88. W. M. Latimer, "Oxidation Potentials," 2nd Edition, Prentice Hall, New York, NY, 1952.

89. B. F. Myasoedov and I. A. Lebedev, Radiokhimiya, 19, 87 (1977).

90. A. S. Saprykin, V. P. Shilov, V. I. Spitsyn, and N. N. Krot, Dokl. Akad. Nauk SSSR, 226, 853 (1976).

91. R. C. Propst, J. Inorg. Nucl. Chem., 36, 1085 (1974).

92. R. R. Rickard, Analytical Chemistry Division, ORNL, private communication, 1980.

93. R. L. N. Sastry, S. R. Yoganarasimhan, P. N. Mehrota, and C. N. R. Rao, J. Inorg. Nucl. Chem., 28, 1165 (1966).

94. K. A. Kraus, F. Nelson, and G. L. Johnson, J. Am. Chem. Soc., 71, 2510 (1949).

95. D. M. Gruen and R. L. McBeth, J. Inorg. Nucl. Chem., 9, 290 (1959).

96. C. Musikas, Thesis, University of Paris, Orsay, France, 1977.

97. P. G. Hagan and J. M. Cleveland, J. Inorg. Nucl. Chem., 28, 2905 (1966).

98. C. Keller, J. Gross, and W. Bacher, Institut für Radiochemie, Kernforschungszentrum und Universität, Karlsruhe, Germany, unpublished work.

99. V. I. Dzyubenko, S. A. Karavaev, V. F. Peretrukhin, and N. N. Krot, Dokl. Akad. Nauk SSSR, 248, 1362 (1979).

100. L. J. Basile, J. R. Ferraro, M. L. Mitchell, and J. C. Sullivan, Appl. Spectrosc., 32, 535 (1978).

101. L. J. Basile, J. C. Sullivan, J. R. Ferraro, and P. LaBonville, Appl. Spectrosc., 28, 142 (1974).

102. W. W. Schulz, "The Chemistry of Americium," Technical Information Center, U.S. Department of Energy, TID-26971 (1976), and references therein.

103. D. E. Hobart, K. Samhoun, R. G. Haire, J. P. Young, M. Jaber, and J. R. Peterson, abstract of paper presented at 10th Journées des Actinides, Stockholm, Sweden, May 27-28, 1980.

104. L. R. Morss and J. Fuger, J. Inorg. Nucl. Chem. (in press).

105. L. B. Asprey and T. K. Keenan, J. Inorg. Nucl. Chem., 7, 27 (1958).

106. L. B. Asprey and R. A. Penneman, Inorg. Chem., 1, 134 (1962).

107. J. Y. Bourges, CEN-FAR, Fontenay-aux-Roses, France, private communication, 1980.

108. V. F. Peretrukhin, E. A. Erin, V. I. Dzyubenko, V. V. Kopytov, V. G. Polyukov, V. Ya. Vasil'ev, G. A. Timofeev, A. G. Rykov, N. N. Krot, and V. I. Spitsyn, Dokl. Akad. Nauk SSSR 242, 1359 (1978).

109. L. J. Nugent, R. D. Baybarz, J. L. Burnett, and J. L. Ryan, J. Inorg. Nucl. Chem., 33, 2503 (1971).

110. Reproduced here with the permission of B. Allard, Chalmers University of Technology, Department of Nuclear Chemistry, Göteborg, Sweden.

VITA

David Edward Hobart was [redacted] He attended public school in Miami, Florida, graduating from Miami Carol City Senior High School in June 1967. In September of that year he entered Rollins College, Winter Park, Florida, and in May 1971 he received a Bachelor of Arts degree with a major in Chemistry. In July 1971 he was married to the former Miss Barbara Jean [redacted] in Winter Park.

In October 1971 he entered active military service in the United States Air Force during which he served as an aircraft electronic sensor systems specialist (reconnaissance) for the Strategic Air Command. He graduated with honors at the Lowry AFB Technical Training Center, Denver, Colorado, and was named Outstanding Airman of the Month in his unit at Beale AFB, California. He was also stationed in Okinawa and Thailand. He was honorably discharged from active duty service in August 1975.

In September 1975 he entered the Graduate School of The University of Tennessee, Knoxville, and was granted a graduate teaching assistantship in the Department of Chemistry for two years. In September 1977 he was granted a graduate research assistantship which enabled him to conduct specialized research at the Transuranium Research Laboratory, Oak Ridge National Laboratory, Oak Ridge, Tennessee. While conducting this research, he had the opportunity to collaborate on several research projects with some international guest scientists, with some projects resulting in publications.

On [redacted] the author's wife gave birth to a baby girl, Michelle Anne Hobart.

The author received the Doctor of Philosophy degree from The University of Tennessee, Knoxville with a major in Chemistry in June 1981.

The author is a member of the American Chemical Society and its Nuclear Chemistry and Technology Division. He presented papers on his research at the 30th Southeastern Regional Meeting of the American Chemical Society, Savannah, Georgia in November 1978 and at the Combined Southeast-Southwest Regional Meeting of the American Chemical Society, New Orleans, Louisiana in December 1980. He has published articles in the Journal of Chemical Education, Journal of Inorganic and Nuclear Chemistry, and Inorganic and Nuclear Chemistry Letters, and is co-author of a chapter on Berkelium in "The Chemistry of the Transuranium Elements," 2nd Edition, J. J. Katz, G. T. Seaborg, and L. R. Morss, Editors, to be published by Chapman and Hall, London.